

SACLANTCEN Conference Proceedings No. 36

AD-A151 779

SACLANT ASW
RESEARCH CENTRE



SACLANTCEN Conference Proceedings No. 36

20000814016

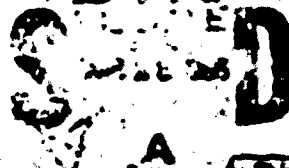
SILENT SHIP
RESEARCH APPLICATIONS AND OPERATION

VOL. II UNCLASSIFIED PAPERS

PROCEEDINGS OF A CONFERENCE
HELD AT SACLANTCEN ON 2-4 OCTOBER 1984

Organized by
Pierre BLIVIER

DTIC



15 JANUARY 1985

This document has been approved
for public release and sale, its
distribution is unlimited.

DTIC FILE COPY

NORTH
ATLANTIC
TREATY
ORGANIZATION

SACLANTCEN
LIVORNO ITALY

This document is unclassified. The information it contains is published subject to the conditions of the legend printed on the inside cover. Short quotations from it may be made in other publications if credit is given to the author(s). Except for working copies for research purposes or for use in NATO publications, reproduction requires the authorization of the Director of SACLANTCEN.

85 09 11 175

This document is released to a NATO Government at the direction of the SACLANCEN subject to the following conditions:

1. The recipient NATO Government agrees to use its best endeavours to ensure that the information herein disclosed, whether or not it bears a security classification, is not dealt with in any manner (a) contrary to the intent of the provisions of the Charter of the Centre, or (b) prejudicial to the rights of the owner thereof to obtain patent, copyright, or other like statutory protection therefor.

2. If the technical information was originally released to the Centre by a NATO Government subject to restrictions clearly marked on this document the recipient NATO Government agrees to use its best endeavours to abide by the terms of the restrictions as imposed by the releasing Government.

Compiled and
Published by



REPRODUCTION QUALITY NOTICE

This document is the best quality available. The copy furnished to DTIC contained pages that may have the following quality problems:

- **Pages smaller or larger than normal.**
- **Pages with background color or light colored printing.**
- **Pages with small type or poor printing; and or**
- **Pages with continuous tone material or color photographs.**

Due to various output media available these conditions may or may not cause poor legibility in the microfiche or hardcopy output you receive.

☐

If this block is checked, the copy furnished to DTIC contained pages with color printing, that when reproduced in Black and White, may change detail of the original copy.

(4)

SACLANTCEN CONFERENCE PROCEEDINGS NO. 36

NORTH ATLANTIC TREATY ORGANIZATION

SACLANT ASW Research Centre
Viale San Bartolomeo 400,
I-19026 San Bartolomeo (SP), Italy.

tel. — national 0187 540111
international • 39 187 540111

telex 271148 SACENT I

SILENT SHIP
RESEARCH APPLICATIONS
AND OPERATION

VOL. II: UNCLASSIFIED PAPER

Proceedings of a Conference held at SACLANTCEN
on 2-4 OCTOBER 1984
Organized by
Pierre Blavier

15 January 1985

This document has been prepared from camera-ready provided by the authors:

- a) The opinions expressed are those of the authors and are not necessarily those of the SACLANT ASW Research Centre.
- b) The legibility of text and figures reflects the quality of the copy received from the authors and not the reproduction processes used by the SACLANT ASW Research Centre.

DTIC
ELECTRIC
S MAR 26 1985
A

This document has been approved
for public release and sale, its
distribution is unlimited.

LIST OF PARTICIPANTS

CANADA

Mr Alexander P. Brown
National Defence Headquarters

Mr Richard F. Brown
Defence Research Establishment

Mr James H. Costain
National Defence Headquarters

DENMARK

Mr Ole V. Olesen
Brüel & Kjaer

Mr Lars Thiele
Oedegaard & Danneskoild-Samsøe K/S

FRANCE

Dr Claude Bercy
Université Pierre et Marie Curie

Mr Georges Bienvenu
Thomson-CSF DASM

Ms Françoise Briolle
DCAN Toulon/GERDSM

Mr Jean-Guy Cailloux
DCAN Toulon/GERDSM

Dr Hubert Debart
SINTRA

Mr Bernard De Raigniac
DCAN Toulon/GERDSM

Mr Georges Elias
Office National d'Etudes et de
Recherches Aéronautiques

Ms Anne Frances
DCAN Toulon/CERDAN CERTSM

Mr Georges Gouillet
DCAN Toulon/GERDSM

FRANCE (Cont.)

Mr Alain Julienne
Office National d'Etudes et de
Recherches Aéronautiques

Mr André Kermabon
SYMINEX

Mr Robert Laval
Société AERO

Mr Jean-Pierre Le Goff
D.R.E.T. (MOD)

Mr Claude C. Leroy
Sintra-Alcatel

Mr Sylvain Marcouyoux
DCAN Toulon/CERDAN CERTSM

Mr Yves Moretti
SURF

Mr Dominique Otero
Sintra-Alcatel

Mr Alain Plaisant
Thomson-CSF DASM

Mr Benoît Raffin
DCAN Toulon/GERDSM

Mr Thierry Rohan
DCAN Toulon/CERDAN CERTSM

Mr Jean-Louis Vernet
Thomson-CSF DASM

GERMANY

Mr Robert Hagen
IABG

Dr Peter Mertens
Krupp-Atlas Elektronik GmbH

Mr Bernd Schmelfeldt
Marine Technik GmbH

List of Participants

GERMANY (Cont.)

WDir Wolfgang Schmidt
Forschungsanstalt der Bundeswehr
für Wasserschall-und Geophysik

BDir Manfred Tode
Forschungsanstalt der Bundeswehr
für Wasserschall-und Geophysik

Dr Gerhard Wittek
Fraunhofer-Institut für Hydroakustik

ITALY

CDR Lucio Accardo
MARICONAVARMI - CEIMM

Ing. Pier Luigi Ausonio
Cantieri Navali Italiani S.p.A

Dr Ing. Franco Bau
Cantieri Navali Italiani S.p.A

Ing. Enzo Cernich
Sonomar SpA

Dr Agostino Colombo
CETENA (Italian Ship Research Center)

Ing. Renato Faresi
CETENA (Italian Ship Research Center)

Ing. Giovanni Guzzo
Sonomar SpA

Dr Luciana Ricciardiello
CETENA (Italian Ship Research Center)

Prof G. Tacconi
Istituto di Elettroacustica
MARIPERMAN

Ing. Giancarlo Vettori
USEA

NETHERLANDS

Dr Ir Alex De Bruijn
TPD, Institute of Applied Physics

Ir Jan H. Janssen
TPD, Institute of Applied Physics

NETHERLANDS (Cont.)

Mr Hendrik F. Steenhoek
TPD, Institute of Applied Physics

Mr Jan Van Der Kooij
NSMP-Marin

SPAIN

CDR Antonio Arredondo de Rio, SN
Estado Mayor

Mr Rafael Carbo-Fite
Instituto de Acustica

CDR Fernando Cominges de Molins, SN
Estado Mayor

Mr Carlos Lanz-Guerra
Instituto de Acustica

UNITED KINGDOM

Mr Cedric M. Hubbard
LYCAB ALGADA (Marine) Ltd

Mr Stephen J. Ryder
ARE, Portland

Mr Gwilym E. Thomas
ARE, Teddington

UNITED STATES

Mr George C. Connolly
NUSC, New London

Mr John W. Fay
NUSC, New London

Dr David Felt
David W. Taylor Naval Ship R&D Center

Mr Ariel W. George
Bolt Beranek & Newman

Mr Keith W. Kaulum
ONR, Arlington

Mr John H. Keegan
NUSC, New London

UNIT STATES (Cont.)

Mr. James H. King
Lt. W. Taylor Naval Shipyard Center

Mr. J. E. Lench
New York

Mr. J. E. Lench
New York

Mr. J. E. Lench
New York

Mr. J. E. Lench
Lt. W. Taylor Naval Shipyard Center

Mr. J. E. Lench

Mr. J. E. Lench (Dept. Director)

Mr. J. E. Lench

Mr. J. E. Lench

Mr. J. E. Lench

Mr. J. E. Lench



A-1

Table of Contents

TABLE OF CONTENTS

	<u>Pages</u>
INTRODUCTION	1
(Sessions 1, 2 and 3 were classified, see SACLANTCEN CP-35)	
<u>SESSION 4 - MAINTENANCE OF SILENT SHIPS - -</u>	
(Chairman: James H. King)	
- Different approaches to economic cruising speeds on a CODOG frigate with due regard to radiated noise, by L. Accardo and M. Stori	a) 1-1 to 1-8
- Propeller leading edge trimming and maintenance: effects on ship's noise operational performances, by L. Accardo and F. Bau	b) 2-1 to 2-8
<u>SESSION 5 - APPLICATIONS OF SILENT SHIPS - -</u>	
(Chairman: Benoit Rafine)	
Incidence du bruit acoustique de thoniers ligneurs et sennieurs francais sur leurs performances de peche by C. Bercy, B. Bordeau, C. Depoutot	c) 3-1 to 3-14
The implications of a silent ship for the investigation of low-frequency acoustic/seismic propagation, by Hassan B. Ali	d) 4-1 to 4-22
<u>SESSION 6 - TECHNIQUES FOR REDUCTION AND MEASUREMENTS OF OWN-SHIP NOISE - -</u>	
(Chairman: Howard Schloemer)	
- Near field propeller radiated noise measurements: model and full scale experimental data comparison, by L. Accardo and A. Colombo	e) 5-1 to 5-15
- Some near-field acoustic imaging techniques in noise ranging, by B. Rafine and G. Elias	f) 6-1 to 6-8
- Mutual coherence and silence, by H.P. Debart	g) 7-1 to 7-9
- Mobile range for measuring ship radiated acoustic noise, by E. Cernich and G.C. Vettori	h) 8-1 to 8-15

INTRODUCTION

Ronald S. Thomas
Deputy Director
SACLANT ASW Research Centre
La Spezia, Italy

The project to construct an acoustically quiet research ship for the SACLANT ASW Research Centre provided a reason for SACLANTCEN to organize a conference on silent ships, their operation and applications. The ship, to be delivered in 1986, will have a strong impact on the Centre's ability to undertake research and to meet its mandate to provide scientific and technical advice on ASW to SACLANT. This is especially true since there is an increasing trend towards research at lower acoustic frequencies, where most of the underwater background noise is generated by ships.

The new ship, the first actually owned by NATO, will be operated by a commercial firm and will, as with the present research ship, be used by a NATO international scientific staff serving on relatively short-term contracts. This higher-than-normal rate of turnover in the research staff leaves flexibility for adjusting scientific programmes, but also accentuates the need for good planning.

The conference was an opportunity to discuss problems related to the operation and applications of quiet ships in a forum in which the participants had an unusual combination of disciplines. The result was a series of stimulating exchanges and a broadening of perspectives for all.

Undoubtedly the conference will influence the Centre in its planning for the management of this specialized quiet ship and will affect thinking for staffing. At the same time it has made more people aware of the new ship that will often participate with NATO nations in joint experimental studies, following the tradition established with SACLANTCEN's previous chartered ships: the MARIA PAOLINA G. and the ARAGONESE.

SACLANTCEN is grateful for the contribution of all participants and hopes that they have also found the conference both informative and enjoyable.

DIFFERENT APPROACHES TO ECONOMIC CRUISING SPEEDS ON A CODOG
FRIGATE WITH DUE REGARD TO RADIATED NOISE

by

Lucio Accardo (CDR, IN) and Massimo Stori (CDR, IN)
Mariconavarmi, MOD Navy
Rome, Italy

ABSTRACT

All Navies, in recent years, have been much more concerned in economic cruising speeds of ships. Frigate type naval ships are usually characterized by two shafts, by multiple propulsion engines per shaft, and by different types of propulsion engines (gas turbines and diesels). When economic cruising speed is essential (for example during transit missions) naval ships are usually operated at asymmetrical shaft revolutions, with one propulsive shaft and the other trailing. This paper illustrates the impact on cavitation (and therefore on radiated noise) of asymmetrical shaft revolutions mode of operation compared to the even shaft revolutions mode of operation.

INTRODUCTION

It is well known that specific fuel consumption of gas turbines increases with decreasing power output. When a gas turbine ship is underway at relatively low speeds the mode of operation with one shaft propelled and the other trailing is more favorable than operation with two propelled shafts. Fuel consumption in this condition is lower, in spite of the additional drag of the trailing shaft.

CODOG ships have the advantage of been able to reach speed not attainable with diesel propulsion in an unconventional way, that is with one shaft propelled by diesel engine at nominal speed, and the other shaft propelled by a gas turbine. In this condition the drag of the slow shaft is reduced, the r.p.m. difference between the two shafts is also reduced, and an overall lower fuel consumption has been measured.

Specific trials have been carried out to investigate this unconventional machinery line-up. The speeds investigated were those corresponding to a Froude number of 0.337 and 0.368. These ship's speeds are attainable with the following propulsion machinery line-ups:

- one gas turbine on each shaft
- one gas turbine on one shaft and the other trailing
- one gas turbine on one shaft and a diesel engine at nominal r.p.m. on the other shaft

ACCARDO & STORI: CODOG frigate

An additional investigation was performed at a Froude number of 0.307, attainable only with one gas turbine on each shaft or with one gas turbine on one shaft and the other shaft trailing.

1. TRIAL DESCRIPTION

The trials have been carried out in the northern Tyrrhenian sea, in the month of April, 1982. Weather conditions were good, with calm sea and variable wind force 1. The ship was at the trial displacement, with clean hull and propellers.

The pitch on controllable pitch propellers was kept at the design value during the trials.

The following variables were measured during the trials :

- ship's speed by Paddist
- shafts' torque by torquemeters
- shafts' n.p.m. by counters
- fuel consumption by on-board fuel meters

The cavitation sketches were taken on the port shaft, equipped with propeller viewing windows.

2. CAVITATION SKETCHES

Tables 1., 2., and 3. summarize the computed values of the torque coefficient K_q and of the cavitation index σ_n based on the values of power and shaft n.p.m. measured during the trials.

The following relationships have been used :

$$F_n = \frac{V}{\sqrt{gL}}$$

$$K_q = \frac{75 P_d}{2\pi \rho N^3 D^5} \quad 216'000$$

$$G_n = \frac{10'150 + 10'25 i}{52,3 N^2 D^2} \quad 3'400$$

where :

- F_n is the Froude number
- L is the ship's length in meters
- g is the acceleration due to gravity in m/s^2
- P_d is the power in horsepower
- N is the propeller r.p.m.
- D is the propeller diameter in meters
- l is the propeller center disk draft in meters

The cavitation sketches at Froude numbers of 0.307, 0.337 and 0.368, with the ship propelled at even shaft r.p.m. by a gas turbine per shaft, are given in Fig. 1, Fig. 2, and Fig. 3 respectively.

The cavitation sketches at Froude numbers of 0.307, 0.337 and 0.368, with the ship propelled at asymmetrical shaft r.p.m. with a gas turbine on one shaft and the other shaft trailing, are given in Fig. 4, Fig. 5, and Fig. 6 respectively.

The cavitation sketches at Froude numbers of 0.337 and 0.368, with the ship propelled at asymmetrical shaft r.p.m. with a gas turbine on one shaft and a diesel engine at nominal speed on the other shaft, are given in Fig. 7 and Fig. 8 respectively. Froude number of 0.307 has not been considered since it is not attainable in this propulsive condition.

3 COMMENTS ON TRIAL RESULTS

Examination of cavitation sketches leads to the following comments :

3.1. at even shaft r.p.m. extension of cavitation is minimum, as expected.

3.2. at asymmetrical shaft r.p.m. :

3.2.1. fast shaft :

back cavitation is always present, and the extension is larger with increasing shaft r.p.m. difference between the two shafts.

face cavitation is present only in the least r.p.m. difference between the two shafts.

3.2.2. slow shaft :

back cavitation is present at Froude numbers of 0.337 and 0.368 only when the slow shaft is connected to the diesel engine.

face cavitation is always present, and the extension is larger with increasing shaft r.p.m. difference between the two shafts.

ACCARDO & STORI: CODOG frigate

4 CONCLUSIONS

The trials carried out have confirmed that :

- optimal conditions, from the point of view of cavitation, are attained with even shaft r.p.m.
- the worst cavitation extension has been observed when the ship is propelled by one shaft and the other is trailing.
- ship's propulsion by one gas turbine and one diesel at moderately asymmetrical shaft r.p.m. is the best from the fuel consumption point of view and represent a good compromise from the cavitation point of view.

ACCARDO & STORI: CODOG frigate

	port shaft (with windows)	starboard shaft
Propulsion 1	gas turbine	gas turbine
K_q	0.0419	0.0419
σ_n	3.30	3.30
Propulsion 2	gas turbine	trailing
K_q	0.0663	=
σ_n	2.53	2.15
Propulsion 3	trailing	gas turbine
K_q	=	0.0635
σ_n	2.33	2.66

Table 1 - Froude number = 0.387 - Computed values of K_q and σ_n .

	port shaft (with windows)	starboard shaft
Propulsion 1	gas turbine	gas turbine
K_q	0.0467	0.0467
σ_n	3.17	3.17
Propulsion 2	gas turbine	trailing
K_q	0.0674	=
σ_n	2.12	5.21
Propulsion 3	trailing	gas turbine
K_q	=	0.0634
σ_n	6.01	2.20
Propulsion 4	gas turbine	diesel
K_q	0.0489	0.0397
σ_n	2.83	3.21
Propulsion 5	diesel	gas turbine
K_q	0.0377	0.0515
σ_n	3.10	2.06

Table 2 - Froude number = 9.337 - Computed values of K_q and σ_n .

ACCARDO & STORI: CGDOG frigate

	port shaft (with windows)	starboard shaft
Propulsion :	gas turbine	gas turbine
K_A	0.0464	0.0464
σ_n	2.59	2.59
Propulsion :	gas turbine	trailing
K_A	0.0693	=
σ_n	1.90	3.03
Propulsion :	trailing	gas turbine
K_A	=	0.0704
σ_n	5.14	1.34
Propulsion :	gas turbine	diesel
K_A	0.0565	0.0304
σ_n	2.26	3.04
Propulsion :	diesel	gas turbine
K_A	0.0343	0.0536
σ_n	3.03	2.24

Table 3 - Froude number = 0.368 - Computed values of K_A and σ_n .

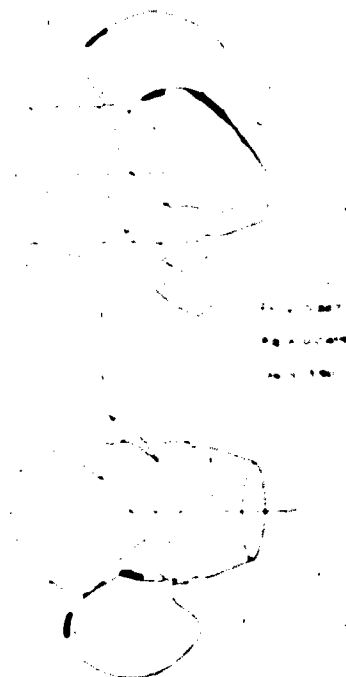


Fig. 1
Even shaft r.p.m. with both shafts
on gas turbine

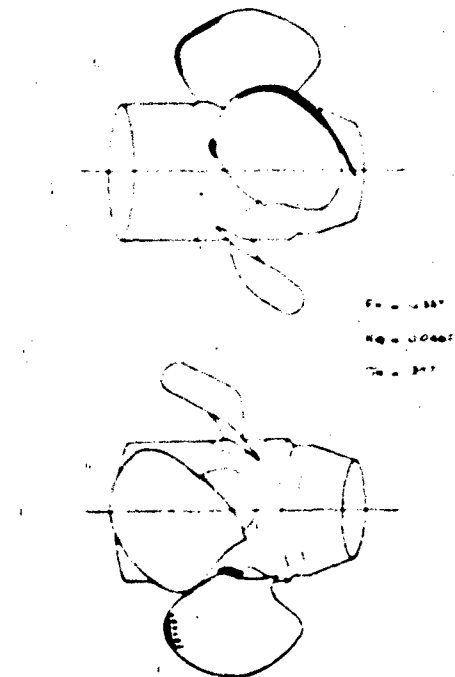


Fig. 2
Even shaft r.p.m. with both shafts
on gas turbine

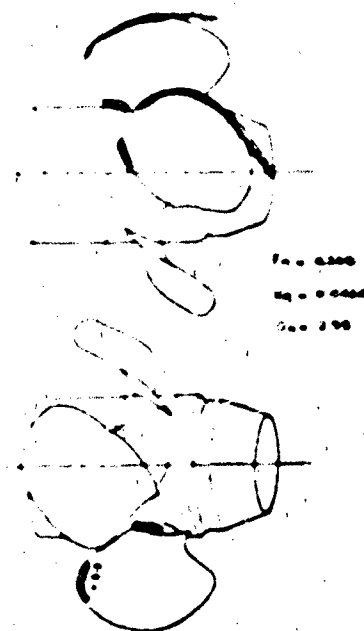


Fig. 3
Even shaft r.p.m. with both shafts
on gas turbine

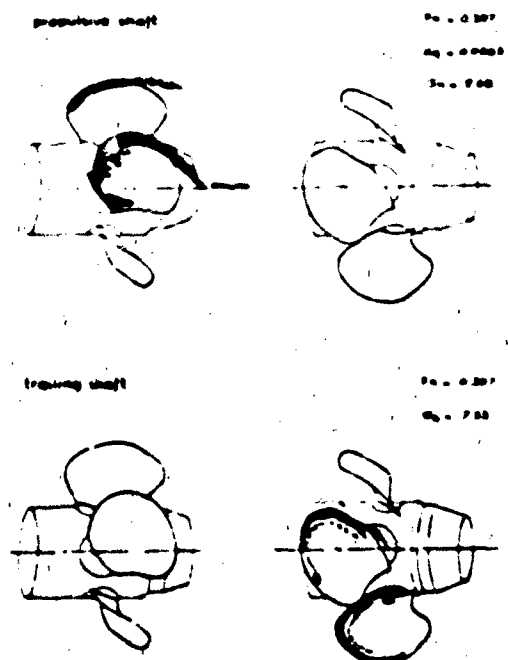


Fig. 4
Asymmetrical shaft r.p.m. with one
shaft on gas turbine and the other
shaft trailing

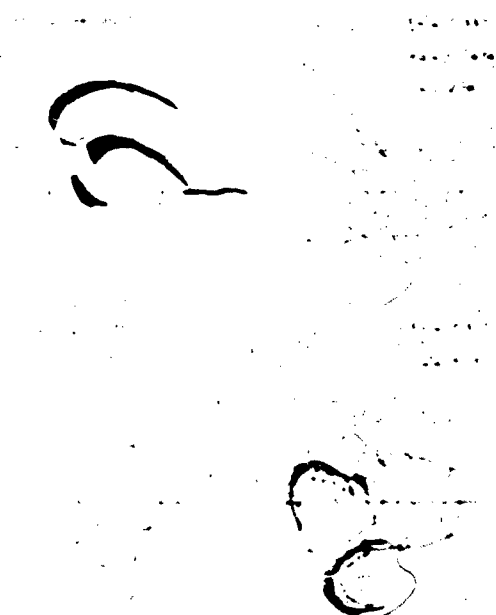


Fig. 5
Asymmetrical shaft r.p.m. with one
shaft on gas turbine and the other
shaft trailing

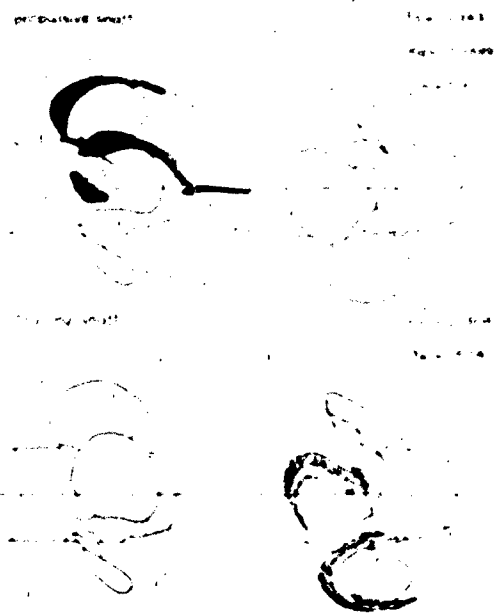


Fig. 6
Asymmetrical shaft r.p.m. with one
shaft on gas turbine and the other
shaft trailing

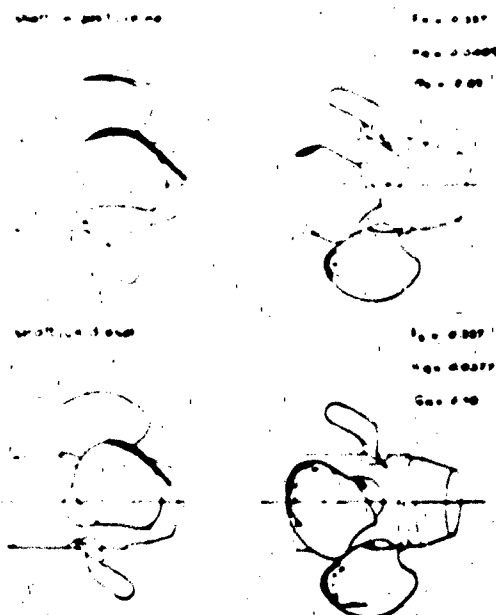


Fig. 7
Asymmetrical shaft r.p.m. with one
shaft on gas turbine and the other
shaft on diesel

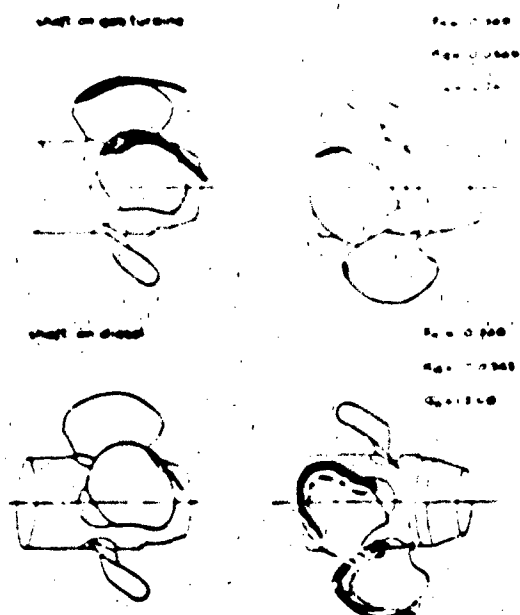


Fig. 8
Asymmetrical shaft r.p.m. with one
shaft on gas turbine and the other
shaft on diesel

PROPELLER LEADING EDGE TRIMMING AND MAINTENANCE
EFFECTS ON SHIP'S NOISE OPERATIONAL PERFORMANCES

by

L. Accardo - M.M.I. - C.E.I.M.N. - Roma (Italy)

F. Bau - FINCANTIERI - C.N.I. - Genova (Italy)

ABSTRACT

In the last ten years, considerable experience has been gathered at CEIMN's cavitation tunnel (Centro Esperienze Idrodinamiche Marina Militare) on the effects of propeller leading edge geometry on cavitation (and noise) performances. The experience has been gained on both model and full scale tests, carried out by using various techniques. Some considerations are also made on the design, manufacture and maintenance needs imposed by today's silent ship design and operation.

INTRODUCTION

It is well known that a fluid surrounding a lifting surface, with foil type sections, undergoes the most important velocity variations in the vicinity of the section's leading edge (1,2).

During one revolution of a propeller blade, the velocity variations are related to the wake distribution at the propeller disc, the propeller working conditions, and the cavitation number (3, 4).

At the initial propeller design stage, some parameters can be suitably chosen to delay cavitation, viz. low RPM, regular wake field, loading distribution, skew, etc., (5,6). Although the whole blade geometry is responsible for a given cavitation behaviour, the leading edge is the region where the cavitation first starts and develops. Due to the important correlation between cavitation and noise, (7,8), any operational requirement which implies quietness makes, therefore, the leading edge geometry very important.

Unfortunately, the leading edge region is difficult to shape properly at the production stage, and even more difficult to check and control accurately and maintain efficiently.

In this paper some examples of propeller leading edge geometry effects on cavitation and noise behaviour of both full scale and model propellers are briefly presented and discussed. The analytical illustration of the effects of geometrical details, working conditions and local Reynolds number on the fluid velocity distribution and cavitation onset of propeller blade is not the scope of this paper; considerable literature can be found on this field (9, 10).

1 DESIGN PROBLEMS

When low noise propellers are to be designed, several computer programs can provide rather accurate theoretical predictions on the cavitation and vibration performances of a given propeller geometry operating at given conditions (11).

One fundamental design parameter is the local full scale wake field, still ill known at this stage. Therefore all designs are developed and optimized under some assumptions about the wake field.

The leading edge is the most sensitive part of the blade with respect to both the local wake pattern and the cavitation. Definite risk exists of local inadequacy of the propeller geometry when the wake field shows unexpected variations. However, leading edge trimming can give positive solution to the problem (12).

2 EXISTING STANDARD AND PROPELLER CAVITATION

Propellers manufactured to the tolerances prescribed by the international ISO 484-81 standard will in general have propulsive performances corresponding to the design and model testing stage predictions.

On the other hands, generous tolerances are allowed in those parts of the blade where the cavitation phenomena first occur (tip, leading edge region, blade root region). Sectional thickness distribution tolerances become quite significant at the leading edge. Experience gathered leads eventually to the conclusion that a "case by case" tolerance must be studied and adopted when special quietness is imposed by operational requirements to a given propeller. Production accuracy, according to international standards, does not represent in such cases a sufficient safeguard against cavitation onset.

Propeller geometry check procedures in blade regions where large curva-

ture variations occur, are difficult. Templates can be used only at given positions, and even there the resulting accuracy is at least doubtful.

Check problems exist also for numerically controlled manufacturing. Spot checks are possible by using the same manufacturing equipment, but the necessary quasi-continuous (high density) check is impractical (13).

3 MAINTENANCE PROBLEMS

Low noise propeller maintenance during the operational life of the vessel is extremely important.

The use of grinding machines can be allowed for cleaning flat areas (subject to some precautions). Their use must be absolutely forbidden where local surface curvature variations exist or where air injection systems are used. Frequent maintenance by suitable brushing and compressed air cleaning must be adopted.

A special problem is encountered when geometry check must be performed on ship propeller during drydock. This check should be performed on a routine basis or when local damages occur. Difficulties in carrying out this geometry checks "on the spot" impose disassembly of blades (in a C.P.P) or dismounting of the whole propeller.

4 LEADING EDGE TRIMMING EFFECTS - A SAMPLE CASE

A practical case might well illustrate the leading edge trimming effects on propellers of twin screw naval vessels. During the design and model testing phases, particular care had been paid to propulsion performances optimization, as well as noise and vibration minimization.

Final trials well confirmed predicted performances, but during the stroboscopic tests an unexpected local cavitation phenomenon was observed on the face of the propeller, at the leading edge, when the blades were at an angular position of about 300 degrees (0 degrees upwards) (14).

Accurate checks led to the conclusion that blade leading edges were to be manufactured according to a closer tolerance, and corrective actions were then undertaken. A successive stroboscopic test did show an improvement, but some problems still existed (15).

Studies were then carried out by means of model tests, where wake field

scale effects were systematically varied, assuming different scale factors. Local wake effects on cavitation onset were also investigated.

A local leading edge trimming was defined as possible solution: a considerable increase on face cavitation inception speed was expected together with a very slight decrease of cavitation performance of the back and, without modifying in practice, propulsive performances (16).

Model modifications and successive tests at the cavitation tunnel proved such a solution. Fig. 1 shows the maximum extent of modifications. After applying the above modifications to the full scale propellers, sea trials were carried out, and a full confirmation of the model cavitation performance was found. Table 1 gives the cavitation onset Froude number values for various cavitation phenomena before and after the trimming (17).

5 LEADING EDGE MAINTENANCE - A SAMPLE CASE

Stroboscopic tests carried out on board another class of naval vessels, show a propeller cavitation behaviour somewhat similar to what already mentioned under para 4 above. A very thin, flashing face (and partially back) leading edge cavitation was observed at rather low speeds (Froude number about 0.19), at about 0.5 R of the propeller blades, as shown in Fig. 2, (18). Local defects (scratches) at the leading edge, where cavitation was observed, were found during successive drydock inspection. Dimensions of scratches were about 80 mm long, 2 mm wide, and 2 mm deep. They could have been caused during one of the blades handling and mounting or by cables in mooring or towing operations or to improper maintenance.

Proper corrective maintenance actions, leading to the elimination of such scratches, kept again the cavitation onset speed at the original value (Froude number 0.23).

6 CONCLUSIONS

Stroboscopic tests results gathered during sea trials when compared with theoretical cavitation predictions can show the presence of unexpected local wake disturbances and/or geometrical inadequacies at the leading edge of the propeller. Corrective actions are possible, in fact the results obtained stressed the importance of both shaping and successive maintenance of the leading edge.

Accurate blade manufacturing and rigorous checking procedures are also ne-

ACCARDO & BAU: Propeller leading edge trimming

cessary. The development and the systematic use of a leading edge geometry measuring equipment (possibly portable) will be a powerful tool for improving the present acoustic performances of silent vessels.

PHENOMENA	ORIGINAL LEADING EDGE	TRIMMED LEADING EDGE
Back sheet cavitation (at leading edge)	0.231	0.231
Face sheet cavitation (at leading edge)	0.207	0.287
Back bubbles	0.415	0.415
Hub vortex	=	0.415

Table 1 - Froude numbers of cavitation onsets

ACKNOWLEDGMENT

The authors thank Miss. L. Ravazzano for her valuable contribution in the preparation of the paper.

ACCARDO & BAU: Propeller leading edge trimming

REFERENCES

- 1) - Abbott, I.H.; Von Doenhoff A.E.; Stivers L.S., " Summary of air-foil data, NACA Report 824, 1945.
- 2) - Brockett, T. " Steady Two Dimensional Pressure Distribution on Arbitrary Profiles ", DTMB Report 1821 - 1965.
- 3) - Van Oassanen, P. " Calculation of Performance and Cavitation Characteristics of Propeller Inducing effects on Non-uniform Flow and Viscosity - NSMB Publication No. 547.
- 4) - Colombo A., Child B. - " Propeller Induced Pressures in a Non-uniform flow " - Program PRESS - CETENA Report no. 1367 - 1981
- 5) - Brown, N.A. " Minimization of Unsteady Propeller Forces that Excite Vibration of the Propulsion System " Propeller '81 SNAME - 1981.
- 6) - Cumming, R.A., Morgan W.B., Boswell R.S. " Highly Skewed Propellers " - Transaction SNAME, 1972.
- 7) - Nilsson, A.C., Persson B., Tyvand, N.B. " Propeller Induced Noise in Ships " - Propeller '81 SNAME - 1981.
- 8) - De Bruijn " Measurement and Prediction of Sound Inboard and Outboard of Ships as Generated by Cavitating Propellers " Symposium on High Powered Propulsion of Large Ships - 1974.
- 9) - Kaplan P., Bentson J. Breslin J.P., " Theoretical Analysis of Propeller Radiated Pressure and Blade Forces due to Cavitation " R.I.N.A. Symposium - 1979.
- 10) - Valentine, D.T. - " The Effect of Nose Radius on the Cavitation Inception Characteristics of Two-dimensional Hydrofoils " - N S R D C Report No. 3813 - 1974.
- 11) - Bau F., Bellone G., Colombo A., Child A., " Propeller Design Optimization : An Integral Theoretical and Experimental Procedure " - Propeller '81 SNAME - 1981.
- 12) - C.E.I.M.M. Report 13/80.
- 13) - C.E.I.M.M. Report 2/83.
- 14) - C.E.I.M.M. Report 0/78
- 15) - C.E.I.M.M. Report 2/78
- 16) - C.E.I.M.M. Report 3/80
- 17) - C.E.I.M.M. Report 13/80
- 18) - C.E.I.M.M. Report 17/82.

ACCARDO & BAU: Propeller leading edge trimming

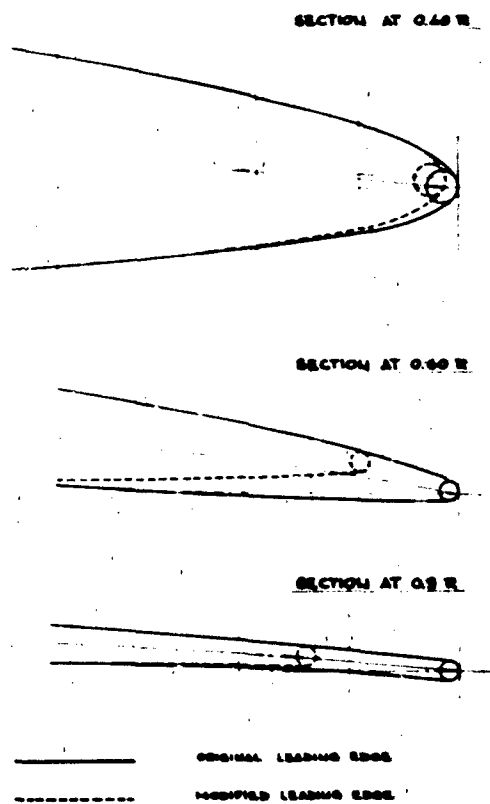
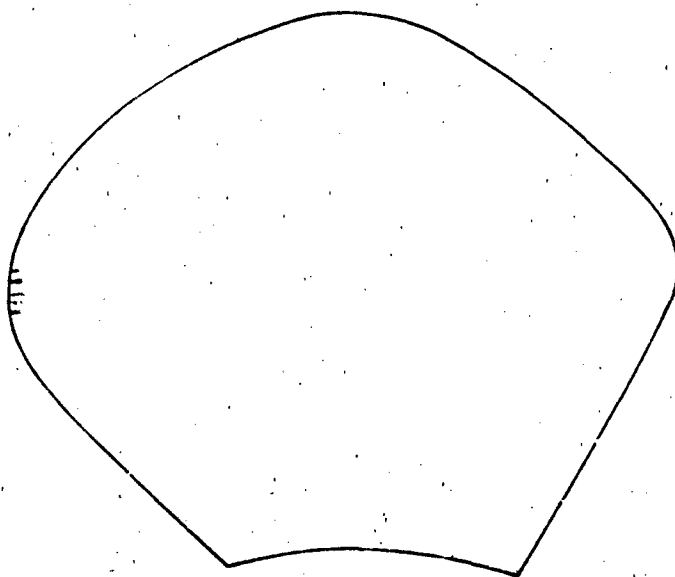


Fig. 2



DISCUSSION

G. Thomas (United Kingdom): What is the significance of Froude number in the context of this study? Is speed the only parameter that is changing?

L. Accardo: The Froude number indicates the increase in ship speed in relation to some other parameters (revolutions, power output, etc.). It has been substituted for ship speed in this unclassified presentation.

"INCIDENCE DU BRUIT ACOUSTIQUE DE THONIERES LIGNEURS ET
SENNEURS FRANCAIS SUR LEURS PERFORMANCES DE PECHE"

C. BERCY - B. BORDEAU - C. DEPOUTOT

RESUME

Les auteurs présentent quelques expertises acoustiques provenant de deux études réalisées par le G.E.R.B.A.M. :

- . la première, sur 95 thoniers ligneurs pratiquant la pêche du germon (*Thunnus alalunga*),
- . la seconde, sur 18 thoniers senneurs pratiquant la pêche du listao (*Katsuwonus pelamis*) et de l'albacore (*Thunnus albacares*).

La structure spectrale du bruit de chaque navire est analysée corrélativement à ses résultats de pêche et aux capacités auditives du poisson.

Des résultats significatifs mettent en évidence l'effet négatif de raies importantes dans la gamme 200-700 Hz (bande auditive des Thonidés), sur les performances de pêche.

Une étude statistique de la flottille germonière, basée sur l'analyse factorielle des caractéristiques des bateaux (âge, longueur, tonnage, puissance, type de coque, résultats de pêche) confirme ces résultats.

Ces premières mesures constituent une base de réflexion pour la réalisation de navires de pêche "peu bruyants" dans la gamme auditive des espèces qu'ils recherchent.

INTRODUCTION

Ces dix dernières années, le droit international en matière d'exploitation des ressources halieutiques a évolué dans le sens d'une forte augmentation des contraintes pour les professionnels de la pêche : mise en place de zones de pêche et de quotas, limitation des engins de capture...

Les Armements Français doivent donc faire face à des difficultés techniques et économiques croissantes.

La pêche thonière dans son ensemble, confrontée à une compétition internationale très vive, est plus particulièrement exposée. L'ajustement des charges et du chiffre d'affaires est de plus en plus difficile à réaliser. La rentabilité des armements est soumise :

- à la stagnation, voire la baisse des cours du thon sur le marché mondial,
- aux difficultés d'écoulement rencontrées par les conserveurs,
- au prix du carburant (1kg de thon équivaut à 0,85 l de fuel),
- à la diminution des stocks de thonidés.

Ainsi, la pêche germonière connaît un déclin important, le nombre d'unités passant de 480 en 1967 à 106 en 1983.

La grande pêche du thon tropical (30 unités) reste, cependant, un secteur dynamique, mais menacé.

Une intensification de la recherche appliquée dans ce domaine se justifie donc particulièrement.

I - BRUIT A BORD DES NAVIRES DE PECHE ET PERCEPTION ACOUSTIQUE DES ESPECES

1.1. PARAMETRES INFLUANT SUR LES PERFORMANCES DE PECHE D'UN THONIER

De très nombreux facteurs jouent sur le rendement d'un thonier, et il serait vain de vouloir en dresser une liste exhaustive.

La pêche du germon est pratiquée en été dans l'Atlantique Nord par des thoniers ligneurs. Le thon est capturé en surface, au moyen de lignes traînantes (18 lignes par bateau au maximum). Cette technique de pêche est basée sur le comportement alimentaire du thon, et le bruit généré par le bateau, à priori et aux dires des pêcheurs, joue un rôle important sur le rendement.

On distingue trois groupes de facteurs influant sur le débarquement global du thonier (Fig 1.) :

- L'ensemble des caractéristiques du bateau (longueur, puissance, type de coque, tonnage...) conditionne directement l'efficacité du navire en présence du banc de thon -ou "puissance de pêche locale". Notons que des caractéristiques très fines, telles que ligne d'eau et sillage, interviennent également.

- La valeur de l'équipage (expérience du patron, habileté des marins pêcheurs...) joue sur la "puissance de pêche locale", mais surtout sur la "capacité stratégique", c'est-à-dire l'aptitude à repérer et se rendre au bon moment sur les zones de pêche les plus favorables.

- Enfin, les facteurs extérieurs, tels que les conditions climatiques et hydrologiques, la densité et l'accessibilité du poisson, conditionnent en partie le débarquement global.

Le bruit du bateau ne dépend que des caractéristiques du navire et agira donc sur le débarquement par l'intermédiaire de la "puissance de pêche locale".

La pêche à la senne est pratiquée toute l'année dans l'Atlantique tropical et, depuis peu, dans l'Océan Indien. La technique utilisée est beaucoup plus brutale : le banc de thons est encerclé rapidement dans un filet circulaire, la senne, qui couvre plusieurs hectares.

Les principaux facteurs d'échec sont :

- la fuite du banc lors de l'approche du bateau,
- la plongée en profondeur des thons pendant la manoeuvre d'encercllement du banc et le déploiement de la senne, qui dure une trentaine de minutes avant la fermeture totale du filet.

Les mêmes groupes de facteurs jouant sur le rendement, cités ci-avant, se retrouvent avec, en plus, quelques paramètres propres aux senneurs, comme les dimensions du filet, et l'utilisation ou non d'un hélicoptère de recherche.

D'autre part, le bruit généré par l'appareil propulsif du bateau, s'ajoute celui de puissants propulseurs d'étraves (300 CV) qui permettent de positionner le navire lors de la manoeuvre d'encercllement, et de "skiffs" (600 CV), embarcations annexes rapides.

1.2. CAPACITES AUDITIVES DES POISSONS

L'appareil auditif présente, chez les poissons, une variabilité macro et micro structurale considérable. Cependant, leur percept on sonore dépend principalement de l'oreille interne, de la vessie natatoire et ses annexes, et du système latéral.

La détermination des seuils d'audition soulève des problèmes complexes [1]. Le plus important est sans doute celui posé par l'existence de deux grandeurs liées au phénomène sonore : la pression acoustique et la vitesse particulière. Actuellement, des dispositifs sophistiqués permettent de contrôler ces deux grandeurs.

II - INCIDENCE DU BRUIT DES THONNIERS LIGNEURS (GERMONIERS) SUR LEURS CAPTURES

2.1. HISTOGRAMMES DES CAPTURES EN FONCTION DU TYPE DE SPECTRE

Nous avons retenu, comme résultats de pêche, les débarquements globaux, en tonnes, des deux premières marées de juillet et août 1983.

A l'examen de l'histogramme des débarquements cumulés sur les deux marées (Fig 6.), on remarque un groupe de 9 bateaux ayant des résultats nettement plus élevés que le reste de la flottille, avec des débarquements cumulés supérieurs à 25 tonnes. Ces unités ont toutes un spectre de type C. De plus, il est frappant de constater que, parmi les 10 meilleures unités, se trouvent 9C et 1B et, à l'inverse, parmi les 10 moins bonnes, se trouvent 7A et 3B.

Les histogrammes par type de spectre montrent une supériorité significative des navires C sur les B, et du type B sur le type A.

D'autre part, les 3 unités à coque polyester se trouvent parmi les 9 meilleures, ce qui confirme la bonne qualité de ce matériau sur le plan de l'acoustique sous-marine.

La figure 7 fait apparaître les résultats de chaque marée. Le "nuage" des points représentant les bateaux C se démarque nettement du reste de la flottille, ce qui prouve leur supériorité, pour chacune des deux marées.

Les moyennes calculées sur 62 bateaux sont présentées dans le tableau suivant :

	moyenne générale (Kg)	moyenne des bateaux A (Kg)	moyenne des bateaux B (Kg)	moyenne des bateaux C (Kg)	% augmentation C par rapport à A
1ère marée (64 bateaux)	10 406	9 239 (26)	9 451 (13)	12 349 (23)	+ 33,66 %
2ème marée (63 bateaux)	8 271	7 294 (27)	8 254 (14)	9 480 (22)	+ 29,97 %
Résultats cumulés sur marées 1 et 2 (62 bateaux)	18 710	16 263 (26)	18 049 (14)	22 024 (22)	+ 35,42 %

Ainsi, l'importance du facteur bruit est telle qu'elle apparaît clairement sur les débarquements globaux, bien que, comme nous l'avons vu, de nombreux autres paramètres interviennent.

2.2. ANALYSE FACTORIELLE DE LA FLOTTELLE GERMONIERE

Une méthode d'analyse multivariable a été appliquée aux données recueillies sur les germoniers pour, d'une part avoir une vision synthétique de la flottille, d'autre part pour tenter d'expliquer la différence d'efficacité entre les ligneurs. Pour cette analyse, nous n'avons retenu que les caractéristiques des bateaux obtenues pour la majorité des ligneurs expertisés en 1983: âge, longueur, tonnage du navire, puissance nominale du moteur, débarquements cumulés, nature de la coque, origine géographique. L'ensemble de ces données a été entièrement rassemblé pour 56 ligneurs.

Le seuil, au niveau minimal détectable, est défini comme le niveau de pression sonore minimale pour lequel le poisson répond directement à la stimulation. Les tracés d'audiogrammes passent par des travaux complexes de conditionnement d'individus. Ils apportent, en bout de leurs limites, des informations utiles sur la nature de sensibilité en fréquence du système auditif des poissons. Le niveau d'audiogrammes intéressant la grande pêche industrielle est donné à ce jour (Fig 2.).

4.2. L'AUDITION DES THONIDES ET BRUITS DES BATEAUX

Les deux Thonides pour lesquels IVERSEN [2] a établi des audiogrammes, l'Albacore (*Thunnus albacares*) et la Thonine (*Thunnus thynnus*), présentent une gamme d'audition comprise auditivement entre 100 et 1000 Hz, avec un optimum à 500 Hz. La différence de niveau acoustique entre les seuils des deux espèces pourrait être due à la présence d'une vessie natatoire chez l'Albacore, inexistante chez la Thonine, et à une vitesse de nage plus élevée de cette dernière.

Les audiogrammes des autres Thonides font défaut. Cependant, il a été démontré que des espèces taxonomiquement proches ont des audiogrammes semblables. Il est probable que les capacités auditives du Thonin (*Thunnus thynnus*) soient comparables, voire meilleures, à celles de l'Albacore.

Les sources de bruit à bord des bateaux de pêche sont nombreuses : ensemble propulsif (moteur, réducteur, arbre, hélice), moteurs auxiliaires, compresseurs, centrale hydraulique, échappements. La participation des vibrations engendrées au spectre acoustique sous-marin dépend, entre autre, de la qualité des isollements, ainsi que des modes de résonance des structures.

Nous avons enregistré et analysé les bruits sous-marins de chalumeurs et de fileyeurs, dans les mêmes conditions. Le bruit de la mer interférant de manière notable sur la qualité des expériences acoustiques, elles ont été réalisées pour des états de mer inférieurs à 4. Les spectres ont été classés selon leur allure dans la gamme 200-700 Hz, qui correspond à la bande d'audition optimale des Thonides (Fig 4.):

- Type A : spectres très perturbés, présentant des pics de plus de 10 dB.
- Type B : spectres dont les pics ont une amplitude comprise entre 5 et 10 dB.
- Type C : spectres réguliers, ne présentant pas de pics de plus de 5 dB.

En rapportant les audiogrammes d'IVERSEN [5] à ces types de spectres (Fig 5.), on constate qu'un bateau de type A sera beaucoup mieux perçu qu'un bateau de type C.

Cette démarche est comparable à celle adoptée par ERICKSON [4], dont l'étude porte sur 154 germoniers américains.

METHODE

Chaque variable est découpée en quatre ou cinq classes, de façon que chacune ait le même "poids" en nombre de bateaux. On définit 24 classes :

CUM1 à CUM5 : débarquements de 9 à 30 tonnes
 AGE1 à AGE4 : âge des bateaux de 1946 à 1982
 LON1 à LON4 : longueur des bateaux de 15 à 31 mètres
 JAU1 à JAU4 : tonnage " " de 29 à 143 tonneaux
 PUS1 à PUS4 : puissance " " de 150 à 510 CV
 COQB, COQA, COQP : bateaux à coque en bois, acier ou polyester.

Le découpage des variables en classes permet de bâtir deux matrices :

- . un "tableau disjonctif complet",
- . un "tableau de contingence" (tableau de BURT) qui croise les 24 classes entre elles.

A partir du tableau de BURT, on construit un nuage de 24 classes dans un espace à 24 dimensions, chaque dimension correspondant à une classe. La distance entre deux points du nuage représentant deux classes, traduit le degré de liaison entre elles, celle-ci étant d'autant plus forte qu'elles seront proches dans l'espace.

Comme il est impossible de se représenter visuellement un espace à 24 dimensions, on analysera le nuage de points par coupes successives. Un plan de coupe est appelé plan factoriel et défini par deux axes orthogonaux correspondant à deux valeurs propres du tableau de BURT.

La figure 8 représente l'axe 3 croisé à l'axe 4, le plan factoriel ainsi considéré représente 20,15 % de l'inertie du nuage. L'analyse de ce plan conduit à distinguer quatre quadrants déterminés en fonction de la variable CUM, qui représente les résultats de pêche.

RESULTATS

La figure 9 montre, en fonction du type de spectre A, B, C, le nombre de bateaux (exprimé en pourcentage) corrélés avec leurs résultats de pêche.

Deux résultats significatifs ressortent :

- . 58 % des bateaux A ont des performances CUM1, ainsi que 55 % en CUM2,
- . 83 % des bateaux C ont des performances CUM5.

L'opposition pyramidale des bateaux A et C est tout à fait représentative (Fig 10.).

L'influence de la composition spectrale du bruit, entre 200 et 700 Hz, sur les résultats globaux de pêche est confirmée par cette analyse.

D'autres remarques peuvent être déduites de cette analyse factorielle :

- la particularité des navires à coque polyester, corrélés à de grandes dimensions (LON4, JAU4), de fortes puissances (PUS4), récents (AGE4), et de très bons rendements (CUM5);
- les navires de petites dimensions et de faible tonnage (JAU1, LON1, PUS2) ont de faibles résultats;
- les bateaux moyens (LON3) réalisent de fortes captures (CUM5), les grandes unités ayant, elles, des résultats (CUM4) inférieurs à ce qu'une relation linéaire longueur-efficacité laisserait prévoir.

Enfin, une distinction des navires par origine géographique (29 unités du Finistère, 4 du Morbihan, 23 de Vendée) met en évidence la supériorité des navires finistériens sur les vendéens.

Dans le quadrant 4 de la figure 8, il n'y a ainsi que 3 vendeens sur 10 unités.

III - THONNIERS SENNEURS.

RÉSULTATS DE PÊCHE EN LIAISON AVEC LA QUALITÉ ACOUSTIQUE

En raison de l'importance économique de la pêche à la senne tournante, l'étude de l'incidence des bruits des bateaux sur leurs résultats a paru évidente.

Actuellement, une trentaine d'unités industrielles opèrent dans le Golfe de Guinée et l'Océan Indien. Dix-huit senneurs de cette flottille franco-ivoiro-sénégalaise ont été expertisés en 1983.

On peut distinguer trois classes de bateaux :

- la classe 1 comprend 7 senneurs de grande dimension (70m), de forte puissance (3600 à 4000 CV), de grosse capacité de stockage (1300 m³);

- la classe 2 compte 9 senneurs de taille moyenne (50 à 60m) et de puissance moyenne (2000 à 3000 CV);

- la classe 3 est représentée par 2 petites unités d'autonomie réduite.

Dans un même groupe, d'un bateau à l'autre, les spectres peuvent être très différents (Fig 11.).

L'analyse des signatures acoustiques retenue est basée sur la typologie A, B, C, déjà utilisée pour les germoniers.

Les chiffres de tonnage global débarqué étant insuffisants pour apprécier l'efficacité des senneurs, nous utiliserons un indice représentant la "puissance de pêche globale". Cet indice est défini comme un rendement de pêche indépendant des facteurs extérieurs.

La figure 12 fait apparaître assez clairement que la puissance de pêche globale, et par conséquent le tonnage moyen, est d'autant plus forte que la taille et la puissance des navires sont importantes.

Cependant, le bruit intervient lui aussi sur les puissances globales : les rendements de pêche des navires de spectre C sont supérieurs de 34,64 % à ceux des bateaux de spectre A, et de 47,41% à ceux des bateaux de spectre B.

Il semblerait qu'une bonne qualité acoustique conférerait aux bateaux C une "puissance locale" importante, leur "capacité stratégique" ayant alors moins d'importance sur leur "puissance globale".

IV - CONCLUSION

Il est évident que le problème de l'amélioration acoustique des navires de pêche ne se pose pas de la même façon, selon la taille et le type de bateau.

Dans tous les cas, il doit être abordé DES LA CONCEPTION du navire, et particulièrement au moment du montage du moteur principal.

- Divers points sont importants pour la réduction du bruit :
- . choix du matériau pour la coque (acier, bois, fibre de verre),
 - . choix du moteur,
 - . type de longerons du bâti moteur,
 - . choix de la suspension (souple ou solide),
 - . dégagement de l'hélice,
 - . choix du système d'échappement (vertical, direct ou à injection d'eau),
 - . isolation acoustique du compartiment moteur,
 - . isolation antivibratile systématique de toute la machinerie.

La conception d'un navire de pêche "silencieux" doit maintenant être abordée, et faire appel aux techniques antivibratiles les plus sophistiquées. Après une sensibilisation accrue des professionnels de la pêche aux problèmes acoustiques, un dialogue constructif doit s'instaurer entre eux et les chantiers navals, les industriels, les scientifiques, afin de prendre en compte les résultats significatifs présentés ci-avant.

R E M E R C I E M E N T S

La réalisation de ce travail n'aurait pu se faire sans le concours actif de la Direction des Pêches/Secrétariat d'Etat à la Mer, de l'ORSTOM/Département C, de l'IFREMER/COB statistique, du Comité Interprofessionnel du Thon, et de tous les Armements et Patrons qui ont accepté de donner leur concours, ainsi que les organisations professionnelles CCPM et UAPP.

BIBLIOGRAPHIE

- [1] TAVOLGA, W.N., POPPER, A.N., FAY, R.R., 1981 (Eds).
"Hearing and sound communication in fishes".
Springer Verlag, New-York.
- [2] IVERSEN, R.T.B., 1967.
"Response of yellowfin tuna (Thunnus albacares) to underwater sound".
In : Marine Bio-Acoustics, Vol 2, 105-121, TAVOLGA, W.N. (Ed)
Pergamon Press, Oxford.
- [3] IVERSEN, R.T.B. 1969.
"Auditory thresholds of Scombrid fish: Euthynnus affinis,
with comment on the use of sound in tuna fishing".
FAO Fish REP., 62, (3), 849-859.
- [4] ERICKSON G.J., 1979.
"Some frequencies of underwater noise produced by boats
affecting albacore catch".
J.A.S.A., Vol 66 (1), 296-299.
- [5] DEPOUTOT C., 1983.
"Typologie acoustique des germoniers français en liaison
avec leurs captures. Etude préliminaire".
Rapport GERBAM. Thèse ENSA/Rennes.
- [6] BERCY C., 1984.
"Campagne germonière 1983. Synthèse de l'étude acoustique
menée sur 65 bateaux de la flottille de pêche".
Rapport GERBAM. Université P. et M. Curie.
- [7] BERCY C., MEPHON D., DEPOUTOT C., 1984.
"Etude statistique de la flottille germonière vendéo-bretonne.
Analyse factorielle des caractéristiques des bateaux en
liaison avec leurs performances et qualité acoustique".
Rapport GERBAM. Université P. et M. Curie.

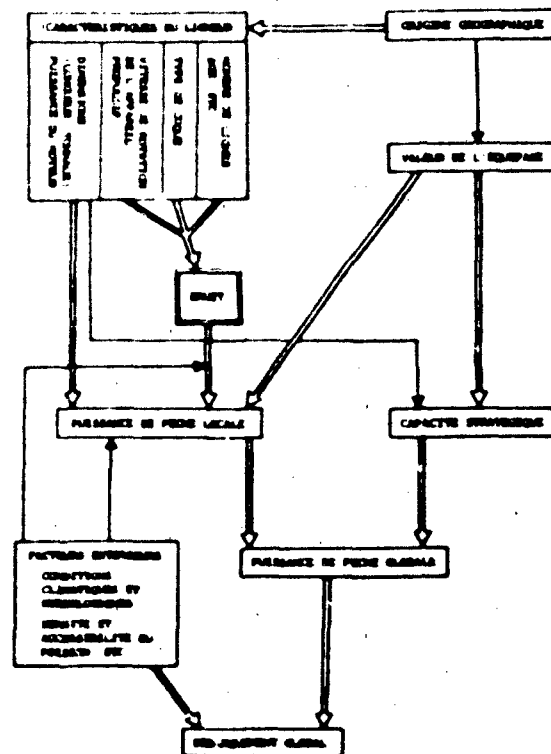


Figure 1

Paramètres influant sur les performances de pêche d'un thonier ligneur.

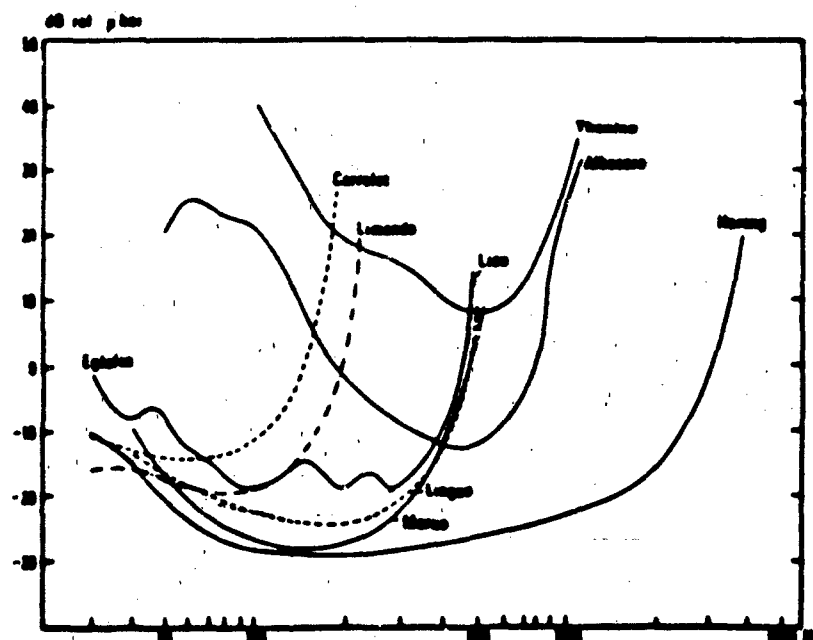


Figure 2 : Audiogrammes de quelques espèces intéressant la pêche
 Thonine et Albacore : d'après IVERSEN (1967, 1969)
 Limande et Carrelet : " CHAPMAN et SANO (1973)
 Lingue, Lieu, Eglefin : " CHAPMAN (1973)
 Merlu : " CHAPMAN et HAWKINS (1974)
 (les niveaux de pression sonore sont établis à 1m et pour 1Hz).

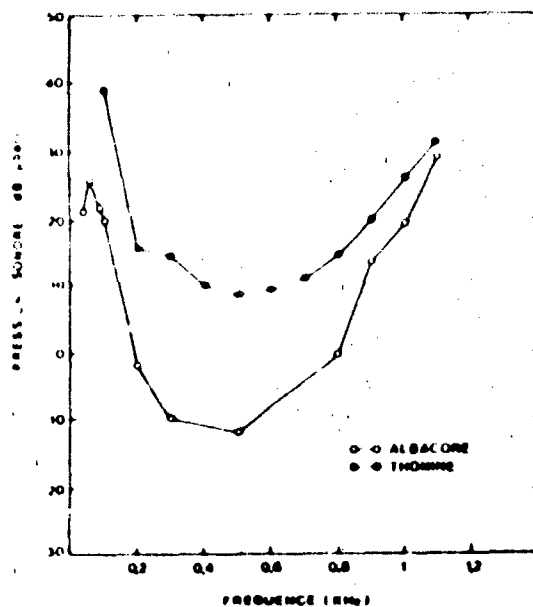


Figure 3

Algorithme de l'Albacore (*Thunnus albacares*) et de la
Thonier (*Thunnus albacares*) d'après IVERSEN (1967, 1969)
Niveau en dB pbar/MHz 2.

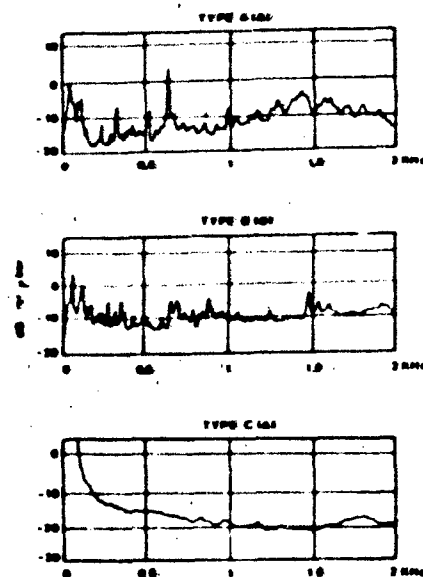


Figure 4

Classement des spectres des thoniers selon
la typologie A, B, C. (les niveaux sonores
sont ici à 35m de l'hydrophone, on obtient
le niveau à 1m en ajoutant 30dB).

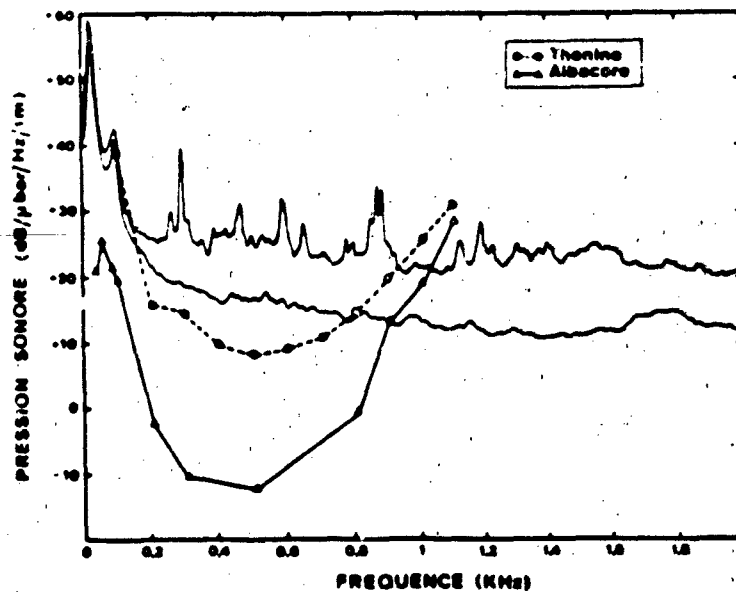


Figure 5 : Perception du bruit des navires par les Thoniers.

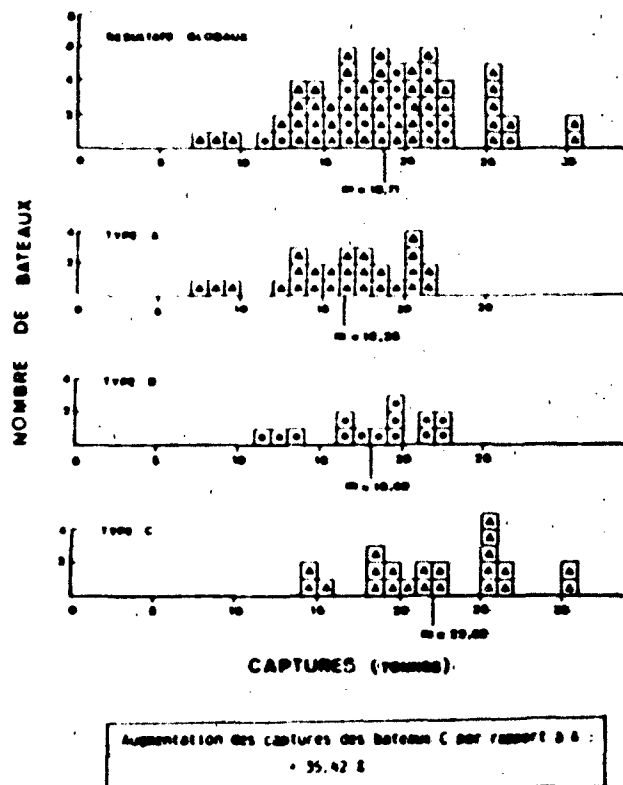


Figure 6 : Histogramme des captures des germoniers par type de spectre (marées 1983).

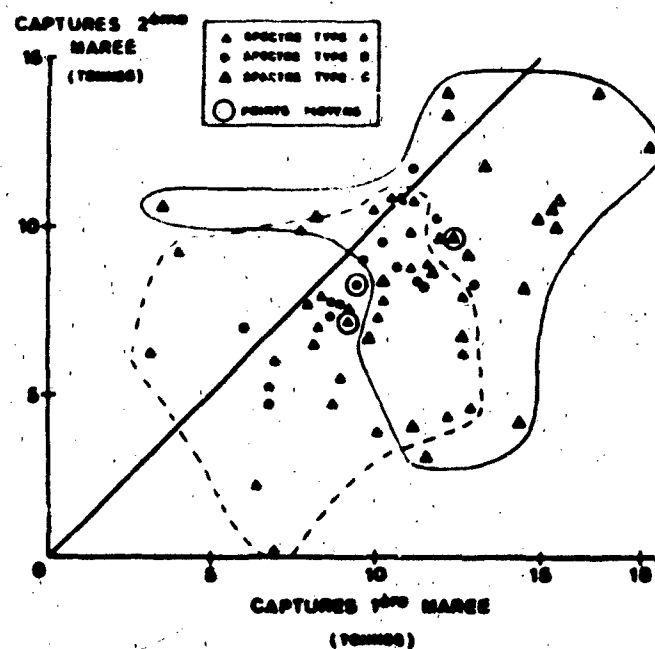


Figure 7 : Corrélation entre les captures des première et deuxième marées 1983.

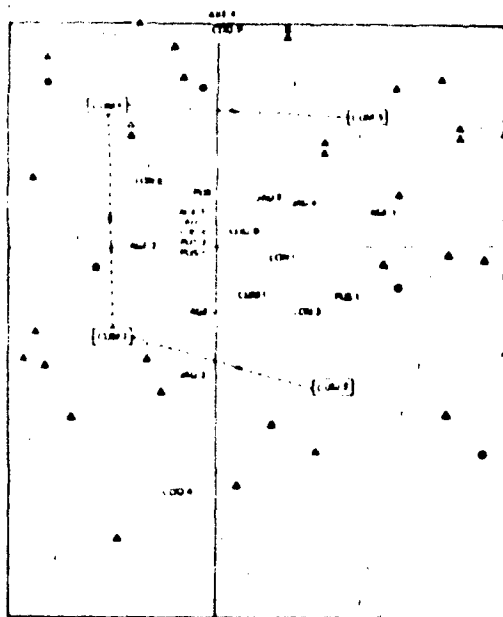


Figure 8
Analyse factorielle de la flottille germonière

	CUR 1	CUR 2	CUR 3	CUR 4	CUR 5
A	50.5	55.5	36.5	40.5	0.5
B	25.5	27.5	27.5	30.5	0.5
C	17.5	18.5	36.5	30.5	0.5
	100.5	100.5	100.5	100.5	100.5

Figure 9

Catégories de résultats de pêche
en fonction du type de spectre.

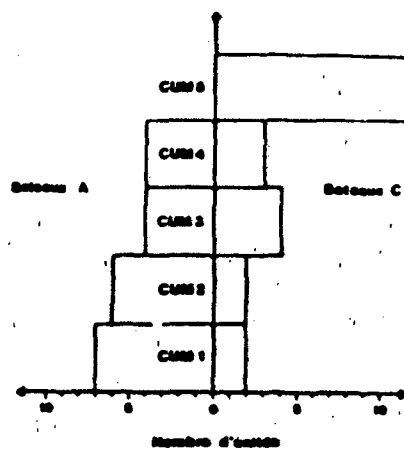


Figure 10

Proportion de bateaux ayant un spectre de
type C dans les cinq classes de captures.

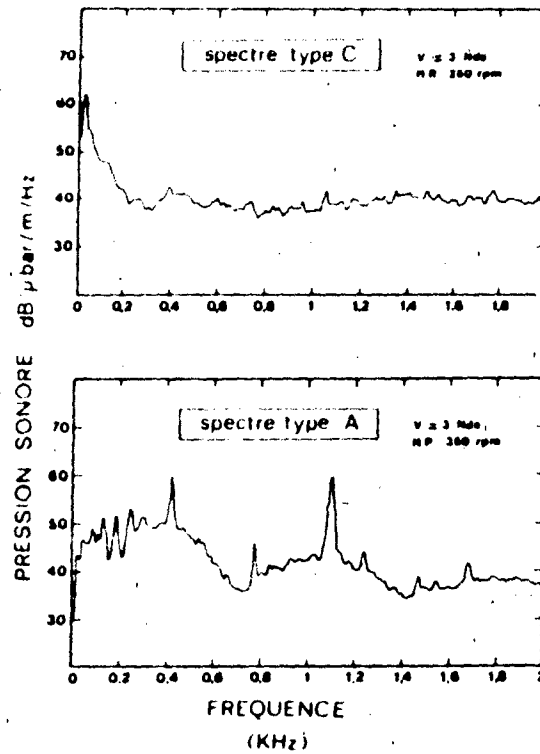
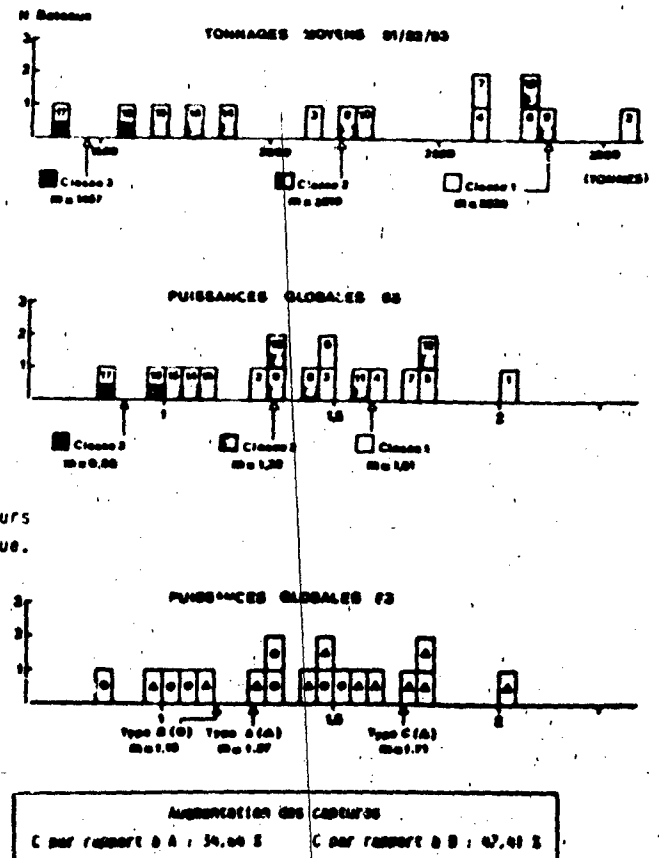


Figure 11

Spectres A et C de deux thoniers senneurs en vitesse d'approche de bancs.

Figure 12

Résultats de pêche des thoniers senneurs en liaison avec leur qualité acoustique.



DISCUSSION

J. H. Janssen (Netherlands): Just to be sure: What were the distances at which the underwater noise spectra were measured? Were they measured in deep water and under the ship?

C. Bercy: The underwater noise spectra were measured at approximately 50 m for the tuna line-fishing boat and at 100 m for the tuna trawler fishing boat. Our apparatus was located in a stationary rubber launch (Zodiac), with the fishing boat circling around the launch. All records were made in the Atlantic (Azores or Gulf of Guinea) in a water depth of 4000 m. Our hydrophone was placed 5 m below the launch. The levels presented in micropascals were at these distances.

B. Schmalfeldt (Germany): Did you correct the radiated noise spectra you showed to 1 m distance?

C. Bercy: The radiated noise of each fishing boat was measured at approximately 50 m (line) or 100 m (trawl). The distance was measured using an optic telemeter (precision ± 5 m). Except for Fig.3, where the levels are referenced to 1μ bar/1 m, the spectra were not corrected to 1 m but were referenced to 1μ Pa. Because we are mainly interested in relative noise levels between three kinds of spectra (type A, B or C) it is not of prime importance to correct noise spectra to 1 m.

THE IMPLICATIONS OF A SILENT SHIP FOR THE INVESTIGATION OF LOW-FREQUENCY
ACOUSTIC/SEISMIC PROPAGATION

by

Hassan B. Ali
SACLANT ASW Research Centre
La Spezia, Italy

ABSTRACT

In certain circumstances the energy emitted from a sound source, including a ship, may travel more readily in the sea floor, as a seismic wave, than in the water column itself. This is particularly true in those cases, such as encountered in shallow water propagation, in which a "cut-off" frequency exists, below which acoustic "propagation" as such does not exist in the water column. The energy in the bottom, on the other hand, contains a potential wealth of information, in the form of seismic interface waves, on both the feasibility of the bottom as a propagation path and on the properties of the bottom itself. The use of a ship to investigate this important regime is, however, complicated by the interference caused by the radiated noise of the ship. The present paper discusses some aspects of very-low-frequency acoustic/seismic propagation and the potential value of a silent ship in the investigation of the latter. Following a brief overview of the ambient noise spectrum in the ocean, including the contribution of ship noise, some comments are made on the effects of the sea bottom on low-frequency propagation. This is followed by a discussion of measurement techniques found useful at SACLANTCEN (and elsewhere) to investigate the propagation of seismic (interface) waves. It is shown that a good deal of useful information has been obtained from these measurements. Nevertheless, questions remain. The role of a silent ship in resolving some of these questions is discussed. In particular, a silent ship can be an invaluable asset in the investigation of such important items as the coupling between the sound source and sea bottom, the ambient noise directionality (using an array of seismic sensors), and the area-dependent behaviour of interface waves. It is concluded that a silent ship will fill a need in the very low frequency region of the noise spectrum of the ocean. Conversely, seismic sensing can provide a measure of what "silent" might mean in this regime.

INTRODUCTION

The propagation of underwater sound is, dependent on the circumstances, greatly affected by the properties of the sea bottom. This is particularly true for shallow water, or equivalently for low-frequency propagation, for which the interaction with the bottom increases with increasing wavelength. It has been known for several decades that shallow water propagation is

characterized by a wave-guide effect — that is, below a certain "cut-off" frequency, which depends primarily on water depth and relative sound speeds, effective acoustic propagation does not take place. Not surprisingly, therefore, underwater acousticians have, until recently, generally considered the regime below cut-off as acoustically uninteresting.

In recent years there has been a growing awareness that the energy in this domain, far from being "lost", contains a potential wealth of information in the form of propagation of seismic interface waves. These interface waves provide not only a "new" propagation path but, by virtue of their bottom-dependent behaviour, an opportunity to investigate the structure of the sea bottom. The knowledge of the existence and properties of these interface waves is hardly new, going back to at least Rayleigh. Moreover, seismologists and geophysicists are quite familiar with them as a source of "noise" to be eliminated from their data. From an acoustic viewpoint, however, the experimental investigation of interface waves is potentially very promising, albeit relatively recent.

For reasons that will emerge later, the most effective platform for studying these phenomena is a research ship. However, its use is a double-edged sword. As often happens in scientific investigations, the measuring techniques can distort the thing to be measured. In this case, the radiated sound from the research ship can contaminate the low-frequency acoustic and seismic propagation being investigated. Thus it is essential that an effective investigation of this area be performed with a silent ship. The purpose of the present paper is thus to examine some aspects of those areas in which the use of a silent ship is potentially most valuable and to suggest relevant measurements.

The subsequent presentation is therefore structured as follows. Beginning with a brief overview of the noise spectrum of the sea, the importance of the low-frequency acoustic/seismic regime is stressed. This is followed by some general comments on the nature of the problem posed by ships — i.e., the characteristics of their radiated noise. The effects of the sea bottom are then discussed within the general context of the propagation of sound in the sea. A quick look at the results of earlier measurements of waterborne/seismic propagation is followed by a discussion of relevant SACLANTCEN experiments. Finally, suggestions are made on the use of a silent ship to investigate those areas warranting further examination.

1 BRIEF SURVEY OF AMBIENT NOISE

Figure 1 <1> is the well-known Wenz curve of the sound-pressure spectrum levels of noise sources in the sea. The frequency regime of primary interest here is the infrasonic region, although, because of its effects on the latter, the region dominated by ship noise is also of interest.

Some aspects of this spectrum are not adequately understood, and the last word is yet to be said. However, the following observations relevant for this paper can be made based on this curve and more recent data:

1.1 Very-low-frequency (infrasonic) regime (<10 Hz)

The region below 10 Hz is dominated by oceanic turbulence and seismic activity, the spectral slope being approximately -8 to -10 dB/oct. We are interested primarily in the region greater than 1 Hz, since, among other reasons, the geophones we are using are generally insensitive below this frequency. However, the region below 1 Hz is in itself quite interesting (especially for seismologists) since it is by no means a "dead" region. In particular, the noise spectrum of microseisms below 1 Hz is characterized by two peaks occurring at about 0.07 Hz and 0.14 Hz, with an energy ratio of the peaks greater than 100. The smaller, primary peak, occurs at the primary frequency at which most ocean waves are observed and has been attributed to the action of waves on coasts (Wiechert, 1904, <2>). The larger, secondary peak, was explained by Longuet-Higgins in 1950 as due to the pressure on the sea bottom below standing ocean waves, which may be formed by waves travelling in opposite directions in a source region of a storm or near the coast. The resulting microseismic frequency is twice that of ocean waves (Aki and Richards, <2>). There is some agreement that primary microseisms derive from shallow waters, and secondary ones from either shallow water or deep water.

There is a great deal of evidence that microseisms propagate essentially as Rayleigh waves, although a Love-wave mode of propagation is not uncommon (Bath, <3>).

Seismic activity is by no means confined to frequencies less than a few hertz. On the contrary, its effects can be felt at frequencies in the hundreds of hertz (Wenz <1>; McGrath, <4>).

Measurements by Perrone <5> and subsequently by McGrath <4> suggest that wind-dependent noise is important in the region from approximately 1 to 4 or 5 Hz, but above this range distant shipping noise predominates in the infrasonic and low-frequency ranges. As will be seen later, relevant seismic measurements in this area are few and far between.

1.2 The Frequency Regime from approximately 10 to 300 Hz

Shipping is the dominant source in this region, the average noise levels having increased in recent years. The spectra in this range are very dependent on proximity to sea lanes and are characterized by tonals, since a major part of the excitation is rotating machinery of propulsion systems. The main sources of ship-radiated noise are well understood. The principal radiators are the propeller (cavitation noise, especially at shaft- and blade-rate frequencies), the hull, and machinery items.

Figure 2 schematically summarizes the frequency regimes of these components. The radiation mechanisms are understood well enough to allow simple predictions of gross levels in many cases. Figure 3, for example, presents a somewhat simplified view of these mechanisms particularly applicable to the behaviour of a slender body (e.g., a submarine).

The problems posed by shipping noise on the investigation of low-frequency acoustic/seismic investigations will become increasingly evident when we

subsequently discuss these investigations. However, some general observations can be made at this point. In particular:

- Pressure fluctuations in the ocean, including those arising from ships, do contribute to the seismic background noise in the sea. The converse, of course, is also true.
- Evidence exists that, at least for deep water, distant shipping noise dominates the infrasonic region at least down to 4 or 5 Hz <4, 5>.
- Since distant shipping noise is restricted primarily to refractive paths (multiple-reflected signals are greatly attenuated) the noise intensity in the low-frequency band is significantly higher for angles close to the horizontal plane (about $\pm 15^\circ$).
- Nearby ship passages affect lower frequency infrasonic noise levels earlier and for longer periods than higher frequencies <4>.
- Because of the greater absorption effects on higher frequencies, the radiated noise from a nearby ship covers a far greater frequency band than that of distant shipping.
- Directionality effects on a received level are influenced not only by the propagation distances involved but also by the directivity pattern of a nearby ship's acoustic radiation.

In short, one arrives at the important, albeit somewhat obvious conclusion, that if a ship is to be used in investigations in the infrasonic region, then either the ship be relatively silent or effective methods be employed to separate the signal and noise. As will be seen, this separation is not always possible in the very-low-frequency acoustic/seismic case since noise and signal have similar propagation characteristics.

2 THE EFFECTS OF THE SEA BOTTOM ON LOW-FREQUENCY SOUND PROPAGATION

In order to place in its proper perspective the discussion on seismic interface waves, it is necessary to briefly review some well-known aspects of sound propagation. The interest here is primarily on shallow water propagation. By "shallow-water" we shall generally mean depths less than an order of magnitude or so of the acoustic wavelengths involved. Implicit in the use of the term shallow water is significant interaction of a propagating signal with the bottom and surface boundaries. The likelihood of bottom interaction is determined largely by the sound-speed profile, whereas the degree to which the signal is affected by the interaction is dependent upon signal frequency, signal-to-noise ratio, grazing angle, and bottom properties (particularly absorption coefficient).

Generally, a negative gradient in sound-speed profile (as in summer conditions) leads to a greater likelihood of bottom interaction and, hence, greater bottom losses. The experimental results of Akal in Fig. 4 <6>, illustrate this effect quite clearly.

Figure 5, also due to Akal, demonstrates the effect of water depth on propagation loss. As seen, the shallower the water, the greater the losses and the higher the optimum frequency of propagation. This is because bottom interaction increases with increasing ratio of wavelength to water depth.

The effect of the type of bottom is well illustrated by Fig. 6, from Akal and Jensen <7>. The figure shows the predicted (FFP model) transmission loss at 10 km for various bottom types arising from a sound source located at a depth of 50 m in 100 m isovelocity (1500 m/s) water. The geoaoustic parameters used in the model are shown in Table 1.

TABLE 1
GEOACOUSTIC PARAMETERS FOR DIFFERENT BOTTOM TYPES

Bottom Type	Density (g/cm ³)	Compress. speed (m/s)	Shear speed (m/s)	Compress. attenuation (dB/λ)	Shear attenuation (dB/λ)
SILT	1.8	1600	200	1.0	2.0
SAND	2.0	1800	600	0.7	1.5
LIMESTONE	2.2	2250	1000	0.4	1.0
BASALT	2.6	5250	2500	0.2	0.5

Several features of interest are noted. With the exception of basalt, the propagation is seen to be divided into two regions: the high-frequency region (5 Hz and above) represents the waterborne path; the region below about 5 Hz represents the seismic path. It is well-known from the work of Rauch and Schmalfeldt <8>, among others, that the sound in the lower region propagates essentially in the form of interface waves. Thus seismic interface waves offer an important propagation path below the cut-off frequency of waterborne propagation.

3 PROPERTIES OF INTERFACE WAVES

Interface waves, also called surface waves, are so-named because their exponentially decaying amplitude away from the interface between a solid and another medium effectively restricts them to the immediate vicinity of the interface. Since these waves depend on shear properties for their existence, at least one of the interface media must be a solid. The other medium can be vacuum, liquid, or solid, the corresponding interface wave being denoted a Rayleigh wave, a Scholte wave, or a Stoneley wave, respectively, as indicated in Fig. 7. Additional relevant characteristics of interface waves are the following <8>:

- a. Particle motion is confined to the radial/vertical plane (with respect to source/receiver direction and guiding interface). Thus there is no transverse deflection.

b. There is a high coherence and stable phase shift of about $\pi/2$ between the radial and the vertical ground displacements, resulting in highly regular elliptical orbits or hodographs.

c. The bottom pressure in the water column and the vertical particle velocity are characterized by phase relations similar to those in (b). The ratio of these quantities is proportional to the bottom impedance.

d. The energy carried in these waves decreases exponentially in the direction perpendicular to the interface, the "penetration depth" being characterized, roughly, by one wavelength. Due to this confinement by the interface, it is quite obvious that the excitation of this wave type improves as the source is located closer to the interface.

e. The associated phase velocities are usually of the order of 100 to 200 m/s and always less than the sound speed in the water column and the shear velocity in the bottom (these velocities are to be considered as frequency-dependent average values weighted over the length of the penetration depth).

The outlined propagation characteristics are mainly affected by the geoaoustical properties of the upper sediment layers and have generally been studied in connection with experiments in which the interface waves were excited by explosive charges detonated close to the bottom. Nevertheless, the characteristic behaviour of these waves is not predicated upon their excitation by any particular type of source. It is this fact that can lead to difficulties in separating "signal" from "noise", as will become evident subsequently.

4 PREVIOUS RELEVANT EXPERIMENTS

Although these characteristics have been known for some time, only recently has there been a recognition of their potential value in the investigation of sound propagation in the bottom. Experiments performed to ascertain the relative merits of waterborne versus seismic paths have not been entirely successful. Table 2 <9> summarizes some of these earlier measurements. A few general observations are in order.

A great deal of useful information was obtained from these measurements; nevertheless, a number of shortcomings are evident in these results. With few exceptions, there appears to be a general lack of awareness of the important role played by interface wave propagation. Although the seismic detection of waterborne sounds was the primary objective of many of these measurements, this was not clearly demonstrated. Further, a number of apparent contradictions were observed between the various experimental results. For example, in particular situations the signal-to-noise ratios of hydrophones were either higher or lower than those for geophones. That is, the "seismic gain" was not consistently positive or negative, but varied from experiment to experiment as well as for geophone orientation. However, it is probably misleading to consider these results to be contradictory, since such a view assumes, implicitly, that these various sensors were responding to identical phenomena. It is difficult to

substantiate such a view for at least two reasons: inadequate understanding of the acoustical characteristics of the sea bottom, and differences in sensor dynamics and/or sensor-to-medium coupling. In particular, some of these measurements did not include any information on seismic ambient noise, let alone its directionality. Further, often neither the structure of the bottom nor the nature of the sensor-to-medium coupling were adequately known. Without this information, the relative merits of waterborne and bottom paths for detection can be little more than conjecture. Further discussions on this question are given in <9>.

It will suffice, at this point, to give two examples of the differences in response arising solely from different sensor-to-medium coupling, (Hecht, <10>). Figure 8a shows the differences in background noise for measurements using a tripod-mounted geophone and one attached to a probe that penetrated the bottom. The probe geophone is much quieter and shows no response to the tide. Even at slack tide more than 6 dB reduction in background noise is obtained by the proper sensor implementation. Figure 8b shows a similar improvement in the signal response to an explosion of a probe geophone over that of a tripod-mounted geophone. The probe's trace is sharp and distinct in character and less noisy than that of the other geophone. It is thus not surprising that apparent contradictions have arisen in earlier results. In fact, unless the characteristics of the medium and its coupling to the sensor are better understood, contradictions will continue to appear.

5 THE SACLANTCEN MEASUREMENTS

The SACLANTCEN measurements have removed some of the preceding ambiguities, although questions still remain. A detailed discussion of these measurements is out of place here, and can, in any case, be found in <9>. A brief discussion is warranted, however.

Figure 9 illustrates a typical deployment of the measurement system. The ocean bottom seismometer (OBS) consists of a tri-axial geophone and an omni-directional hydrophone mounted outside the OBS or floating above it <11>. Since the digitized data from the OBS were transmitted to the receiving ship, normally the SACLANTCEN Research Vessel MARIA PAOLINA G. (MPG), as an fm-modulated, vhf signal, the MPG was anchored at a distance of approximately 1 km from the OBS unit. This required proximity of the MPG to the OBS is clearly a limitation if one is interested in investigating the background sound free from ship-interference. On the other hand, if it is the ship's noise that is to be seismically sensed, then this closeness increases the likelihood of such sensing. This is clearly illustrated by Figure 10, which shows the power spectral density of the horizontal (X) component of the geophone's response (solid line) compared with the background seismic noise. Over most of the frequency range shown, the ship's response is clearly higher than the ambient noise - particularly at 3 Hz, corresponding to the 180 rev/min shaft rate of the MPG.

The distribution of the power spectral density with azimuthal angle (bearing) is shown in Fig. 11. Although not evident here, the axis of the

dipole-like pattern points in the direction of the MPG, as explained in <9>. It is clear that the transverse component of the particle velocity is negligible compared with the radial component.

Further information on the mechanism and direction of the propagation is revealed by examination of the relevant coherence and phase spectra, shown in Fig. 12. Figure 12a shows the squared coherence between the radial and vertical components, $\rho^2_{R,z}$, while the corresponding phase spectrum $\phi_{R,z}$ is shown in Fig. 12b. As seen, a remarkably high value of approximately 0.9 is obtained for the squared coherence in the vicinity of the 3 Hz source frequency. Further, a reasonably stable phase shift of $+\pi/2$ is evident in the same frequency interval, the positive sign of this shift indicating propagation in the direction from the MPG to the OBS. Similar plots for the transverse component, not shown here, reveal insignificant coherence and phase behaviour in the same frequency interval. The corresponding hodograph, that is, the trace of the particle orbit in the radial/vertical plane, Fig. 13, shows the expected elliptical patterns.

Figures 11 to 13 confirm that the disturbance from the source to the OBS is propagated as a seismic interface wave. Several comments, as well as caveats, are in order concerning this result. On the one hand, it is clear that the presence of a nearby ship can seriously complicate the investigation of low-frequency acoustic/seismic phenomena. On the other hand, the seemingly obvious conclusion that waterborne sound sources can be seismically detected below cut-off frequencies must be tempered with other information. It is well-known, for example, that there is a correlation between the nature of the sea-bottom material and the propagation characteristics of interface waves. In fact, this characteristic behaviour allows one to use interface waves to study bottom properties. This suggests, however, that clear seismic detection of waterborne sounds in one particular location does not allow one to infer, a priori, similarly good detection in another area. This result has been demonstrated by Sevaldsen in a recent SACLANTCEN conference <12>.

Moreover, total reliance on the previously described properties of interface waves to resolve ambiguities is unwarranted. In particular, the use of these wave characteristics to separate signal from noise — regardless of which — is not as easy as might be thought. It has already been pointed out that the "natural" seismic background disturbances have been found to travel as interface waves. This has also been demonstrated by the SACLANTCEN measurements.

In particular, Fig. 14 shows, for the ambient noise, the squared coherence and phase between the vertical particle velocity and the bottom pressure in the water column. The very high coherence and stable phase shift of $\pi/2$ up to approximately 3 Hz suggests that the seismic ambient noise is propagating in the form of interface waves. Further evidence is provided by Fig. 15, which compares the measured seismic noise sensed by the tri-axial geophone with the predicted vertical and horizontal responses of interface wave propagation. [The measured response below 1 Hz (Fig. 15a) has been deleted since the geophones are insensitive in this region]. The predictions are based on SACLANTCEN's Fast Field Program (SAFARI), a completely modified version of the FFP model. The bulk wave shear attenuation assumed in the model was 0.25 dB/ λ , the same as the measured

interface wave attenuation. It turns out <13> that the replacement of interface wave attenuation for bulk shear attenuation is not unreasonable. On the other hand, several choices of compressional wave attenuation revealed little effect on the behaviour at the lower frequencies.

Figure 15 clearly suggests that the seismic ambient noise has a behaviour that is characteristic of interface wave propagation (the region below about 6 Hz in the theoretical result) and not of waterborne propagation. The qualitative agreement between these two plots is more striking if one takes into account the fact that the model assumes a rather specialized acoustic input (white noise), and, therefore, the source characteristics of the two cases are different. A brief investigation of the predicted responses for several ranges produced best agreement with the measured results for a source distance of 40 km. The inference that the sound sources of the measured data are therefore at a distance of 40 km is probably an unwarranted speculative jump, tantalizing though it may be.

It is therefore apparent that the separation between seismic signal and noise may not be a trivial task. Moreover, one cannot rely on presumed directionality characteristics of the signal to permit such a separation. It is well known that waterborne ambient noise does display directionality, often "pointing", as it were, in the direction of busy ports and the like. From what has been said before, it is not unreasonable to expect that seismic ambient noise, too, will display directionality. Therefore, in potential applications, this directivity must be determined, if not for its own sake, then in order that it be "subtracted" from the data to prevent possible confusion with whatever signal is to be sensed.

As a final point on the data, we would like to comment on a somewhat puzzling result from the SACLANTCEN measurements, concerning large differences in measured results even from the same area. In particular, up to 25 dB differences in very-low-frequency spectral density levels were observed between runs that differed, essentially, only in the aspect of the MPG relative to the receiving OBS. Propagation effects, induced by variations in sedimentary layering of the sub-bottom, appear to be a likely explanation. However, until the mechanisms whereby waterborne sound is converted into seismic waves are better understood, this explanation is merely conjecture. It is generally taken for granted that at those very low frequencies (less than 5 Hz) directivity effects should be negligible because of the presumed large wavelength. However, this view may, in fact, be erroneous, since the low frequency is offset by the very low phase velocity of interface waves. For example, for an interface wave travelling with a phase speed of 70 m/s at a 5 Hz frequency, the associated wavelength would be 14 m. A 14 m sound wave in water, on the other hand, would be associated with a frequency of 107 Hz. Put differently, directivity effects can be important in interface wave propagation at frequencies well below those required to observe similar effects in waterborne sound.

6 ACOUSTIC SPECIFICATIONS OF SACLANTCEN'S NEW RESEARCH SHIP

In the preceding it has been stressed, convincingly we hope, that ship-radiated noise can interfere with the investigation of low-frequency acoustic/seismic propagation. In view of all that has been said, the question of the degree of interference posed by SACLANTCEN's new ship begs itself. Regrettably, the question cannot be answered now. An examination of the proposed acoustic specifications of the new ship, Figure 16, helps explain why. As seen, the important region below 20 Hz is conspicuous by its absence. Therefore, it seems to me, if interest in this region is really genuine, high priority should be given to conducting a radiated noise survey in the frequency regime from 1 to 20 Hz. Such a survey would satisfy two needs. Apart from providing the low-frequency noise levels of the ship, it would - assuming the ship really is "quiet" in this regime - allow an effective test of the feasibility of seismically sensing low-level waterborne sounds. In other words, the ship could serve as a "calibration point", as it were, of the seismic sensing system.

The question still remains as to what radiated noise levels would cause interference with seismic measurements. This is a difficult question, requiring for its answer a realistic transfer function between waterborne sound sources and seismic responses in the bottom. However, this presupposes an understanding of the relevant coupling mechanisms. Or, at the very least, one needs realistic values of what Urlick calls the "seismic gain": the difference in decibels between the signal-to-noise ratio of a geophone and that of a hydrophone. But clearly this is precisely one of the unknown quantities that the investigation is attempting to understand. Nevertheless, based on the results of earlier measurements, and using predicted transfer functions such as shown in Fig. 15b, some very approximate answers may be obtained.

In a recent experiment, the response of a distant ship was monitored until the received signal recorded on the bottom-mounted hydrophone was barely perceptible above the background noise. Using this level, coupled with reasonable assumptions concerning the spreading loss and rate of shear attenuation of interface wave propagation, one arrives at the number 140 dB re μPa at 1 m as the source level at which one would expect interference with seismic noise measurements at 2 Hz. The calculation has assumed $10 \log R$ (cylindrical) spreading losses, a shear attenuation of $0.25 \text{ dB}/\lambda$, an interface wave phase velocity of 600 m/s and a ship distance of 10 km. The assumptions are believed to be "reasonable", not infallible. It is assumed, in particular, that a large part of the 10 km range is traversed through the bottom, that a phase velocity of 600 m/s is a conservative number, albeit somewhat larger than the usually measured numbers, and that the shear attenuation of $0.25 \text{ dB}/\lambda$ is most reasonable, since it agrees with measurements. At these low frequencies a 1/3 octave band correction is a subtlety unwarranted by the grossness of the other assumptions. It cannot be overemphasized that the resulting number is little more than an educated guess. The expectation of more precise numbers at this stage runs the risk of falling into the well-known trap of confusing precision with accuracy.

CONCLUSIONS AND RECOMMENDATIONS

An attempt has been made to indicate the importance of the low-frequency (infrasonic) regime for the investigation of acoustic and seismic propagation. An understanding of this area will not only clarify the conditions under which one can expect effective seismic sensing of waterborne sounds, but lead also to a reliable means of probing the structure of the sea-bottom. As already indicated, numerous unresolved questions remain in both areas.

It has been emphasized that a silent ship can play an essential role in this effort, particularly in the study of the nature of the ambient noise background and the mechanisms involved in coupling waterborne sounds into the sea bottom. By way of summary, a few comments are made on each area.

a) Seismic ambient background

Current knowledge of the nature of the seismic ambient background is inadequate. Among the items requiring further investigation are its directionality, statistics, fluctuations, the nature of its propagation, and its origin.

As already indicated, the determination of directionality is necessary to avoid confusion with the directivity of other sources, particularly that of a nearby ship. A single OBS unit is inadequate for this purpose. What is needed is an array of OBS units, as shown schematically in Fig. 17 <9>.

The statistics of seismic noise, including analysis of its temporal fluctuations, would help clarify some problems. Auto- and cross-spectral densities between several OBS units would be most helpful in this analysis, providing coherence information as a function of sensor separation, among other things. Similarly, additional information on the nature and origin of interface waves would be useful. The Wenz curve <1> is somewhat qualitative in the very low infrasonic region. A correlation of results of seismic measurements in this region with a thorough analysis of shipping distributions would perhaps fill in some of the gaps. Currently, long-term seismic noise measurements are being conducted by SACLANTCEN's EAG group.

b) Coupling of waterborne sound into the sea bottom

From earlier results it is quite evident that the mechanism whereby originally waterborne sound is converted into an interface wave is poorly understood. This was exemplified by the large differences in measured results for ship runs that differed merely in relative geometry.

A step in the right direction would be to conduct an experiment using both fixed and towed sources, cw as well as explosive, to excite interface waves. Since interface waves are excited better the closer the source is to the bottom, towing sources at various depths, and also at several distances from the receiving OBS, would allow one to study some aspects of

the coupling. Naturally, such a thorough study should be conducted in several areas characterized by different bottom structures.

The comparison of the responses of geophones and both bottom-mounted and free-field hydrophones to sources with clearly understood characteristics (e.g., cw sources) would enable the measurement of seismic gain and thereby provide some information on the acoustic-source/seismic-response transfer function.

REFERENCES

1. WENZ, G. M. Acoustical ambient noise in the ocean: spectra and sources. Journal of the Acoustical Society of America, 34, 1962: 1936-1956.
2. AKI, K. and RICHARDS, P.G. Quantitative Seismology: theory and methods, Vol. 1, San Francisco, CA, W.H. Freeman and Company, 1980.
3. BATH, M. Spectral Analysis in Geophysics. Amsterdam, The Netherlands, 1974.
4. McGRATH, J.R. Infrasonic sea noise at the Mid-Atlantic Ridge near 37°N. Journal of the Acoustical Society of America, 60, 1976: 1290-1299.
5. PERRONE, A.J. Infrasonic and low-frequency ambient noise measurements on the Grand Banks. Journal of the Acoustical Society of America, 55, 1974: 754-758.
6. AKAL, T. Sea floor effects on shallow-water acoustic propagation. In: Kuperman, W.A. and Jensen, F.B. eds. Bottom-Interacting Ocean Acoustics. Proceedings of a conference held June 9-12, 1980 at the NATO SACLANT ASW Research Centre, La Spezia, Italy. New York, NY, Plenum Press, 1980: pp. 557-575.
7. AKAL, T. and JENSEN, F.B. Effects of the sea-bed on acoustic propagation. In: Pace, N.G. eds. Acoustics and the Sea-bed. Proceedings of an Institute of Acoustics, Underwater Acoustics Group Conference held at Bath University on 6-8 April, 1983. Bath, U.K. Bath. Bath University Press, 1983: pp. 225-232.
8. SCHMALFELDT, B. and RAUCH, D. Explosion-generated seismic interface waves in shallow water: Experimental Results, SACLANTCEN SR-71, La Spezia, Italy, SACLANT ASW Research Centre, 1983. [AD A 134 551]
9. ALI, H.B. and SCHMALFELDT, B. Seismic sensing of low-frequency radiated ship noise, SACLANTCEN SR-77, La Spezia, Italy, SACLANT ASW Research Centre, 1984.
10. HECHT, R.J. Background of the problems associated with seismic detection of signal sources in the ocean. In: Proceedings, workshop on seismic propagation in shallow water, 6-7 July, 1978, Arlington, Va., Office of Naval Research, 1978: 1/1-1/23. [AD A 063 163]

11. BARBAGELATA, A., MICHELOZZI, E., RAUCH, D., and SCHMALFELDT, B. Seismic sensing of extremely-low-frequency sounds in coastal waters. In: Institute of Electrical and Electronics Engineers, Acoustics Speech and Signal Processing Society. Proceedings, IEEE International Conference on Acoustics, Speech and Signal Processing, (ICASSP 82) Paris, France, 3-5 May 1982. Piscataway, N.J., IEEE Service Center, 1982: pp. 1878-1881.
12. SEVALDSEN, E. Low frequency seismic and hydroacoustic noise measurements in a Fjord. In: Wagstaff, R.A. and Bluy, O.Z. eds. Underwater Ambient Noise. Proceedings of a conference held at SACLANTCEN on 11-14 May 1982. La Spezia, Italy, SACLANT ASW Research Centre, CP-32, Pt 1, 1982: 4-1 to 4-25.
13. SCHMIDT, H. SACLANT ASW Research Centre, La Spezia, Italy. Private communication.

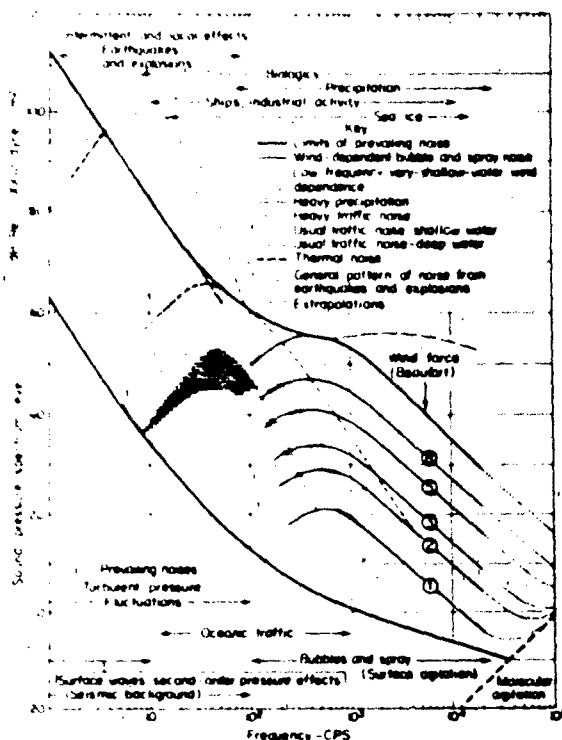


Fig. 1
Ambient noise spectra in the
Ocean (after <1>)

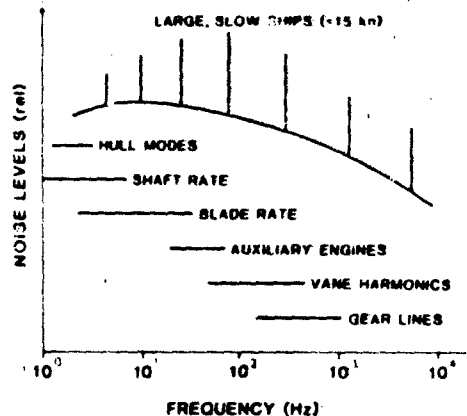


Fig. 2
Generalized spectrum of radiated
ship noise

Frequency	Structural Behaviour	Acoustic Radiation
Very low (1 Hz)	Rigid Body	Dipole
$\lambda = l$	Beam Flexural Modes	Distributed Simple
$\lambda = l/2$	Accordion Modes	Sources
$\lambda = R$	Cylindrical Shell Modes	Orthotropic Plate
$\lambda \ll R$ (70 Hz)	Compartment Vibration	
	Frame Vibrations	Ribbed Plate

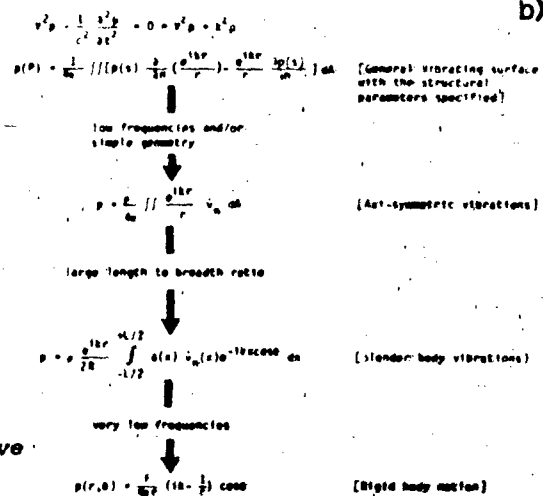


Fig. 3
Radiation mechanisms of a vibrating
body (a) qualitative (b) quantitative
representations

$$\nabla^2 u = 0$$

$$\nabla^2 p = 0$$

$$\left(\frac{\partial^2}{\partial t^2} \right) u = \text{low } \frac{\partial^2}{\partial t^2}$$

[Infinite,
thin vibrating
plate.]

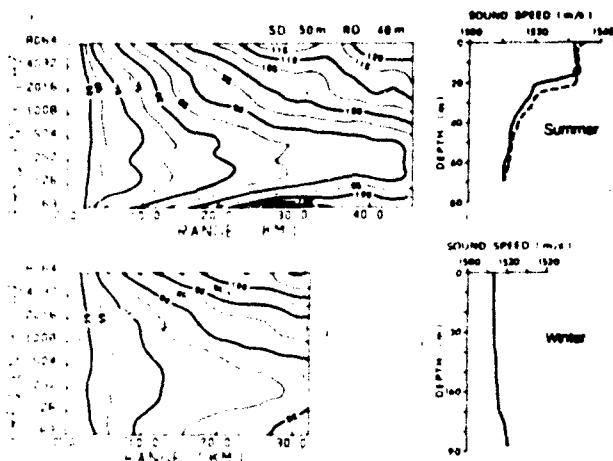


Fig. 4
Transmission losses measured over the
same propagation path under summer
and winter conditions (after <6>)

Table 1
Geoacoustic parameters for different bottom types

Bottom type	Density (g/cm ³)	Compress. speed (m/s)	Shear speed (m/s)	Compress. attenuation (dB/λ)	Shear attenuation (dB/λ)
SILT	1.8	1600	200	1.0	2.0
SAND	2.0	1800	600	0.7	1.5
LIMESTONE	2.2	2250	1000	0.4	1.0
BASALT	2.6	5250	2500	0.2	0.5

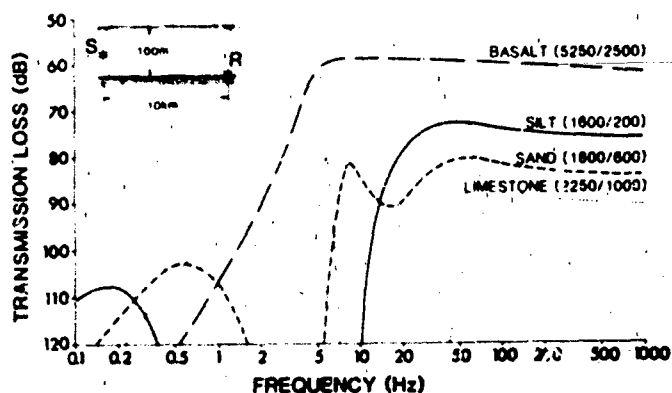


Fig. 6
Broadband propagation characteristics for
different bottom types. Numbers in
parentheses are compressional and shear
speeds, respectively. (after <7>)

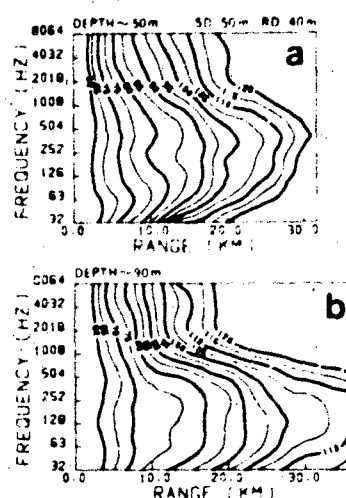


Fig. 5
Experimental evidence of the
effect of water depth on prop-
agation.
(a) 50 m water depth,
(b) 90 m water depth.
(after <6>)



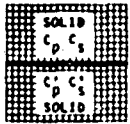
CLASS OF INTERFACE	TYPE OF FREE INTERFACE WAVE
VACUUM 	RAYLEIGH WAVE $C_R = n' C_S$ $0.873 < n' < 0.956$
LIQUID 	SCHOLTE WAVE $C_{Sch} = \min \left\{ \frac{C_p}{C_s}, \frac{C_s}{C_p} \right\}$
SOLID 	STONELEY WAVE $\max \left\{ \frac{C_R}{C_s}, \frac{C_s}{C_R} \right\} < C_S < \min \left\{ \frac{C_s}{C_s}, \frac{C_s}{C_s} \right\}$

Fig. 7
Classification of the basic
interface-waves, with an
estimation of their phase
velocities (after <8>)

Table 2
Selected previous measurements on waterborne/bottom-
path comparisons (after [9])

EXPERIMENTER	SOURCE(S)	SENSORS	WATER DEPTH (SOUND RANGE)
Worley & Wain (1943/1944)	Underwater explosion	Two hydrophones One uniaxial geophone (vertical component)	15 to 190 m 0.5 to 40 km
Worley & Walker (late 1950s)		Hydrophone Two axes (horizontal and vertical geophones)	27 m 0.5 to 40 km
Woods et al. (Columbia Univ.) (late 1950s) Krauth & Clay	Towed air source	Several uniaxial (vertical) geophones	118 to 593 m Up to 9 km
Melroy (1961)	Broadband air minesweeper source	One hydrophone One triaxial geophone	Shallow water 18 m Several km
Crick (1968)	Freighters and tankers	One hydrophone One triaxial geophone	18 m Up to 6 km
Melroy (1968)	Explosions air minesweeper source	Array of 7 triaxial geophones and six bottom-mounted hydrophones	20 m; 30 m 16 km 100 km
Schirmer (1976)	Explosions	Three tri-axial geophones	130 m 0.8-6 km
Easen et al (1977)	Explosions	Six tri-axial geophones	1 m 0.5-1.2 km
Lopez Island (1978)	Explosions and mechanical transients	12 seismometers One hydrophone 1 m above bottom 3 "standard systems"	6 to 7 m Variety of distances
Northrop (1979)	Explosions c/ projector	Hydrophones Triaxial geophones	"Deep" and "shallow" waters Up to 81 km

Table 2 (contd)

PARAMETERS	COMMENTS/CONCLUSIONS	EXPERIMENTER
Mainly 10 to 40 Hz some up to 100 Hz	(a) Results derived on the ground wave. (b) Limited quantitative information. (c) No background noise measurements.	Marshall-Paing (1943/1944)
15 to 25 Hz	(a) Zero seismic gain for vertical geophone. (b) Horizontal geophone failed. (c) Limited quantitative information.	Warner & Nelson (late 1950s)
10, 24, 40, 100 Hz	(a) No comparisons with hydrophones. (b) Propagation losses were or less consistent with spherical spreading.	Warner Lab, Columbia Univ (late 1950s Blain & Clay)
~ 10 to 700 Hz	(a) Up to 20 dB seismic gain for horizontal geophones; zero seismic gain for vertical geophones. (b) Scholte wave detected.	McLennan (1960)
~ 25 to 300 Hz	(a) 5 to 10 dB seismic gain for horizontal geophones; 0 dB seismic gain for vertical geophones.	Yeh (1968)
2 to 1000 Hz	(a) High seismic gain for all geophones. (b) S/N for radial and vertical geophones higher than those for transverse geophones.	McLennan (1976)
4.5 Hz	(a) Scholte wave detected in range 3.5-5.5 Hz; its attenuation measured (≈ 7 dB/km). (b) Response of vertical geophone much greater than that of either horizontal geophones. (c) No hydrophone measurements.	Schiermeier (1976)
4.5 Hz	(a) Two groups of dispersive Rayleigh waves were observed at ~ 4 Hz. (b) For both groups, transverse geophone response was much smaller than either of other two components. (c) Radial/vertical geophone responses were different for the two wave groups.	Essex et al (1977)
< 100 Hz	(a) Hydrophone data simpler than geophone data. (b) Seismic ambient noise propagated as dispersive Scholte waves.	Lopez Island (1978)
< 50 Hz	(a) For short ranges (< 10 km), 5 to 8 dB seismic gain. (b) Propagation and noise greatest in radial direction. (c) Generally, transverse geophones and buried hydrophones had highest S/N.	Buchrop (1979)

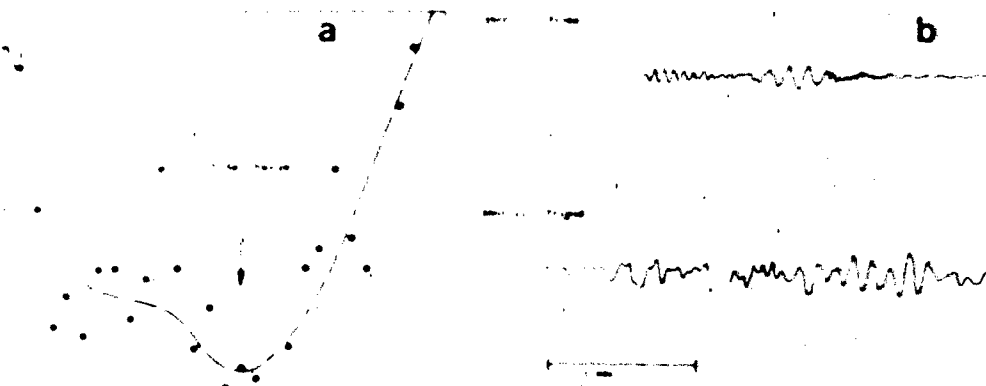


Fig. 8
Comparative responses of probe- and tripod-mounted geophones (a) background noise measurements, (b) explosive source (after <10>)

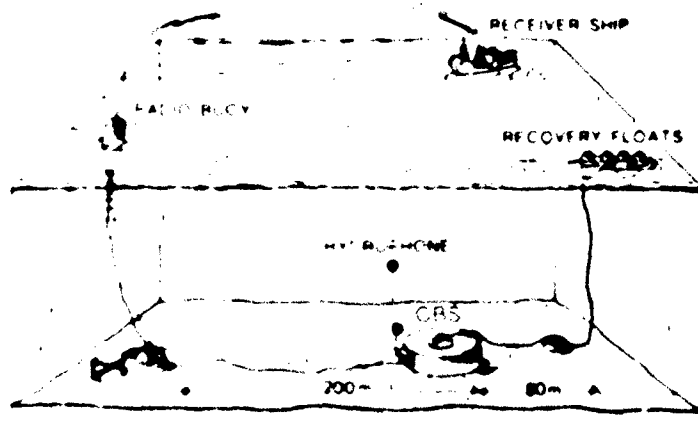
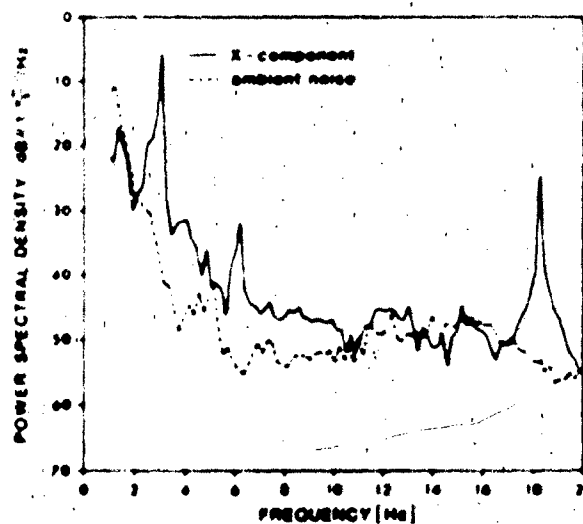


Fig. 9
Deployment of the SACLANTCEN system (after <11>)

Fig. 10
Power spectral density and background seismic noise recorded by the horizontal component of the geophone (after <9>)



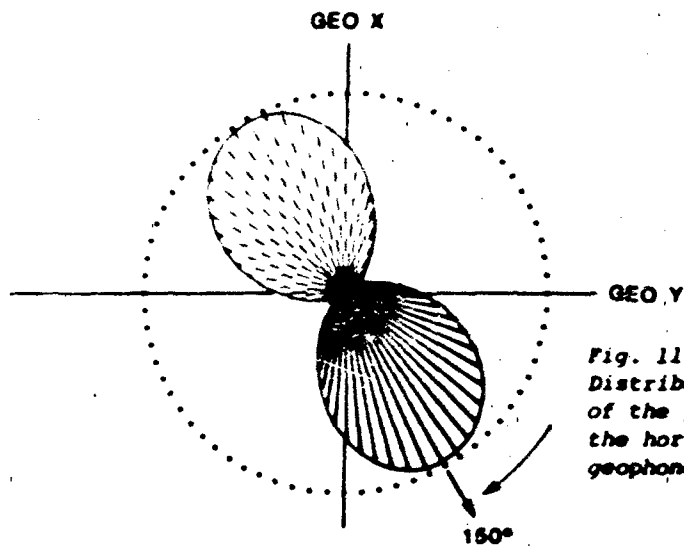


Fig. 11
Distribution with azimuthal angle
of the power spectral density of
the horizontal component of the
geophone (after <9>)

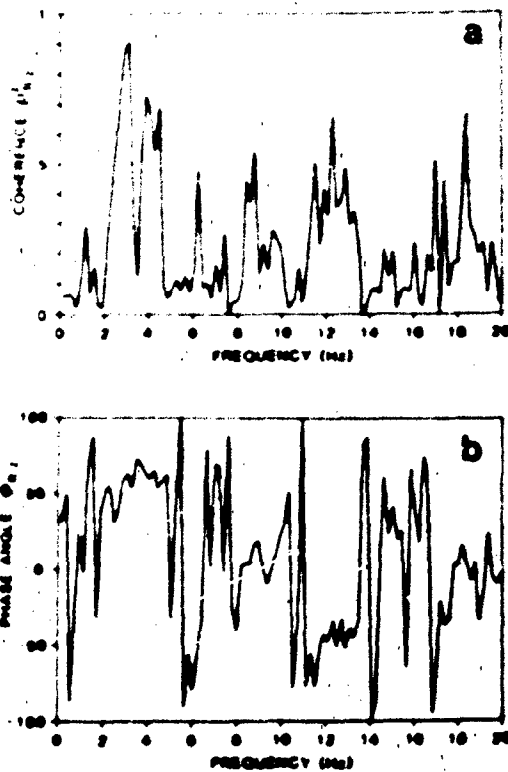


Fig. 12
Coherence and phase spectra between
the radial and vertical components
of the geophone, (a) squared coher-
ence (b) phase angle (after <9>)

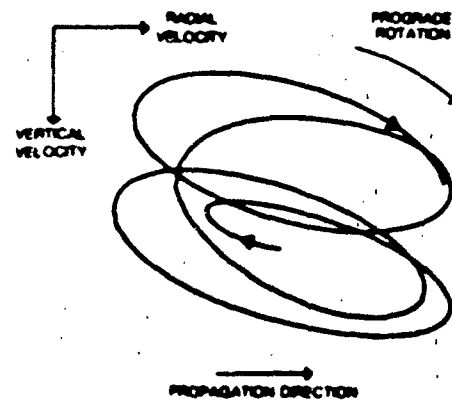


Fig. 13
Trace of the particle orbit
(hodograph) in the radial/
vertical plane at the 3-Hz
source frequency (after <9>)

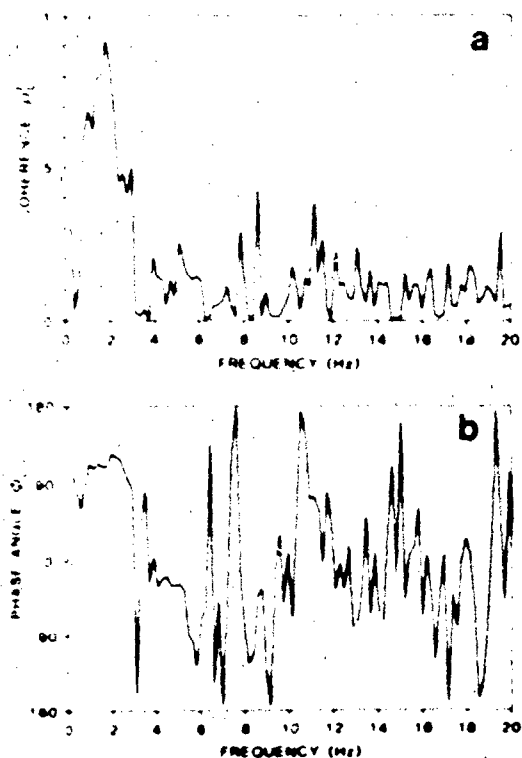


Fig. 14

Coherence and phase spectra between the radial particle velocity and the bottom pressure in the water column for the seismic ambient noise. (a) squared coherence (b) phase angle (after <9>)

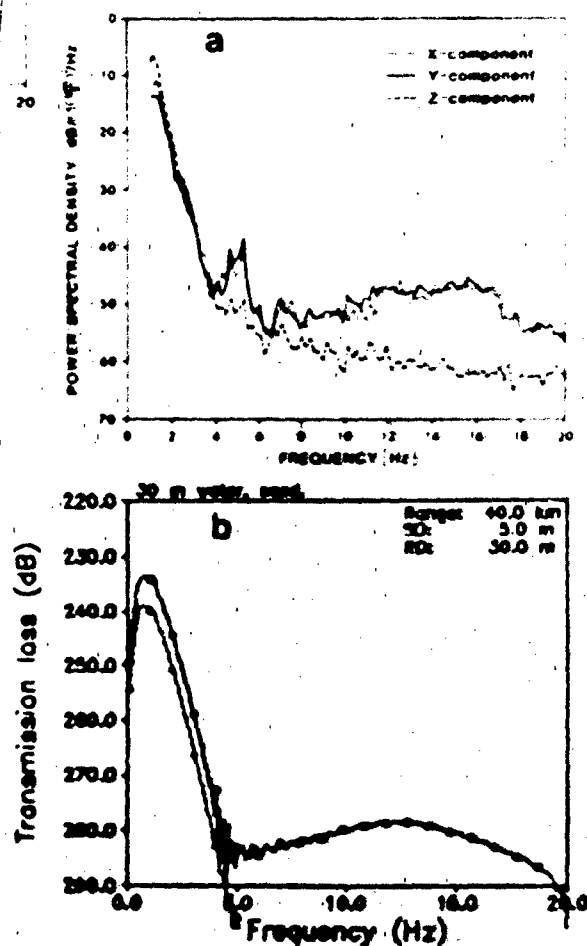


Fig. 15

Comparison of measured and predicted seismic response (a) measured seismic ambient noise (after <9>) (b) predicted (SAFARI) vertical and horizontal interface-wave components

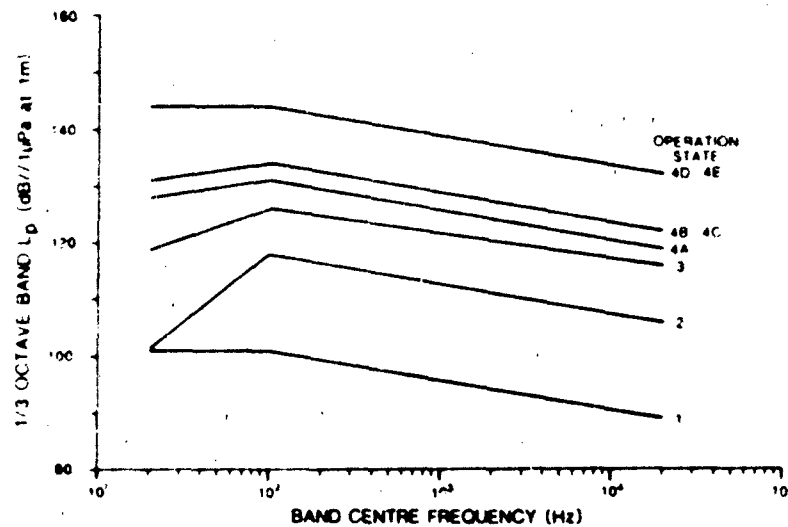


Fig. 16
Proposed underwater radiated noise specifications for
SACLANTCEN's new research ship

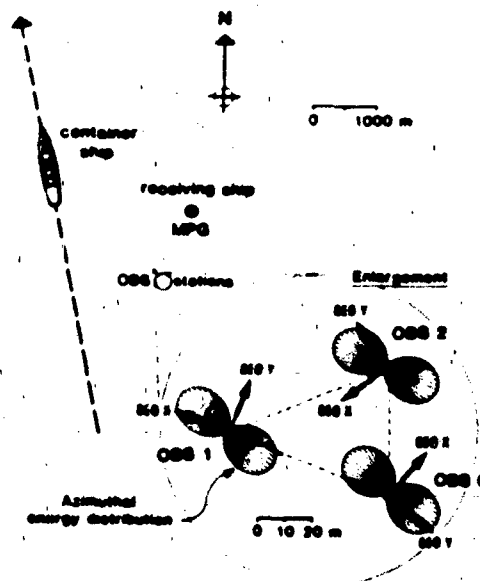


Fig. 17
Array of OBS units in a recent
SACLANTCEN experiment (after <9>)

DISCUSSION

B. Ratine (France): Is it possible to calibrate your sources and sensor at such very low frequencies?

H. Ali: Our geophones are calibrated in the laboratory using very low frequency exciters (shake tables), as is done in accelerometer calibrations. The geophones we use are quite sensitive down to about 1 Hz, below which there is a rapid drop-off in sensitivity.

B. Schmalfeldt (Germany): Usually you calibrate the OBS system on a shake table, which we have not done yet. I know that there is a facility for this at the Centre Oceanologique du Bretagne (COB) in Brest (France).

NEAR FIELD PROPELLER RADIATED NOISE MEASUREMENTS:
MODEL AND FULL SCALE EXPERIMENTAL DATA COMPARISON

by

Lucio Accardo, (CDR.IN), MARICONAVARMI, MDM, Roma
Agostino Colombo, CETENA, Genova

ABSTRACT

The ever rising interest related to the underwater noise originating from cavitating propellers prompted the Italian Navy to study this aspect of naval architecture in an experimental way.

This was accomplished carrying out extensive model tests in the Italian Navy cavitation tunnel (CEIMM) and full-scale tests in cooperation with CETENA.

This paper outlines the measuring technique the acoustic behaviour of the cavitation tunnel as well as the measuring technique and analysis of full scale tests carried out with hull-mounted hydrophones.

Some problems arising from both these kinds of measurements and their analysis methodology are highlighted. A technique to take account hull boundary and hull vibrations, during full-scale tests, is also discussed.

Finally some results of "near field" propeller noise, obtained from both model and full-scale measurements, are shown and compared.

INTRODUCTION

The noise radiated by the external elements of the ship's propulsion system and in particular by the propeller can become predominant and representative of the global noise level if the operative conditions of the propeller are such as to cause inception and development of cavitation phenomena on its blades /1/.

Under these conditions, the propeller radiates directly into the flow a noise level, which not only consists of a certain number of distinct lines in

the low frequency range (linked to the blade frequency and to its multiples), but also becomes predominant in the whole field of high frequencies which are essentially related to cavitation phenomena.

It therefore appears obvious how important the propeller is in the "acoustic signature" of a ship and thus in the possible identification of the ship itself by modern detection systems of underwater weapons.

In this light one of the main aims of the measurements carried out by means of hydrophones, located at the ship stern above the propeller disk, consists in defining both this source of noise and its levels related to the various operative conditions of the ship.

The problem of propeller radiated noise is furthermore considered to be a subject for experimental research at cavitation tunnels world-wide and in particular at the Italian Navy Cavitation Tunnel /2/.

The present method of recording and analysing noise data at this specific tunnel has been established as a result of numerous tests, carried out both on two-dimensional foils as well as on propeller models in order to optimise the calibration of the adopted measurement set-up and essentially to investigate the effects, in terms of acoustic noise, which the inception of the various types of cavitation involve /3/, /4/.

One of the aspects which is still under investigation in this model experimental research is a univocal definition of the parameters able to formulate correct transfer laws, from model to full-scale conditions, of the noise level generated by the propeller.

To this purpose and independently of the various solutions to this problem formulated by different researchers, the availability of full-scale experimental data of the quantities under review, provides a useful opportunity to verify the prediction laws adopted.

This report describes the testing methodology and the setting-up of the tests, used both in model and full-scale conditions.

Some of the results obtained from this experimental investigation are described below.

1 TESTING METHODOLOGY AND SETTING UP OF INSTRUMENTATION

1.1 FULL-SCALE MEASUREMENTS

The usual assessment of this kind of test consists in installing some (generally two) hydrophones at the hull bottom above the propeller disc as well as a number of pressure transducers (4-6) and a number of accelerometers located in proximity of the hydrophones themselves.

The hull transducers, used for noise measurements, are B&K hydrophones, type 8103 (the technical characteristics and relative response curve are well-known). The signal, via a B&K amplifier, type 2635, is visualized during the acquisition on an oscilloscope and recorded directly onto magnetic tape, "Scotch 3M" using a Nagra IVS.J. tape recorder (recording speed : 38 cm/sec).

The transducers used to measure the pressure induced on the hull are of the inductive type P11 from HBM, whereas the accelerometers located close to both the pressure transducers and the hydrophones are of the B&K type 4371, with a cut-off frequency of around 2500 Hz.

The signals of the pressure transducers and of the accelerometers, suitably amplified, are recorded on magnetic tape by means of a Sangamo tape recorder for further processing.

A general outline of the set of instruments used is shown in fig.1 in which, the disposition along the ship of the various transducers and of the acquisition terminal is also shown, for the measurements which constitute the subject of this paper. The positioning on the hull of the two hydrophones and of the pressure transducers is better illustrated in fig.2 in which the stern area of a naval vessel, on which this kind of measurements were performed, is shown.

More details on the instrumentation set adopted by CETENA in such full-scale tests is reported in /5/.

1.2 NOISE MEASUREMENT SET UP AND ACOUSTIC CHARACTERISTIC OF THE C.E.I.M.M. CAVITATION TUNNEL

- Measurement chain

The noise measurement chain used at the C.E.I.M.M. tunnel is illustrated in the block diagram in fig.3. It corresponds, essentially, to the one suggested by the ITTC /6/.

- Positioning of the hydrophone receiver

Several experiments and measurements were carried out in order to establish the best geometric position for the hydrophone receiver and the most suitable link between the structure of the tunnel and the casing of the hydrophone, so as to reduce to a minimum the signal distortions /7/, /8/.

The hydrophone positioning used at the present by C.E.I.M.M. for noise tests is as follows (compare fig.4) :

- a) in correspondence with the propeller plane, in a water filled box mounted on the testing section, from which it is separated by a perspex window which guarantees acoustic transparency. This box is resiliently mounted on the tunnel window;
- b) at 1,65 m from the propeller model, either wall flush-mounted or in a

water filled box resiliently mounted on the tunnel wall.

- Acoustic characteristic of the tunnel

The frequency response of the working section of the tunnel has been obtained by using a hydrophone emitter placed in correspondence with the propeller shaft. This type of hydrophone emits a noise signal, produced by a generator and then amplified, its spectral components being uniformly distributed along the frequency range concerned (white noise).

In order to check the acoustic characteristics of the tunnel testing section, two series of tests, using the same C.E.I.M.M. measurement set up, were carried out at I.N.S.E.A.N. towing tank basin n.1 (430mx13mx6.80m). These experiments were carried out by placing the hydrophones along the centre line of the basin, at a depth of 3.4 m, at a distance between the emitter and the receiver of respectively 0.4 m and 0.8 m. The results of the above-mentioned tests are shown in fig.5 from which the following observations can be deduced :

- a) the acoustic characteristic of the tunnel is fairly similar to that of the basin;
- b) it is possible to transfer with fair approximation the noise levels obtained, from measurements carried out at 0.4 m (tunnel) between the source and the receiver to the standard distance of 1 m, between the propeller and the receiver, by applying the law of spherical propagation of sound.

- Background noise of the tunnel

The reliability of the measurements carried out on propeller models depends to a large extent on the acoustic behaviour of the tunnel.

The C.E.I.M.M. tunnel was built (1962-1964) without specific consideration for the attenuation of the background noise.

In order to identify both the frequencies themselves and their ranges influenced by background noise in the tunnel (due to : dynamometer, main rotor, stator, etc.,) a series of experiments were carried out, systematically varying the number of revolutions of the dynamometer, the number of revolutions of the main rotor and the pressure in the testing section.

The results of the investigation have shown that the pressure in the testing section, the flow speed and the number of revolutions contribute in different ways to the background noise :

- the variation in the number of revolutions of the dynamometer has most influence on the background noise and it becomes louder as the speed of the water decreases
- the variation of the pressure in the testing section influences the background noise on frequencies above 10 KHz

- the variation of flow speed in the testing section influences the background noise at flow speeds of more than 9 m/sec.

The experiments carried out until now have, moreover, shown noise levels for some frequencies for which the relevant source has been identified.

It is, however, important to stress that the background noise can be disregarded when the noise level of the propeller under testing is relatively higher (10 dB) than the background noise level associated with the same functioning conditions. Otherwise, the levels and the noise spectra of the propeller must be corrected for the level of the background noise.

The background noise of the C.E.I.M.M. cavitation tunnel, recorded for the experiments carried out until now, has always been negligible, particularly in the frequency field typical of cavitation.

- Testing methodology

The tunnel cavitation experiments are carried out disregarding the Froude number parity in order to achieve, for a given cavitation index and a given advance coefficient, a Reynolds number sufficiently high to reduce as far as possible cavitation scale effects.

This essentially involves carrying out the experiment using a high number of propeller-revolutions, the highest possible in relation to the strength of the model and therefore at a higher static pressure than would be necessary to adopt according to Froude's law.

Such a testing method also has advantages related to noise testing, as it allows a reduction in the quantity of air bubbles which form in the testing section thus ensuring the correct acoustic transmission of the water.

It should also be noted that by using high pressure values it is possible to perform the tests with a fairly high air content (around 0.6) which is positive for what concerns the tunnel-sea correlation in terms of cavitation phenomena /2/.

2 ANALYSIS METHODOLOGY AND DATA PROCESSING

Given the complex nature of the acoustic noise signal, the methods of analysis of the signal can be differentiated, depending on the type of information which needs to be obtained.

There are basically two ways of analyzing the radiated hydrodynamic noise :

- a) the so-called "broad-band" analysis which, depending on the type of analyser, can be carried out in octave bands, one third octave bands (more common), one tenth octave bands, etc.

- b) the "narrow-band" analysis, which involves analysing the signal with a higher frequency resolution so as to define the energy content of the noise on a much higher number of frequencies.

The first is typical of the noise measurements radiated at relatively long distances from the ship ("Far-Field") and the results are shown as a function of the values of the central frequency of the various bands as being twenty times the logarithm of the root mean squared value (R.M.S.) of pressure referred to a reference value ($P_o = 1 \mu$ Pascal), thus :
 (Band level) $BI = 10 \lg [\hat{P}_{rms}^2 / \hat{P}_o^2] = 20 \lg [\hat{P}_{rms} / \hat{P}_o]$.

Generally, the "level" is shown in a spectral form (and thus corrected for the width of the band so as to refer it to 1 Hz according to the formula :

("Spectrum Level") $SL' = BI - 10 \lg (\Delta f)$,

and finally reduced to the distance of 1 metre from the source, by means of the formula :

("Spectrum Level") $SL = SL' - 10 \lg (R/1 \text{ m})$,

where R = distance in metres, according to the hypothesis of omnidirectional spherical waves. The usual notation is thus as follows :
 "Spectrum Level" $SL \text{ (dB)} \text{ . ref } 1 \mu\text{Pa, 1m, 1 Hz}$.

The second type of analysis, on the other hand, provides more detailed information about the frequency field by identifying all the predominant lines of the spectrum. The presentation is simply made in terms of "levels" (referred to $1 \mu\text{Pa}$ and to 1 m), indicating the width of the narrow band used.

2.1 TECHNIQUES USED

Both of these analysis techniques were applied to the data obtained.

The broad-band analysis was carried out in one third octave bands using a Bruel & Kjaer type 2131 analyser which supplies, directly onto video, the acoustic "levels" as a function of the frequency centres of the various bands starting from 1.6 Hz up to 160 KHz. The levels were obtained with linear averages and relative mean times of 32-64 seconds.

Some results will be illustrated in the next paragraph.

The full scale data analysis was limited to the up frequency of 20 KHz and all the relevant results are reported in /9/.

As far as the analysis relative to the signals of the pressure transducers and the accelerometers placed on the ship stern is concerned, this was carried out using the Fast Fourier Analyzer, type .P. 5451 B, in use at CETENA Data Processing Centre, which allows the spectral distribution of the pressure values induced by the propeller and the vibration values in terms of local acceleration, to be obtained. All the relevant results are reported in detail in /10/.

2.2 EFFECT OF THE HULL ON THE FULL-SCALE MEASUREMENT AND CORRECTION METHODS

The complementary measurements carried out by means of pressure and accelerometer transducers aim to define both the pressure levels induced by the propeller at low frequencies (first blade frequency and its multiples) and the local as well as global vibration levels which occur in correspondence with the hydrophones thereby affecting the response.

The simultaneous analysis of these signals allows the right corrections at noise level picked up by the hull-mounted hydrophones to be carried out so as to eliminate both the effect of the presence of the hull (solid boundary) as well as the effect due to the vibrations of the hull itself.

The corrective factor due to the first effect is defined as the relationship between the pressure measured at the hull and the pressure radiated in the free field and it is of course, a function of the form and material of the surrounding surface.

In the case of a rigid plate of infinite dimension, this factor takes on the value 2. Moreover, this value has been confirmed also for stern shapes similar to those of the above-mentioned ship as proved by previous experimental tests [11].

Therefore, all the collected pressure values must be divided by 2, which means a reduction of 6 dB (in the low frequency range) on the directly measured noise levels.

A second problem which must be taken into consideration is that of the global and local structural vibrations (of panels) to which the hydrophones, rigidly mounted on the hull, are subjected.

It is above all the local vibrations which can induce very high pressure values in the immediate vicinity of the hull surface so that the hydrophone in the hull also records the effects of this contribution due to the vibrations.

In order to obtain noise levels comparable with the tunnel test results, it is therefore necessary to establish the influence of the global and local vibrations and thus the pressure by them induced.

As far as the effect of the global vibration of the hull is concerned, it is necessary to measure the pressure and the vibration both in conditions of forced excitation (by means of a hydraulic exciter) as well as in natural excitation when the ship is underway.

Relative to the effect of local (panel) vibration, a series of additional measurements, using accelerometers, are needed by locally exciting the panel in order to define its resonance frequency (or frequencies). By simultaneously recording the signal from the hydrophone mounted on the panel the transfer function between pressure and vibration can also be obtained.

For frequencies near the local resonance frequency of the panel, variations

of pressure can be found in the nearby flow which can even be far higher to those induced by the cavitating propeller, as experimentally proved by several researchers [12], which require corrections of up to 15 dB on the spectral content of the measured noise levels.

A measure on the effects of the vibration of the ship stern structure, by means of accelerometers, was carried out during the trials the results of which are discussed in this report.

The pressure due to the global vibrations was obtained from these measurements and was of the order of 5% of the total one for the first blade harmonic and of the order of 25% for the second one.

This requires a further correction of the noise level measured by the hydrophone of the order of 1-2 dB.

The local panel vibration measurements, for which it is necessary to use an accelerometer (piezoelectric) with a high cut-off frequency (with a linear response from 0 Hz to at least 12000 Hz) were not carried out on this occasion. Therefore a check on the actual correction to be made to the spectral noise levels, due to this local vibrational effects, was not possible.

The uncertainty concerning the validity of a comparison between noise levels remains, within the middle-frequency range, even if these experiments have enabled a more correct methodology to be identified, both for acquisition as well as analysis to be used in the future.

3 PRESENTATION OF RESULTS

All the results obtained from the experimental full-scale trials performed on an Italian Navy frigate are reported in detail in [9].

Measurements and analysis of propeller radiated noise have been carried out at increasing ship speed from a ship' $F_N = 0.140$ up to $F_N = 0.400$ in order to investigate both on the effects that the different propeller cavitating conditions have on the radiated noise as well as on the efficiency of two air insufflation system with which the ship is equipped.

In this report the radiated noise spectrum levels measured by means of the hull flush-mounted hydrophone for two most significant ship speeds ($F_N = 0.246$, corresponding to back shet and tip vortex cavitation inception, and $F_N = 0.400$ corresponding to the highest investigated speed) are reported.

The two noise spectrum levels are shown in fig.6 and 7 respectively, where the corresponding spectra obtained from test carried out in model scale at Cavitation Tunnel for the same propeller operating conditions, are shown and compared. In the same figures the "far field" ship radiated noise spectra, as measured by the fixed hydrophones of an acoustic range, are also

indicated.

The transfer laws adopted to scale-up both frequencies and sound pressure levels from model to full scale conditions are summarized in fig.8 and are basically derived from ref. /13/.

As concern the two respective propeller cavitation patterns observed both in full scale and model conditions, they are shown in figg.9, 10 where the extent of suction and pressure side cavitation is illustrated.

4. OBSERVATION AND COMMENTS

From the results discussed in this paper the following can be noted :

- the noise spectra measured in the tunnel and scaled are lower than those obtained in full-scale conditions.

Possible explanation for this discrepancy can be found from the following factors :

- in the tunnel the noise emitted from the propeller alone is measured whereas in full-scale, the measurements are also influenced by the global noise produced by the ship
- the extent of the cavitation on full-scale propeller blades, although fairly reproducing the simulated one in the cavitation tunnel, shows some varied local phenomena which are unreproducible in the tunnel due to many physical reasons, not least different manufacturing tolerances /14/ between the model and full-scale propeller
- the adopted noise scaling law, according to the TNO formulation /13/, should be refined on the basis of both further tunnel and full-scale experiments.

In this context it must be pointed out that one of the main recommendations put forward by the last ITTC'84 Cavitation Committee concerns "the implementations of noise scaling laws by utilizing results from this kind of full-scale tests".

5. CONCLUSION

This report has described some fundamental aspects related to the problem of noise radiated by a ship (in particular by its propeller) at sea and some general concepts relating to experimental techniques and noise processing are also summarized.

Prediction of the propeller radiated noise in full scale conditions is not

not assessable in a reliable and integral way.

The results obtained to date show that:

- the testing methods both in model and full-scale conditions have been adequately checked and has proved their reliability also in terms of the instrumentation used

- the hydrophones mounted on the ship hull, despite the complexity of the signal conditioning as already mentioned, offer the opportunity of having qualitative noise spectrum even without an acoustic range and, additionally, provide the opportunity to monitor possible damage and/or excitations occurring on the propeller blades

- to compare directly the propeller noise spectrum obtained from measurements carried out on model scale (Cavitation Tunnel) with results obtained by means of hydrophones mounted on the ship hull, it is necessary to take into account the different boundary conditions between the two measurement systems, which can be adequately evaluated using complementary measurement techniques as already mentioned

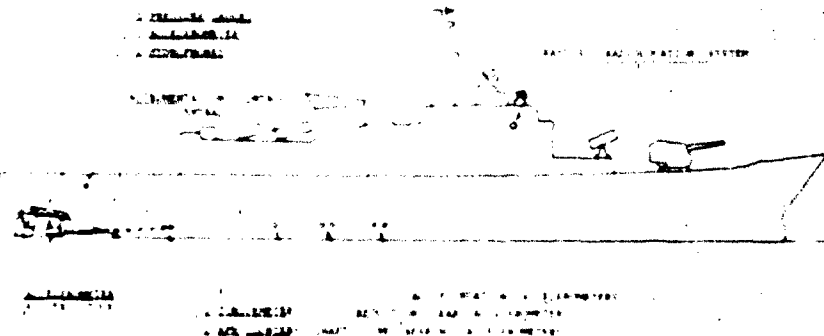
The cavitation tunnel with its instrumentation equipment represents a flexible and reliable facility for a relative evaluation of the noise levels associated with various propeller cavitation phenomena. As a confirmation of this statement some results of comparative noise measurements, suggested by ITTC Cavitation Committee carried out by some international tunnels on the same propeller model under different cavitating conditions are reported in figg.11+13, where CEIMM' results are also shown and compared /15/.

It is the Authors' and their respective Organizations' aim to continue the studies concerning correlations of both noise levels and propeller induced pressures between model (Cav. Tunnel) and full-scale experimental conditions.

Of course the amount of full scale experimental data will definitely be increased once an acoustic range is available in Italy.

REFERENCES

- / 1/ H.G. Flynn, "Physics of acoustic cavitation in liquids", A.P.L. Dept. Electr. Eng., Rochester University, New York.
- / 2/ L. Accardo, V. Gregoretti, "Cavitation prediction by model experimental tests at Italian Navy Cavitation Tunnel", R.1+/80, CEIMM.
- / 3/ L. Accardo, A. Gaudolino, "Noise measurements at CEIMM Cavitation Tunnel", R.4/83, CEIMM presented at 'Noise Control on Board ships', CETENA Symposium, Genova, June 1983.
- / 4/ L. Accardo, "Sydney Express Prop. HSVA. = 28. Radiated Noise Measurements", R.5/83, CEIMM.
- / 5/ A. Colombo, "Hydrodynamic radiated noise. Full scale measurements and signal analysis methodologies", Paper presented at 'Noise control on board ships' CETENA Symposium, Genova, June 1983.
- / 6/ 15th ITTC Proceedings, "Proposed procedures for documenting cavitation noise test", 1978.
- / 7/ V. Gregoretti, L. Accardo, M. Marino, "Acoustic measurements on scale model propeller", R.9/81, CEIMM, Presented at 'IMAEN.81'. Trieste.
- / 8/ L. Accardo, L. Fabbrini, "Studies on noise radiated by cavitating foils and propeller", R.5/82, CEIMM.
- / 9/ A. Colombo, S. De Gaetano, G. Macca', "Propeller Radiated Noise. Full-scale measurements by means of hull stern mounted hydrophones", CETENA Report n.1709, March 1983.
- /10/ S. De Gaetano, G. Macca', P. Scavia, "Propeller induced pressure measurements at stern of an Italian Navy Frigate", CETENA Report n.1767, April 1983.
- /11/ S. Martinelli, B. Della Loggia, L. Cortellini, A. Colombo, "Experimental investigation on propeller induced pressures on a naval ship stern, and their correlation with cavitation phenomena", Presented at 'Advanced Hydrodynamic Testing Facilities Symposium', The Hague, The Netherlands, April 1982.
- /12/ A.C. Nilsson, "Propeller induced hull plate vibrations", Journal of Sound and Vibration, 1980.
- /13/ A. De Bruijn, T. Ten Wolde, "Measurements and prediction of sound in board and out board of ships as generated by cavitating propellers", TNO, - TN Report, Delft, The Netherlands.
- /14/ L. Accardo, F. Bau', "Propeller leading edge trimming and maintenance: effects on ship's noise operational performances", Paper Presented at 'Silent Ship Symposium, La Spezia, October 1984.
- /15/ L. Accardo, A. Colombo, "Cavitation Noise Measurements with the Sydney Express ship propeller model", CETENA Report n.1878, Written Contribution to the Cavitation Committee of ITTC'84.



1. Description of instrumentation set adopted by Intena for noise and vibration measurement on a naval vessel

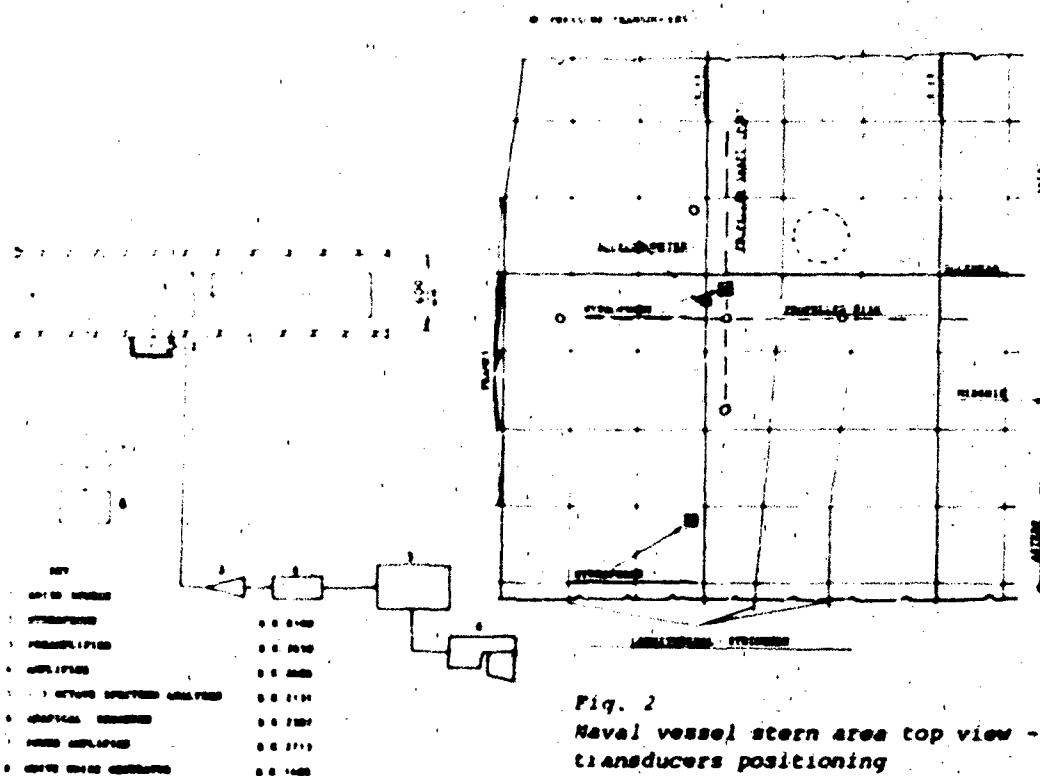


Fig. 2
Naval vessel stern area top view -
transducers positioning

Fig. 1
CEIMM cavitation tunnel - noise
measurement set-up

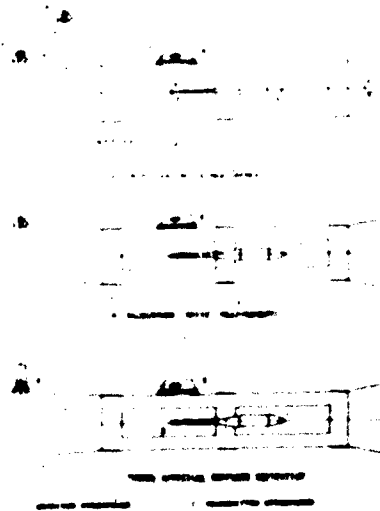


Fig. 4
CEIMM cavitation tunnel -
hydrophone positioning

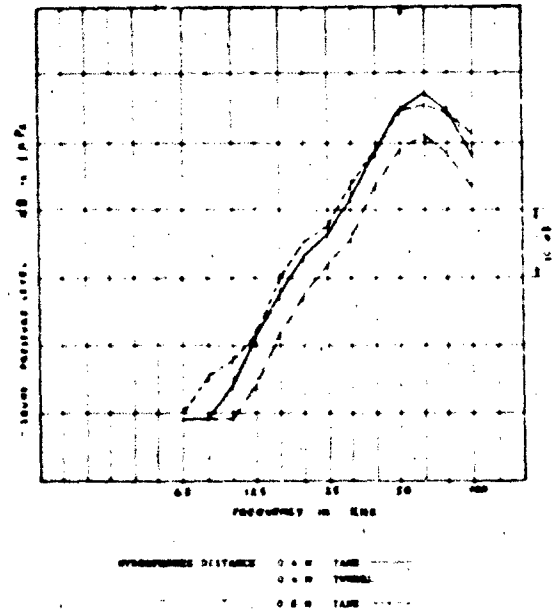


Fig. 5
Acoustic characteristic response
of in-sean towing tank and CEIMM
cavitation tunnel

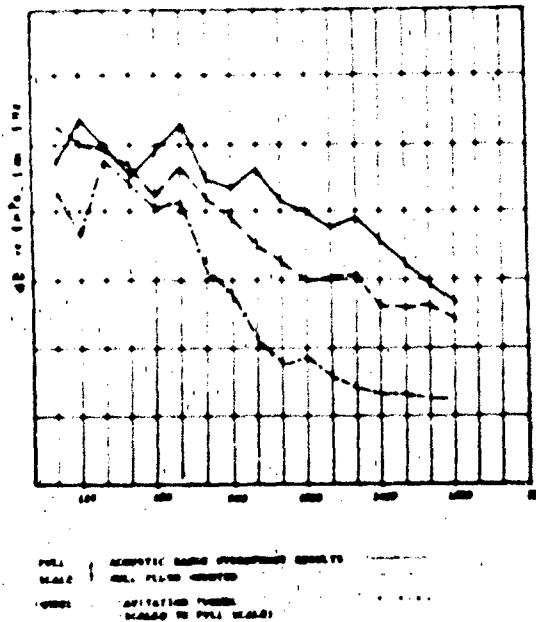


Fig. 6
Sound spectrum levels comparison
Ship's $P_n = 0.266$

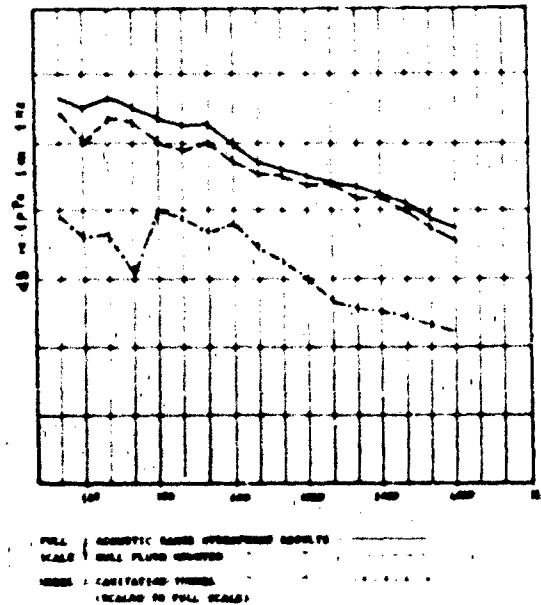


Fig. 7
Sound spectrum levels comparison
Ship's $P_n = 0.40$

ACCARDO & COLOMBO: Propeller noise measurements

6 (A, A) UDA 8760000000

θ^m $\theta^{-1} \theta$ $3.4 = 2.6 \cdot 1.4 = 3.6$

Q. 2. 2. 2. 2.

5. 1999. 10. 10. 11. 12. 13. 14. 15. 16. 17. 18. 19. 20. 21. 22. 23. 24. 25. 26. 27. 28. 29. 30. 31. 32. 33. 34. 35. 36. 37. 38. 39. 40. 41. 42. 43. 44. 45. 46. 47. 48. 49. 50. 51. 52. 53. 54. 55. 56. 57. 58. 59. 60. 61. 62. 63. 64. 65. 66. 67. 68. 69. 70. 71. 72. 73. 74. 75. 76. 77. 78. 79. 80. 81. 82. 83. 84. 85. 86. 87. 88. 89. 90. 91. 92. 93. 94. 95. 96. 97. 98. 99. 100. 101. 102. 103. 104. 105. 106. 107. 108. 109. 110. 111. 112. 113. 114. 115. 116. 117. 118. 119. 120. 121. 122. 123. 124. 125. 126. 127. 128. 129. 130. 131. 132. 133. 134. 135. 136. 137. 138. 139. 140. 141. 142. 143. 144. 145. 146. 147. 148. 149. 150. 151. 152. 153. 154. 155. 156. 157. 158. 159. 160. 161. 162. 163. 164. 165. 166. 167. 168. 169. 170. 171. 172. 173. 174. 175. 176. 177. 178. 179. 180. 181. 182. 183. 184. 185. 186. 187. 188. 189. 190. 191. 192. 193. 194. 195. 196. 197. 198. 199. 200. 201. 202. 203. 204. 205. 206. 207. 208. 209. 210. 211. 212. 213. 214. 215. 216. 217. 218. 219. 220. 221. 222. 223. 224. 225. 226. 227. 228. 229. 230. 231. 232. 233. 234. 235. 236. 237. 238. 239. 240. 241. 242. 243. 244. 245. 246. 247. 248. 249. 250. 251. 252. 253. 254. 255. 256. 257. 258. 259. 260. 261. 262. 263. 264. 265. 266. 267. 268. 269. 270. 271. 272. 273. 274. 275. 276. 277. 278. 279. 280. 281. 282. 283. 284. 285. 286. 287. 288. 289. 290. 291. 292. 293. 294. 295. 296. 297. 298. 299. 300. 301. 302. 303. 304. 305. 306. 307. 308. 309. 310. 311. 312. 313. 314. 315. 316. 317. 318. 319. 320. 321. 322. 323. 324. 325. 326. 327. 328. 329. 330. 331. 332. 333. 334. 335. 336. 337. 338. 339. 340. 341. 342. 343. 344. 345. 346. 347. 348. 349. 350. 351. 352. 353. 354. 355. 356. 357. 358. 359. 360. 361. 362. 363. 364. 365. 366. 367. 368. 369. 370. 371. 372. 373. 374. 375. 376. 377. 378. 379. 380. 381. 382. 383. 384. 385. 386. 387. 388. 389. 390. 391. 392. 393. 394. 395. 396. 397. 398. 399. 400. 401. 402. 403. 404. 405. 406. 407. 408. 409. 410. 411. 412. 413. 414. 415. 416. 417. 418. 419. 420. 421. 422. 423. 424. 425. 426. 427. 428. 429. 430. 431. 432. 433. 434. 435. 436. 437. 438. 439. 440. 441. 442. 443. 444. 445. 446. 447. 448. 449. 450. 451. 452. 453. 454. 455. 456. 457. 458. 459. 460. 461. 462. 463. 464. 465. 466. 467. 468. 469. 470. 471. 472. 473. 474. 475. 476. 477. 478. 479. 480. 481. 482. 483. 484. 485. 486. 487. 488. 489. 490. 491. 492. 493. 494. 495. 496. 497. 498. 499. 500. 501. 502. 503. 504. 505. 506. 507. 508. 509. 510. 511. 512. 513. 514. 515. 516. 517. 518. 519. 520. 521. 522. 523. 524. 525. 526. 527. 528. 529. 530. 531. 532. 533. 534. 535. 536. 537. 538. 539. 540. 541. 542. 543. 544. 545. 546. 547. 548. 549. 550. 551. 552. 553. 554. 555. 556. 557. 558. 559. 560. 561. 562. 563. 564. 565. 566. 567. 568. 569. 570. 571. 572. 573. 574. 575. 576. 577. 578. 579. 580. 581. 582. 583. 584. 585. 586. 587. 588. 589. 590. 591. 592. 593. 594. 595. 596. 597. 598. 599. 600. 601. 602. 603. 604. 605. 606. 607. 608. 609. 610. 611. 612. 613. 614. 615. 616. 617. 618. 619. 620. 621. 622. 623. 624. 625. 626. 627. 628. 629. 630. 631. 632. 633. 634. 635. 636. 637. 638. 639. 640. 641. 642. 643. 644. 645. 646. 647. 648. 649. 650. 651. 652. 653. 654. 655. 656. 657. 658. 659. 660. 661. 662. 663. 664. 665. 666. 667. 668. 669. 670. 671. 672. 673. 674. 675. 676. 677. 678. 679. 680. 681. 682. 683. 684. 685. 686. 687. 688. 689. 690. 691. 692. 693. 694. 695. 696. 697. 698. 699. 700. 701. 702. 703. 704. 705. 706. 707. 708. 709. 710. 711. 712. 713. 714. 715. 716. 717. 718. 719. 720. 721. 722. 723. 724. 725. 726. 727. 728. 729. 730. 731. 732. 733. 734. 735. 736. 737. 738. 739. 740. 741. 742. 743. 744. 745. 746. 747. 748. 749. 750. 751. 752. 753. 754. 755. 756. 757. 758. 759. 760. 761. 762. 763. 764. 765. 766. 767. 768. 769. 770. 771. 772. 773. 774. 775. 776. 777. 778. 779. 780. 781. 782. 783. 784. 785. 786. 787. 788. 789. 790. 791. 792. 793. 794. 795. 796. 797. 798. 799. 800. 801. 802. 803. 804. 805. 806. 807. 808. 809. 810. 811. 812. 813. 814. 815. 816. 817. 818. 819. 820. 821. 822. 823. 824. 825. 826. 827. 828. 829. 830. 831. 832. 833. 834. 835. 836. 837. 838. 839. 840. 841. 842. 843

— 5 —

• • •

100-443887-100

SECRET

• • •

[illegible]

7-42-50

Figure 1 is a line graph showing the percentage of total energy expenditure (TEE) for different activities over a 24-hour period. The Y-axis is 'Percentage of TEE' (0-100) and the X-axis is 'Time of Day' (0-24). The legend indicates: Sleeping (hatched), Sedentary (white), Light (diagonal lines), Moderate (cross-hatch), and Vigorous (solid black). Sleeping is highest at night (~30-40%). Sedentary is highest in the morning (~20-30%). Light activity is highest in the afternoon (~10-20%). Moderate and Vigorous activities are highest in the afternoon and evening (~10-20%).

Figure 1 is a schematic representation of the experimental design. It shows a sequence of events: 'Pretest' (a small box), followed by 'Training' (a larger box), and then 'Test' (a box). The 'Training' box is divided into 'Pretest' and 'Test' sections. The 'Test' section is further divided into 'Pretest' and 'Test' sections. The 'Test' section is further divided into 'Pretest' and 'Test' sections. The 'Test' section is further divided into 'Pretest' and 'Test' sections.

1

DECLASSIFICATION LEVELS

$$G_p = \frac{r' \cdot p'}{p \cdot c \cdot R \cdot p \cdot n}$$

- P = distanza di un punto osservato da P_0
- $\langle P \rangle$ = media quadratica delle posizioni sempre nel punto di osservazione
- R_0 = raggio medio delle collisioni
- N_0 = numero delle volte di collisione generata per unità di tempo
- ρ = densità fluida
- σ_0 = probabilità di collisione
- C = coefficiente del numero medio

•••••

CONFIDENTIAL

2 . 2

2. D

$$\frac{P_1^* \cdot P_2^*}{P_{12} \cdot C_{12} \cdot R_{12} \cdot P_1 \cdot P_2 \cdot N_{12}} = \frac{P_1^* \cdot P_2^*}{P_{12} \cdot C_{12} \cdot R_{12} \cdot P_1 \cdot P_2 \cdot N_{12}} \quad (7)$$

$$\frac{D_1' + P_1' + N_1'}{D_1 + P_1 + N_1} = \frac{D_2' + P_2' + N_2'}{D_2 + P_2 + N_2}$$

$$\frac{(P_1)'}{D_1 P_1 N_1} = \frac{(P_2)'}{D_2 P_2 N_2} \quad (8)$$

$$\frac{p_1}{p_2} = \frac{p_1 p_2 N_2}{p_2 p_1 N_1} \quad (2)$$

$$\frac{N_1^2}{N_2^2} = \lambda^2 \frac{N_1^2}{N_2^2} \quad \text{da cui}$$

$$L_0 - L_\infty = 40 \log \lambda - \frac{2}{\lambda}$$

Fig. 8

Frequency and sound pressure level scaling laws

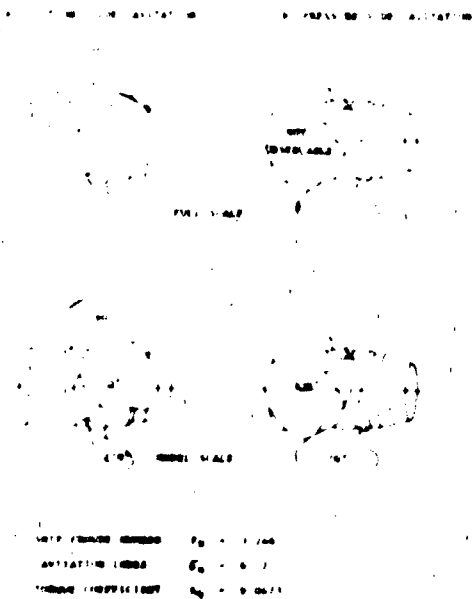


Fig. 9
Propeller cavitation pattern
observation

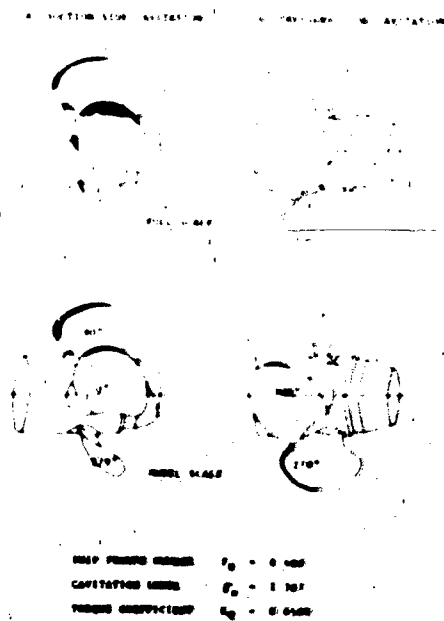


Fig. 10
Propeller cavitation observation

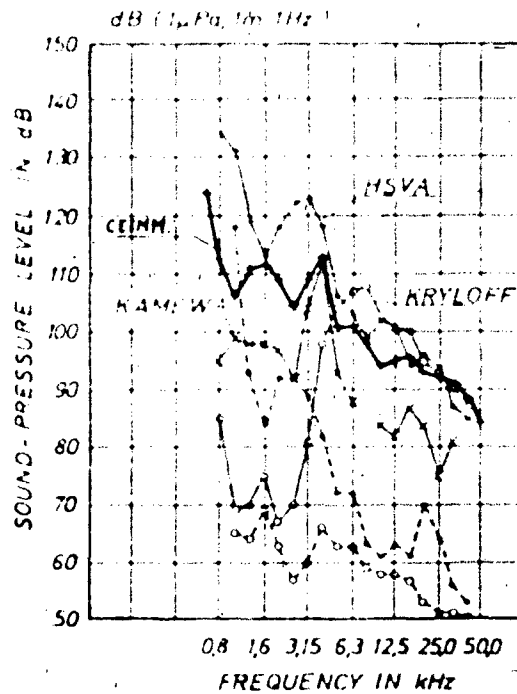


Fig. 11
Noise measurements of conventional
tunnels (suction side cavitation)

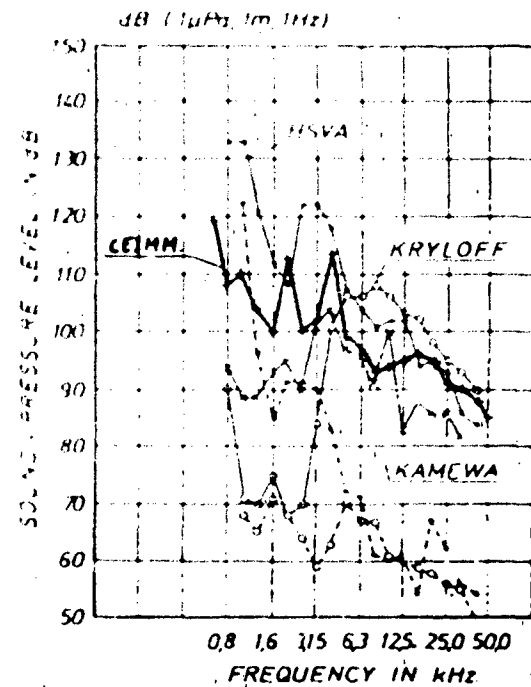


Fig. 12
Noise measurements of conventional
tunnels

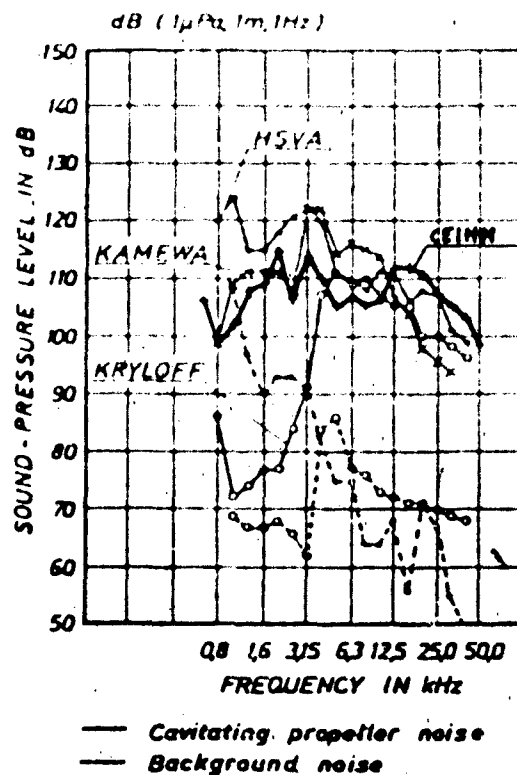


Fig. 13
Noise measurements of conventional
tunnels (pressure side cavitation)

NEAR-FIELD ACOUSTIC IMAGING TECHNIQUES IN NOISE RANGING

by

B. RAFINE
DEAN TOULON - GERDSM
Le Brusq 83140 SIX FOURS LES PLAGES FRANCE

G. ELIAS
Office National d'Etudes et de Recherches
Aerospaciales (ONERA)
29 avenue de la Division Leclerc
92320 - CHATILLON FRANCE

ABSTRACT

Acoustical imaging of ship radiating noise sources requires the development of near field array processing. Performance analysis of a linear processing with static sources together with its adaptation to moving sources imaging are presented. Application of this processing to experimental measurements with static and moving electroacoustic sources is shown. Experimental results and theoretical analysis are in good agreement.

INTRODUCTION

Improvement of ship acoustic discretion requires the identification of radiating noise sources. An interesting way to achieve this purpose is to locate the radiating regions on the hull of the ship.

The acoustical facility could be a measurement station where the ship should follow, with fixed operating condition, a straight line parallel to a multihydrophones linear array.

Usually the aim of acoustic imaging is to identify the directions of a set of individual independent sources. Here, the situation is different. Sources are distributed on a ship of finite length, and they are to be separated spatially along the ship length in his own frame, rather than in angular direction in the observation frame. The relevant representation is therefore the amplitude of the noise source pressure as a function of frequency and axial position on the ship. The structure of the noise sources function may be complex, due to the number of independent sources, to their spatial dimensions (compact or distributed), and to their spectral or temporal content. In addition, this acoustic imaging must take into account the motion of the ship.

Although other techniques may be developed, the approach followed in this paper consists in adapting to imaging the classical beamforming technique.

1. NEED FOR NEAR FIELD IMAGING

Classical beamforming with sources in the far field of the array (plane wave approximation) allows the spatial position of the sources to be determined if their radial distance D is known (see fig. 1 for definitions). The measurement of θ_0 yields $X_0 = D \sin \theta_0$. The angular resolution of such an array being approximately $\Delta(\sin \theta) \sim \frac{\lambda}{L}$ (λ is the acoustic wavelength), its spatial resolution will be

$$(1) \quad \Delta X \sim D / \cos^3 \theta_0 \cdot \frac{\lambda}{L}$$

The best resolution seems to be obtained when $D \ll L$ but the plane wave approximation becomes irrelevant. The shortest distance D for this approximation is controlled by the limit of the Fresnel zone of the array

$$D_m \sim \frac{2\pi L^2 \cos \theta_0}{\lambda}, \text{ so that the minimum value of } \Delta X \text{ is :}$$

$$(2) \quad \Delta X_m \sim 2\pi L / \cos^2 \theta_0$$

To improve the angular resolution, the length of the array must be large with respect to the wavelength, so that $\Delta X_m \gg \lambda$. To obtain a better spatial resolution, the measurement has to be made in the near-field of the array, and the curvature of the wave fronts has to be taken into account.

Even in this case, the spatial resolution will never be very much smaller than the wavelength. If additional information on the sources is not known. Without such an information, the source function is not uniquely determined by the radiated pressure field, according to the Kirchhoff integral. One must then choose a particular representation for the noise source pressure description. Here, this representation will be the simplest one : an equivalent monopole source distribution along a straight line. The array processing presented here is the adaptation to this near-field imaging of the classical linear beamforming.

2. NEAR-FIELD ARRAY PROCESSING AND PERFORMANCE ANALYSIS IN THE STATIC CASE (ref.1)

In presence of a single plane wave and additive uncorrelated noise of same variance σ^2 on each sensor, the optimal estimation for its amplitude and direction is obtained by classical beamforming. For a near-field array of N sensors, the equivalent of the plane wave is given by a single monopolar source of amplitude A and location \vec{z}_0 (fig.1). The pressure on the sensor i of location \vec{y}_i is

$$(3) \quad p(\vec{y}_i) = A \frac{e^{ik|\vec{y}_i - \vec{z}_0|}}{|\vec{y}_i - \vec{z}_0|} + b_i, \text{ with } \langle b_i b_j \rangle = \sigma^2 \delta_{ij} \text{ and } k = \frac{2\pi}{\lambda}$$

It can be shown that the optimal estimate $\hat{\vec{z}}_0$ of \vec{z}_0 maximizes the function

$$(4) \quad B(\vec{x}) = \left(\sum_{i=1}^N 1/|\vec{y}_i - \vec{x}|^2 \right)^{-1} \left| \sum_{i=1}^N p(\vec{y}_i) \frac{e^{-ik|\vec{y}_i - \vec{x}|}}{|\vec{y}_i - \vec{x}|} \right|^2$$

and the optimal estimate \hat{A} of A is :

$$(5) \quad \hat{A} = \left(\sum_{i=1}^N 1/|\vec{y}_i - \hat{\vec{x}}|^2 \right)^{-1} \sum_{i=1}^N p(\vec{y}_i) \frac{e^{-ik|\vec{y}_i - \hat{\vec{x}}|}}{|\vec{y}_i - \hat{\vec{x}}|}$$

As in classical beamforming, these estimates will be used, even with an unknown multipole source distribution. They are obtained by focusing the array and looking for the points giving the best contrast. The performance of this array processing is the following :

- the spatial resolution defined by the difference between the maximum of $B(\vec{x})$ and the first zero-crossing of $B(\vec{x})$ around $\vec{x} = \hat{\vec{x}}$ is

$$(6) \quad \Delta X = \frac{\lambda D}{L \cos \theta_0} \quad \text{if } L \leq D$$

if $L \gg D$, $B(X)$ is close to $J_0(k|X - X_0|)$, so that

$$(7) \quad \Delta X = 0.38 \lambda$$

For a fixed distance D , it is therefore not very useful to increase the length L when $L \geq D$.

Figure 2 shows simulated results for $B(X)$ when the source is at location $X = 0$ for various values of the reduced wave-number $K = kL$, with $D = L$ and $N = 21$.

- the depth of field is approximatively :

$$(8) \quad \Delta \sim 3.3 \lambda \left(\frac{D}{L} \right)^2 \quad \text{when } L \leq D$$

Figure 3 shows simulated results for the same source and array parameters as in figure 2 and for some values of K .

- with N sensors equidistant of Δy [$(N-1)\Delta y = L$], $B(X)$ shows spatial side-lobes like in classical beamforming. Also spatial aliasing appears, at angular positions $|\sin \theta - \sin \theta_0| \sim \lambda/\Delta y$, but with shape and amplitude different from far-field beamforming (fig.4).

3. EXPERIMENTAL RESULTS IN THE STATIC CASE

To evaluate the performance of a near-field array, an experiment has been carried out in the Castillon's facility of GERDSM. The array consists of 19 hydrophones spaced of 0,5 m and immersed horizontally at 20 m. Two electroacoustic transducers have been placed in front of the array at different positions; they are driven at different frequencies (sine or triangular waves). Some results of the array processing are shown in fig. 2 to 7. It appears that the experimental performance in spatial resolution and depth of field of the array are in good agreement with the prediction.

4. ADAPTATION TO MOVING SOURCES

The same near-field array processing can be adapted when the sources are in motion at a constant speed V . The principle is then to catch a set of single pictures of the sources in the frame of the array, each of them corresponding to a small displacement δX of the sources. The pictures are then averaged after shifting them in the sources frame with the help of additional information related to its trajectory.

Let T be the duration for a single picture ($T = \delta X/V$), and Δf the frequency resolution ($\Delta f = 1/T$). Due to the Doppler effect, the various array sensors do not receive the same frequency for a source at a frequency f . The maximum difference between two received frequencies must remain within Δf for a significative computation of $B(X)$. Let φ_i be the angle giving the position of the source with respect to sensor i (fig.1). The Doppler shift on this sensor is: $f_d = f M \sin \varphi_i$ ($M = V/c \ll 1$),

and the maximum differential Doppler shift is $\delta f_d = f M \cos \theta_0 \Delta \varphi$ with $\Delta \varphi \approx \omega \theta_0 \frac{L}{D}$ ($D \gg L$).

With the spatial resolution $\Delta X = \frac{\lambda D}{L \cos^3 \theta_0}$,

$$(9) \quad \delta f_d = \frac{V}{\Delta X}$$

Therefore $\delta f_d < \Delta f$ if

$$(10) \quad VT = \delta X < \Delta X$$

In conclusion, the condition required to get each picture is that the displacement of the source must be smaller than the spatial resolution of the array.

An experimentation was done at the Lake Castillon facility with a vertical array of 19 hydrophones and an electrodynamic transducer mounted in a guided streamlined body (fig.8). The source location information was given by a revolution counter. The speed of the source was about 3 m/s. Figures 9-10 give typical results of this test that show the ability of the technique.

CONCLUSION

The experimental results show that the imaging technique based on near-field array processing is valuable for static or moving sources.

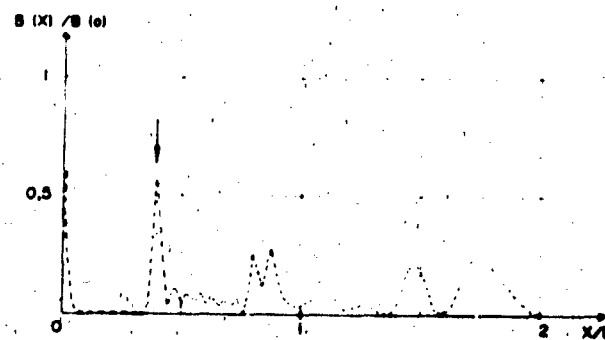
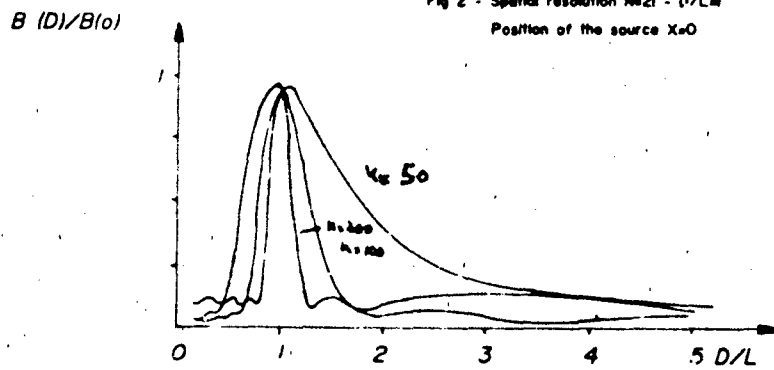
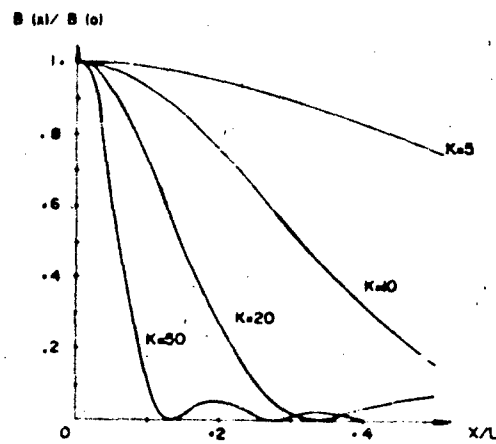
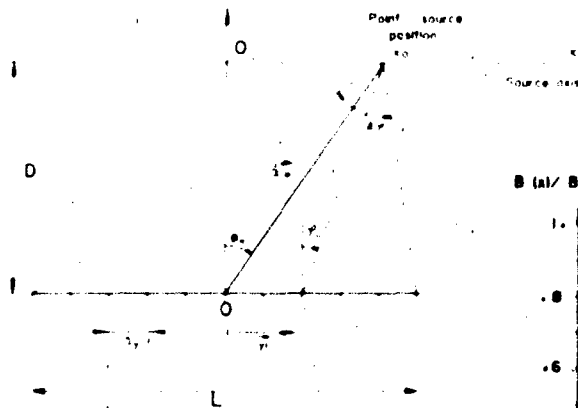
The applications of this linear processing are limited by the spatial resolution and the monopole source model. The spatial resolution limited to the wavelength becomes very poor at low frequencies and this technique becomes irrelevant when the wavelength is not small with respect to the extent of the ship.

The acoustic image of the sources may be difficult to read if the real spatial structure is far from being of a monopolar type. To overcome such problems, particular signal processing techniques already developed for far-field location could be adapted to the near-field situation. It should be necessary to take into account the Doppler effect and have relevant information on the sources to model them.

REFERENCE

1. ELIAS, G. & PALARNEY, C. Utilisation d'antenne focalisées pour la localisation des sources acoustiques. 11th ICA Paris 19-27/7/83 Vol 6 p. 165-166.

RAFINE & ELIAS: Acoustic imaging



RAJINE & ELIAS: Acoustic imaging

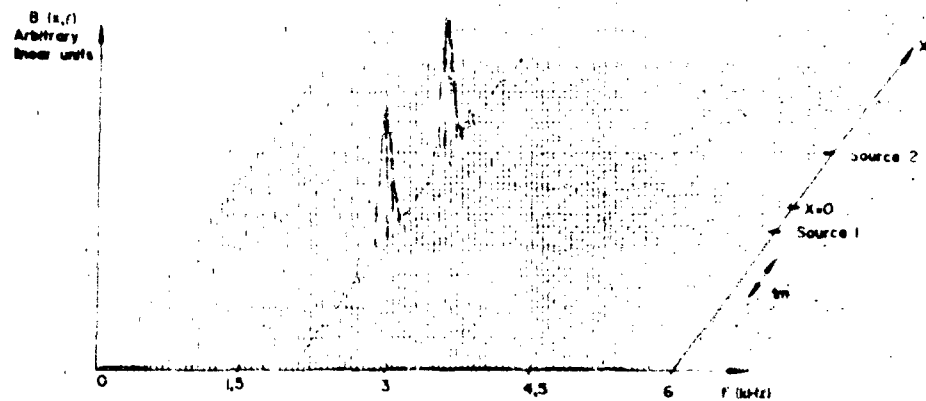


Fig 5 - Acoustic image $B(x, f)$ of two electroacoustic sources excited with a sine wave at 4 kHz
 $N=19$, $L=8m$, $D=7.2m$

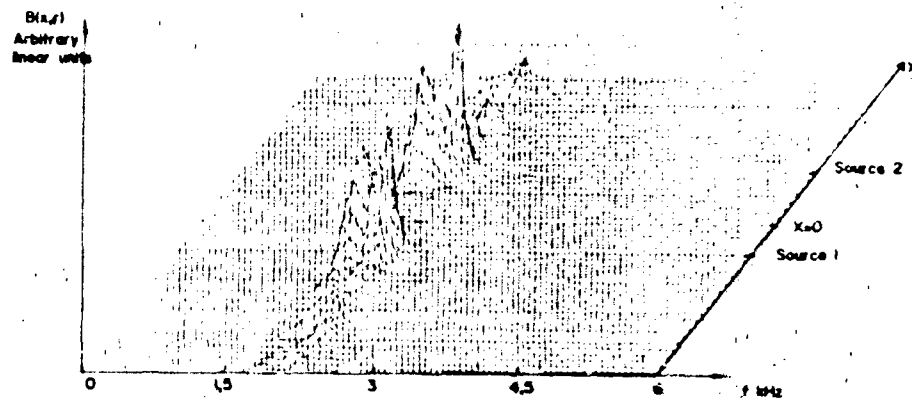


Fig 6 - Acoustic image $B(x, f)$ of two electroacoustic sources excited with a third octave band of 2 kHz $N=19$, $L=8m$, $D=7.2m$

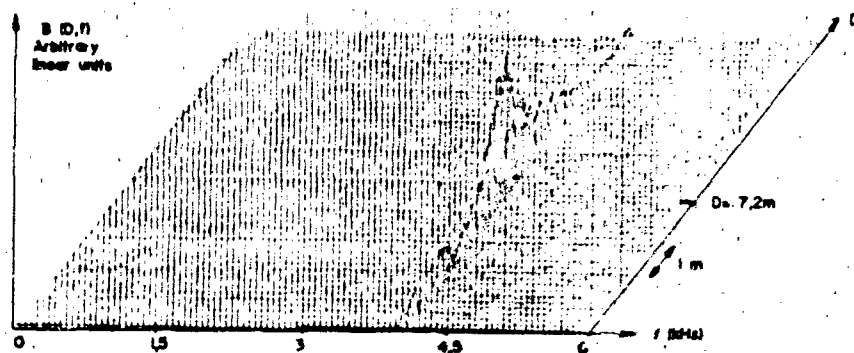
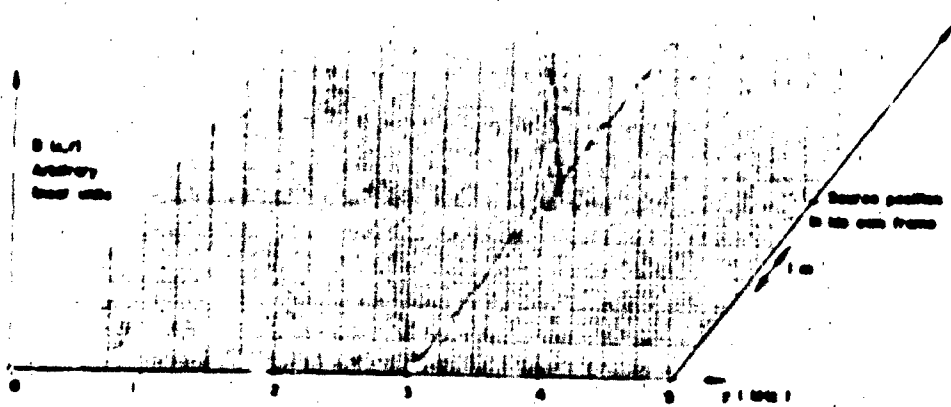
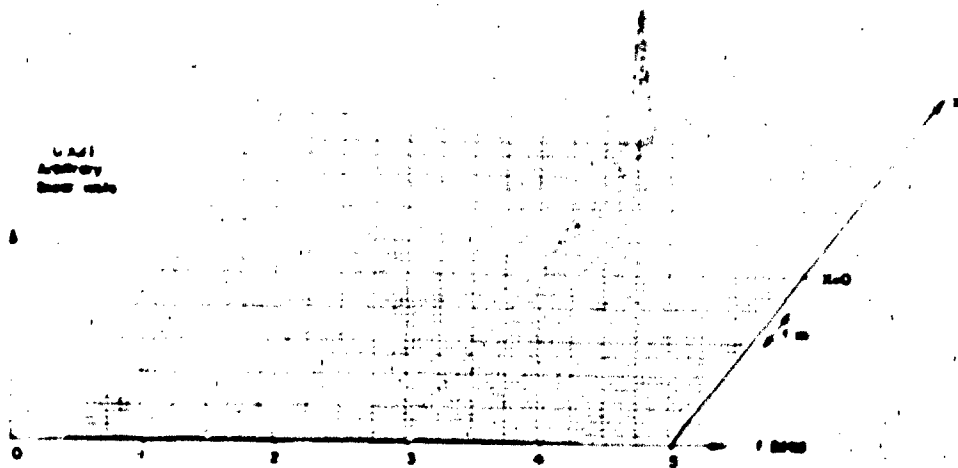
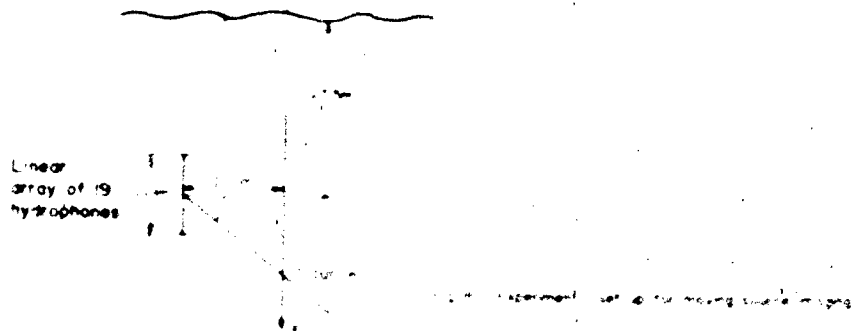


Fig 7 - Depth of field Acoustic image of an electroacoustic source excited by a sine wave at $f=4$ kHz - $N=19$, $L=8m$
 Source position $X=1.5m$ - $D=7.2m$



MUTUAL COHERENCE AND SILENCE

DEBART. Mutual coherence and silence

ABSTRACT

In this paper we are developing the theoretical principle of a modification of the "high resolution" method for angular measurements. Its objective is making inefficient the measurements achieved by a detector. More precisely, the detector is intended to use a "high resolution" method for angular determination. The concept underlying this approach is the mutual coherence of the wavefronts.

1. INTRODUCTION

The term "mutual coherence" is to be understood in its strict significance, i.e., it refers to the power level sent by the ship.

However, it is clear that the idea according to which the acoustical emission of the ship, at a rather high level, lures the detector and induces it to make measurements, its ears becoming deaf to the received sound.

In order to make possible this possibility, we are going to recall the principles of the "high resolution" method for angular measurements using an antenna, and to investigate how the emission is to be modified to make it inefficient.

2. MUTUAL COHERENCE AND ITS PROPAGATION

The "high resolution" methods use a treatment of the covariance matrix of narrow band analytic signals sent by the ship to a set of sensors.

If (x_1, x_2) is a couple of sensors, $s(x_1), s(x_2)$ the analytic signals received by this couple, the corresponding term of the matrix is

$$s(x_1) s^*(x_2)$$

($*$ time average)

DEPART: Mutual coherence and silence

Two signals are said to be "mutually coherent" and only if:

1. the band of the signal is sufficiently narrow, i.e. if a signal $s(t)$ is shaped as $s(t) = A(t) \sin \omega_0 t$, the signal in quadrature $s(t) = A(t) \sin \omega_0 t$ coincides with the original signal $s(t)$.

2. the signal is "quasi-monochromatic".

The signal is said to be "quasi-monochromatic" in the sense of the propagation. The signal is said to be "quasi-monochromatic" if it is an extended source and reach an extended antenna. The difference of propagation time between couples (sending point - receiving point) is limited by a quantity Δt . It corresponds to this quantity, Δt , the width of the band equal to Δf .

3. the signal is "quasi-monochromatic" through the band of the signal. If the bandwidth is small, it results in the condition:

A signal which satisfies with these conditions is said "quasi-monochromatic" and is associated to a frequency f_0 simply associated to it.

Let us now consider a sending surface (source) and (x_1, x_2) two points on

the mutual coherence MC of the quasi-monochromatic analytic signals for this couple:

On the other hand, we consider a receiving area (antenna) and (x_1, x_2) a couple of points on it:

$$C(x_1, x_2) = s(x_1) s^*(x_2)$$

is the MC associated to this couple.

According to these hypotheses, the MC obeys to a second order wave equation and to a "HUYGHENS principle" associated (fig.1).

It can be written

$$C(x_1, x_2) = \iint_{S_1, S_2} \frac{e^{iK(r_1 - r_2)}}{r_1 r_2} dS_1 dS_2 \quad (1)$$

where K is the wave number for the centre of the band, r_1, r_2 the distances (x_1, x_2) to the source.

APPENDIX 1. A SHIP AND AN ANTENNA

The ship and the antenna are represented as two segments. IO is the straight line connecting the centers of the ship and the antenna. The directions are given with reference to IO . The lengths are R (ship), L (antenna).

P, M is a couple of points on the ship

P_1, M_1 is a couple of points on the antenna (fig. 2)

with reference to a system of coordinates whose origin is O (O, O_1) the coordinates of P, M are

$$P: (R \cos \alpha, R \sin \alpha)$$

$$M: (L \cos \beta, L \sin \beta)$$

where

$$P, M: R^2 = R^2 \cos^2 \alpha + R^2 \sin^2 \alpha = R^2 (\cos^2 \alpha + \sin^2 \alpha) = R^2 \quad (2)$$

$$P_1, M_1: R_1^2 = R^2 + L^2 - 2RL \cos(\alpha - \beta) = R^2 + L^2 - 2RL \cos(\alpha - \beta) \quad (3)$$

This expression can be expanded up to second order in (L/R)

$$R_1^2/R^2 = 1 + \frac{L^2}{R^2} - \frac{2L}{R} \cos(\alpha - \beta) + \frac{L^2}{R^2} \cos^2(\alpha - \beta) = 1 + \frac{L^2}{R^2} - \frac{2L}{R} \cos \alpha \cos \beta + \frac{L^2}{R^2} \sin^2 \alpha \sin^2 \beta + \frac{L^2}{R^2} \sin^2 \alpha \cos^2 \beta + \frac{L^2}{R^2} \cos^2 \alpha \sin^2 \beta \quad (4)$$

The quantity of use for introduction in formula (1) is

$$P_1, M_1 - P, M = (1 - \frac{L^2}{R^2}) \cos \alpha \cos \beta - \frac{2L}{R} \sin \alpha \sin \beta + \frac{L^2}{R^2} \sin^2 \alpha \sin^2 \beta + \frac{L^2}{R^2} \sin^2 \alpha \cos^2 \beta + \frac{L^2}{R^2} \cos^2 \alpha \sin^2 \beta \quad (5)$$

The MC for (x_1, x_2) can be expressed in terms of the MC for (ξ_1, ξ_2) by use of the formula (1).

DEBART: Mutual coherence and silence

$$\frac{1}{2} \left(\frac{1}{p} \sin^2 \theta \right) \sin^2 \theta \quad (6)$$

$$\frac{1}{2} \left(\frac{1}{p} \sin^2 \theta \right) \sin^2 \theta \quad (7)$$

the essential quantities are the essential quantities

allows its determination

allows the determination of the wavefront and allows the determination of the

PERFECTLY INCOHERENT SOURCE

the emission of the ship is seen as punctual acoustical sources, entirely independant to each other, the situation is exactly the astronomical situation, in which the optical sources in two points of the sum for example are independant.

In this case:

$$I(x_1, x_2) = I(x_1) \cdot I(x_2)$$

I is the acoustical intensity in each point, and the integral J reduces to a simple integral :

$$J = \frac{1}{R} \int \frac{e^{i k (x_1 - x_2)}}{R} \sin^2 \theta I(x) dx \quad (8)$$

where J is the Fourier transform of the function I (acoustical power on the surface). This result is well known and referred by the astronomers as "Van Cittert-Shotter theorem".

To evaluate the influence of this factor J , it is convenient to suppose a finite number of point-like sources on the ship:

$$J(x_1, x_2) = \sum_{m=1}^M I_m \delta(x_1 - x_m) \delta(x_2 - x_m) \quad (9)$$

where the term of the covariance matrix (X_1, X_2) can be expanded in a sum corresponding to the distinct contributions. If the antenna has a very high resolving power, they are seen as distinct, if not they are seen as an unique source whose angular location is between the extremities of the ship.

4. PARTIALLY COHERENT SOURCE

This situation is modified if the ship bears a repartition of acoustical sources, with a MC function finite between any couple of points.

To study this phenomenon, let us suppose that this MC takes the form

$$J(x_1, x_2) = e^{-\frac{(x_1 - x_2)^2}{2\rho^2}} e^{-\frac{(x_1 + x_2)^2}{2\rho^2}} \quad (10)$$

Its modules is decreasing with the distance, ρ is a radius of correlation. It can be supposed also that the argument is variable (linearly) with a characteristic length λ (λ can be infinite if no variation of the argument exists).

Hence it can be written:

$$J = e^{iK(x_1 - x_2)\cos\alpha} e^{-\frac{(x_1 - x_2)^2}{2\rho^2}} \times \dots \times \exp\left[-\frac{(x_1 - x_2)^2}{2\rho^2} \sin^2\alpha + \frac{(x_1 + x_2)^2}{2R} \sin^2\alpha + \frac{(x_1 - x_2)^2}{2\rho^2}\right] d\xi_1 d\xi_2 \quad (11)$$

In order to evaluate this integral, let us suppose that ρ is very small versus λ .

and adopt new variables, according to the transformation

DEBARI. Mutual coherence and silence

$$\frac{1}{2} \left(\frac{1}{R} + \frac{1}{2R} \sin^2 \theta \right)$$

... by removing the limits of integration for the variable u .

$$\exp \left\{ - \frac{1}{2} \left(\frac{1}{R} + \frac{1}{2R} \sin^2 \theta \right) (x_1 + x_2) \sin \theta \sin \phi - \frac{1}{4R} V \sin^2 \theta \right\} du dv \quad (12)$$

$$\text{where } \dots \quad (13)$$

The calculation can be achieved with no trouble and gives :

$$J = \exp \left\{ - \frac{1}{2} \left(\frac{1}{R} + \frac{1}{2R} \sin^2 \theta \right) (x_1 + x_2) \sin \theta \sin \phi - \frac{1}{4R} V \sin^2 \theta \right\} \times e^{- \frac{1}{2} (x_1 - x_2) \sin \theta \sin \phi \frac{1}{R}} dv \quad (14)$$

If the source is sufficiently remote, the V^2 -term in the exponential can be neglected. Hence, if we drop the constant factor :

$$J = \frac{e^{-(a+ib)}}{a+ib} = \frac{e^{-(a+ib)}}{a+ib} \quad (15)$$

where :

$$a = \frac{1}{2R} \sin^2 \theta + \frac{1}{2} \left(\frac{1}{R} + \frac{1}{2R} \sin^2 \theta \right) (x_1 + x_2) \sin \theta \sin \phi \quad (16)$$

$$b = \frac{1}{2R} (x_1 - x_2) \sin \theta \sin \phi$$

The variation of the argument of J versus $(x_1 - x_2)$ is approximately the same as the variation of the argument of $a+ib$

$$\text{Arg}(a+ib) = \text{Arctan} \left(\frac{b}{a} \right) = \dots = \text{trg } J$$

$$J = \frac{1}{2R} \int_{-L}^{+L} (x_1 - x_2) \sin \theta \sin \theta' dx_1 dx_2 \quad (17)$$

$$J = \frac{1}{2R} \int_{-L}^{+L} (x_1 - x_2) \sin \theta \sin \theta' dx_1 dx_2$$

$$J = \frac{1}{2R} \int_{-L}^{+L} (x_1 - x_2) \sin \theta \sin \theta' dx_1 dx_2 \quad (18)$$

in the same conditions (very remote source).

If the radius of correlation is very small, $\theta \approx \pi/2$ for any distance between the sensors (x_1, x_2): it is again the case of a totally incoherent source.

If not, let us recall that $(x_1 - x_2)$ vary from $-L$ to $+L$ if L is the length of the antenna.

Let us define a radius of correlation from the condition:

$$\theta = \frac{\pi}{4} \text{ for } x_1 - x_2 = \pm \frac{L}{2} \quad (19)$$

$$\frac{L}{2} \sin \theta \sin \theta' = 1$$

If (usual conditions) $\theta = \theta' = \frac{\pi}{4}$ $\sin \theta \sin \theta' = \frac{1}{2}$

$$\frac{L}{2} = 1 \quad \text{or} \quad L = \frac{2}{\sin \theta \sin \theta'} \quad (20)$$

The argument of J vary quasi-linearly from $-\frac{\pi}{2}$ to $\frac{\pi}{2}$ if $x_1 - x_2$ vary from $-L$ to $+L$ and the angular measurement the antenna can achieve is false (the argument of the characteristic factor takes any value according to $x_1 - x_2$).

If, for example $L = 20 \text{ m}$ $\theta = K \cos \alpha = \frac{2\pi}{\lambda} \cos \alpha$

$$\theta = 1 \text{ m} \quad \alpha = \frac{\pi}{4} \quad \lambda = \pi \sqrt{2}$$

$$\lambda = \frac{20}{2\sqrt{2}} = 1,5 \text{ m}$$

DEBART: Mutual coherence and silence

REALIZATION

1) Repartition of acoustical sources whose correlation is shaped as

is to be achieved by a sum of sources of certain structures and random amplitudes, according to the Loeve-Karhunen theorem

$$s(t) = \sum_n s_n(t)$$

is an extended source whose repartition is roughly sinusoidal

$$s_n(t) = a_n \cos(a_n t) + b_n \sin(a_n t)$$

The correlation function can be approximated by a few sources.

CONCLUSION

The theoretical possibility to make inefficient the high resolution method is thus shown. However, achieving this result involves a modification of the acoustical emission of the ship, and this problem must be studied from the point of view of its practical realization.

DEBART: Mutual coherence and silence

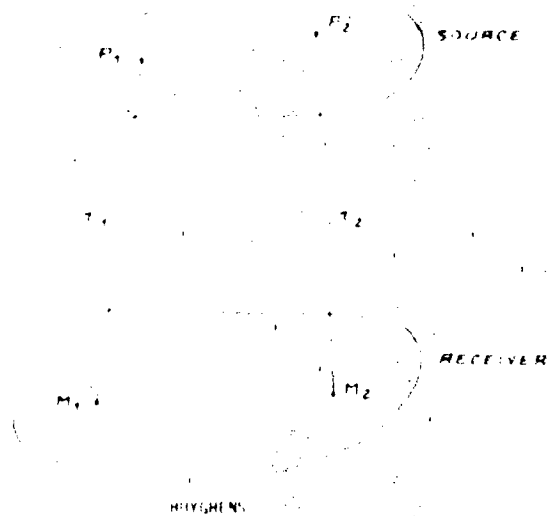


Fig. 1 : Secondorder Huyghens Principe

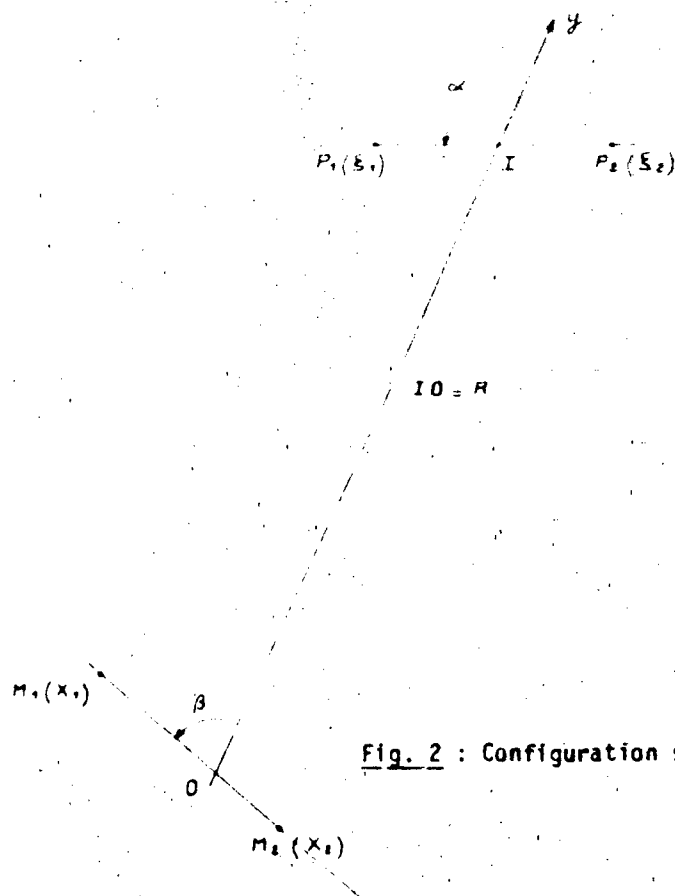


Fig. 2 : Configuration ship-antenna

CERNICH & VETTORI: Mobile range

MOBILE RANGE
FOR MEASURING SHIP RADIATED ACOUSTIC NOISE

by

Enzo Cernich
Sonomar S.p.A.
Sarzana, Italy
and
Giancarlo Vettori
USEA S.p.A.
Lerici, Italy

ABSTRACT

The Mobile Range described in this paper allows measurements of noise radiated from both surface ships and submarines in open seas with bottom depths from less than 100m to 400 meters. The range is being developed and built by Sonomar under contract with the Italian Navy. The system is semifixed, that is, it can be launched, utilized and recovered in short time or else, with some precaution, can be left operational for longer periods. In this paper a description of the system is given; the design criteria for the at-sea measuring equipment, the navigation of the vessel being tested and for at-shore data analysis are discussed.

INTRODUCTION

The system described in this paper will be used to measure the noise radiated by surface ships and submarines in both dynamic and static conditions, in open sea with a bottom depth from less than 100m to 400 meters.

The system is semi-fixed, that is, it can be launched at sea, utilized and recovered in a short space of time, or else it can be left operational for longer periods, provided certain precautions are taken.

The mobile range is now being developed and built under contract with the Italian Navy.

In this paper a description of the system is given; the design criteria for

CERNICH & VETTORI: Mobile range

the existing equipment, the navigation of the vessel being tested and the data reduction analysis are discussed.

1.1.1. REQUIREMENTS

The requirements for the mobile range are as follows:

The range must be able to be initiated by submarines and surface ships with a maximum range of 100 km.

- Measurements to be conducted in areas with bottom depth up to 400 meters; water state conditions up to 2; survival of the in-water equipment at higher temperatures.

- The launch and recovery of in-water equipment to be performed by a small ship with a minimum of expendable parts.

- Flexibility to launch and recover the range and to conduct the measurements from the surface ships to be tested.

- Maximum use of reliable commercially available equipment.

- Computer based analysis of existing facilities.

1.1.2. DESCRIPTION OF THE SYSTEM

The system consists of:

- a) In-water subsystem, formed by three mooring supporting the required hydrophone stations, a marker buoy and a radio buoy transmitting data to an assist ship.

- b) Navigation subsystem, located on the test vessel, having the purpose of giving navigational control with respect to the moorings.

- c) Signal acquisition subsystem, located on the assist ship (or else on the test vessel if it is a surface ship), with the purpose of receiving and recording on magnetic tape the signals transmitted from the radio-buoy and controlling the quality of them.

- d) Signal analysis subsystem, located on land, utilizing part of the

acquisition subsystem and an HP-1000 computer.

2.1 - In-water Subsystem

Fig.1 shows the basic schematic configuration of the in-water subsystem shown for operating on a typical bottom of 200 meters depth. It consists of 2 moorings A,B,C. The hydrophone stations (H_1, H_2, H_3 , and H_4) are suspended from moorings A and B as indicated in the diagram and at the required depths. H_1, H_2 and H_3 are called Beam hydrophones and H_4 is called Track.

The range configuration is flexible so that, starting with the basic configuration in Fig.1, it can be adapted for either surface ships or submarines or changed according to marine currents or to the bottom depth on which the system must operate. For operations with submarines hydrophone H_4 is not used.

The composite structure of the cable enables the position of the hydrophone stations to be changed and also to intervene on each connecting electric cables separately.

Moorings A and B both have a Release-Transponder unit (RT) suspended at a depth of 100mt. These units act as an acoustic responder and free the moorings when receiving an appropriate acoustic control signal.

The two moorings A and B are anchored to the bottom (AN in the diagram). They are supplied with two buoyancy units and connected together at the Connection Unit (UC) by means of a hydrophone cable (CAB-3). Mooring A is connected to the Radio-buoy by means of a Vibrating Insulation Module (VIM) that has the purpose of isolating the buoy's oscillations from the mooring and by the piece of cable, CAB:7, which also has a damping function.

The radio-buoy contains the electronics (EL) necessary for the conditioning the hydrophone signals and for the transmission via radio link of the signals and reception of commands from the assist ship to the buoy.

The radio buoy is easy to connect and disconnect from mooring A in case it is required to disactivate the range and leave it in the sea for a period of time.

The radio buoy is about 5 meter high above the sea surface to make it visible from a distance both optically by periscope and by radar (this applies also to the marker buoy). Oscillations due to sea motion are limited within the vertical aperture of the transmitting/receiving antenna.

GERNICH & VETTORI: Mobile range

The system is a computerized mechanical system for the measurement of the range between two vessels. Both the target and the test vessels are equipped with a transponder unit for the exchange of data.

Navigation and range measurement system

The system is composed of two parts. It is divided into two parts: the first part is the navigation system, the second part is the range measurement system. The two parts are connected by a common data link.

The navigation system is obtained measuring the distance between the test vessel and the target vessel, plotting the data and graphically representing on a display. It also provides the data for the course correction. The above data are plotted on a display together with the time (digital clock). The data are also stored in a memory. A VHF radio channel is used for communicating between the target ship and test vessel and also permits the synchronization of the digital clocks. The first part of the navigation system is the test vessel, and the second part of the acquisition system is the target ship.

The system is also equipped with test vessel's underwater telephone transducer; the system is also equipped with installing a proper transducer is required.

Navigation and range measurement system aboard the assist ship

The system is shown schematically in Fig. 1. It provides magnetic recording of the hydrophone signals received by radio and a preliminary data quality control in a 1st octave analyser and proper recorder. Digital clock data, information on operating parameters of the electronics are also recorded.

The system enables one to choose the hydrophone channels to be used as well as their gain, equalization and to calibrate them.

- Auxiliary functions provided by the subsystem are:

a) Measurement of the geometric deformation of the range due to the water current by interrogation of the two transponder units.

b) The possibility of steering the test vessel from the assist ship; this function duplicate the one implemented on board the test vessel and is

particularly relevant for operations with a submarine.

- d) Rapid electroacoustic calibration in situ of the various hydrophone channels.
- e) Possibility of measuring precisely the distance between the test vessel and each hydrophone.
- f) Activation of the release function of the transponders for recovery of the at-sea equipment.

2.4 - On-land analysis subsystem

Fig.4 is a block diagram of the subsystem. It enables the following operations to be carried out for each hydrophone channel.

- a) Reconstruction of the distance between the test vessel and the hydrophone and choice of the sections of the run to be used for signature data.
It makes use of some of the components of both the acquisition and navigation subsystem.
- b) Analysis and signature in 1/3 octave bands from 10 to 40000Hz.
- c) Narrow band analysis and signature between 5 and 5000Hz.
- d) Compensation for the effects of surface and bottom interference.
- e) Calculation of statistical averages.

3 - ANALYSIS OF SOME CRITICAL DESIGN PARTS

The performances and reliability of a mobile range is a large number of factors and operations. While setting up the system it has been found that after designing the data telemetry and vibration isolation of the hydrophones the most challenging problems to solve were:

- Measuring hydrophone positions in the range.
- Navigation accuracy and safety of vessel navigating inside the range.
- Launching and recovering of at-sea equipment.
- Compensating of surface and bottom interference in the measurements.

In the following paragraphs the solution being implemented of the above mentioned problems are discussed.

3.1 - Mooring deformation in their positions

It is to be expected that in any operational area a current will be present, detouring the lay-out of moorings from a straight line. In the mobile range system has been used to dimension buoyancies and anchors moored to obtain equilibrium and minimize deformation of moorings, but in fact that deformation cannot be totally eliminated.

For example, Figs. 1 and 2 show the deformation of mooring A and B when, at a deep configuration is affected by the following current profile:

- a) zero from 0 to 100 meters;
- b) 10 cm/s on the bottom;
- c) linearly decreasing between 100 meters and the bottom.

In Fig. 1 and 2 the current is assumed perpendicular to the phase containing mooring A and B; in Fig. 3 the current is assumed parallel to this plane.

From Figs. 1 and 2 it can be observed that there is an offset between the axis of base line H_1-H_2 and the axis of base line joining the two transponders used for navigation of the vessel under test.

Therefore, in order to navigate the ship under test over H_4 (TRACK Hydrophone), the offset must be taken into account. It can be observed that for navigation purposes only the offset in the Y/Z plane is relevant. Therefore a simple last mean square algorithm is used to estimate precisely the projections on plane YZ of distances between H_1 , H_2 , H_3 , H_4 , and the two transponders. Measurements are taken from the assist ships before the vessel under test starts a measurement run. Estimated navigation accuracy over H_4 is of the order of 5 meters.

3.2 - Observations on the test vessel's navigation system

Reference is made to Fig. 8. This diagram represents an example of the positions on the horizontal plane of the buoys (B_1 -radio buoy) the two responders RT_1 and RT_2 and the hydrophones H_1 and H_4 at the head of moorings A and B respectively. Because of the deformation caused by the

current H_1 and H_4 are displaced with respect to RT_1 and RT_2 .

The navigation of the test vessel will have several phases (see Fig.8):

a) Approach and radar-optical alignment.

The test vessel "sees" the two buoys B_1 and B_2 and sets an appropriate course in correspondence to the radar axis perpendicular to B_1-B_2 and passing through the midpoint.

This phase precedes the use of the acoustic navigation data and, in the case of a submarine, takes place at periscope depth, before diving.

b) Approach and acoustic alignment.

The test vessel modifies its course, moving into the acoustic navigation axis by utilizing the data supplied by the HP-9836 computer.

c) Maintenance of the course.

The test vessel must be on the correct course some time before reaching the maximum distance DM at which radiated noise measurements begin. (DM is about 1200mt for RT_1-RT_2 , 200mt and minimum aspect angle of 10°).

The test vessel continues on its course with small corrections, as indicated by the computer, up until the end of the course (a distance DM beyond the range).

d) Manoeuvre for moving away with an eventual return towards the range from the opposite side, repeating the above mentioned operations.

The following observations should be made regarding navigation across the range.

- Safe navigation for the submarine.

The navigation system must ensure a 100% non-interference with the structure of the range. The system has been designed to offer this safety; it has in fact been verified that when the distance between the anchorages is 200mt, the deformation of the range, even under the influence of unusual current conditions, leaves ample space for navigation.

Moreover the system supplies the data with a precision far superior (1m) to that required to ensure the non-interference.

- Validity of the measurement.

The most critical case is the passage of a surface ship across the hydrophone track (H_4). The assist ship should pass above the hydrophone H_4 with an offset error not greater than the width of the surface vessel. This can be achieved by means of the proposed system that, owing to the combination of high precision measurements with filtering, allows one to

tain the required precision.

The navigation system utilizes hardware already widely tested both for its functionality and reliability in the offshore field and suitably adapted to the present application.

The test vessel may navigate at maximum speed (30 knots) provided that the induced noise at the transducer installed on the test vessel is contained within the established limits.

The elements installed on the range that are required for the navigation of the test vessel are the two responders RT_1 and RT_2 consisting of the RT units, installed as shown in Fig.8 and defining a system of cartesian coordinates.

The transponders are the reference points with respect to which the test vessel calculates its position. To do this the test vessel interrogates the two transponders RT_1 and RT_2 at a frequency f_1 ; these respond at different frequencies f_2 and f_3 .

The test vessel receives the two responses and recognizes the two units on the basis of their frequencies. Using the time intervals between interrogation and response, distances R_1 and R_2 between the test vessel and RT_1 and the test vessel and RT_2 are measured.

The position of the test vessel is found from the distances R_1 and R_2 . The off-board computer elaborates this information by numerically filtering. Filtering is used to eliminate the effect of the delay in the estimation of the position caused by acoustic propagation time, to estimate the direction and velocity of navigation without the necessity of a gyrocompass and log and to reduce the effect of measurement errors on the global precision of the system.

Errors are essentially:

- Error in the measurement of the delays due to variations in the sound speed.

The effect is minimized by estimating the appropriate average value from the temperature/velocity profile.

- An intrinsic error in the measurement of the time delays due to the instruments used for the measurements.

- Error in the estimation of the transponder positions.

The preliminary measurements for estimating the precision of the system

minimize this error.

An extensive simulation study has been carried out in order to calculate the global errors in the positioning of the navigation system. These have proved to be of the order of 1 meter relative to RT_1 and RT_2 . The functioning of the navigation system, including the operator, has also been simulated in order to verify the ease with which it can be used. Fig.9 is an example of this simulation showing graphically the horizontal plane containing the range (RT_1 and RT_2).

The y axis represents the navigation axis desired V_0 , X_0 , Y_0 and χ_0 represents respectively the speed, the coordinates and the heading of the test vessel measured with respect to the Y axis at starting point. The crosses are the successive positions of the vessel estimated by the system. The system also supplies numerically the successive X and Y values together with the angle. The solid curve represents the real course of the test vessel.

3.3 - Launching and recovering of the system

The method for launching and recovering the range has been designed to operate with an assist ship provided with one derrick, one winch and two auxiliary craft (rubber dinghies).

To carry out the operation with the above hypotheses and the limited manoeuvring capability of the assist ship the sea state must be less or equal to 2 and the direction of the wind must be constant.

The procedure for launching the moorings A and B is a combination of the "anchor first" and "anchor after" methods: each mooring is launched in two sections as shown in Fig.10 (the bottom setting lowered in depth and the top section floating).

The submerged sections are suspended from a reinforced balloon and connected by means of a rapid-release hook.

The two moorings A and B, as shown in Fig.11 are then spaced apart so that there is the desired distance between them (about 200m). The rubber dinghies are used to join together on the surface the two sections of connecting hydrophone cable together with the sinker, kept temporarily on the surface by means of a suitable balloon.

The rubber dinghies are used to uncouple the two supporting balloons.

For recovery, the assist ship activates acoustically the uncoupling of the mooring A releaser and subsequently that on mooring B. The rubber dinghy takes the radio-buoy back to the assist ship and recovery on board begins according to the sequence: radio-buoy, mooring A, mooring B.

An emergency recovery method has been foreseen. This would take place, with the help of divers and only in the unlikely situation in which one of the releasers doesn't work.

3.4 - Compensation for the effects of surface and bottom interference

In order to calculate the acoustic levels at the reference distance of 1 metre from the source using the measured levels, it is necessary to know the propagation loss between test vessel and hydrophone.

Within the geometric conditions foreseen for the range, such losses can be modelled using the classical law (spherical divergence + absorption minus the incoherent contribution of the surface reflections) only for frequencies above 1KHz. For lower frequencies, the difference between the propagation model required and the classical model, becomes greater (and hence also compensation), the lower the frequency.

The order of magnitude of the systematic error by utilizing the above classical model can be of 10-15dB for frequencies of hundreds of Herz and of 15-30dB for frequencies below 100Hz.

This error is caused by interference formed at the hydrophone between the direct sound field and the surface reflected and bottom reflected fields. The bottom reflected field depends upon the frequency and the geometry and nature of the bottom.

A preliminary study, conducted in cooperation with Mr. Schmidt (Saclantcen) using models NISSM and FFP, on propagation over a reflecting bottom has indicated that for frequencies above 1000Hz compensation for incoherent addition of surface and bottom contribution and averaging over values obtained from the 3 hydrophones (spacial diversity) gives a reliable result if bottom characteristics are known.

For frequencies below 1000Hz there is no simple rule available. Some modelling work has been started and shall be verified in known areas using the range itself.

4 - CONCLUSION

The system must be delivered for acceptance test in summer '85. Sea trials are also foreseen in order to verify at sea operations of the various parts of the system in Fall '85.

CERNICH & VETTORI: Mobile range

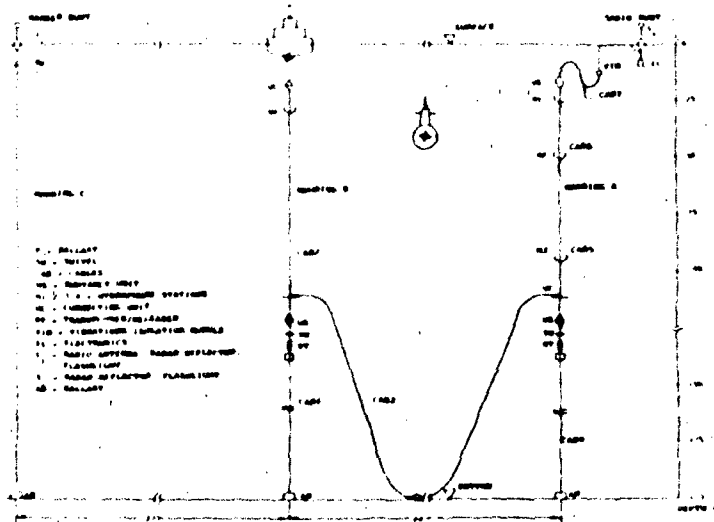


FIG. 1 - AT-SEA SUBSYSTEM. BASIC CONFIGURATION

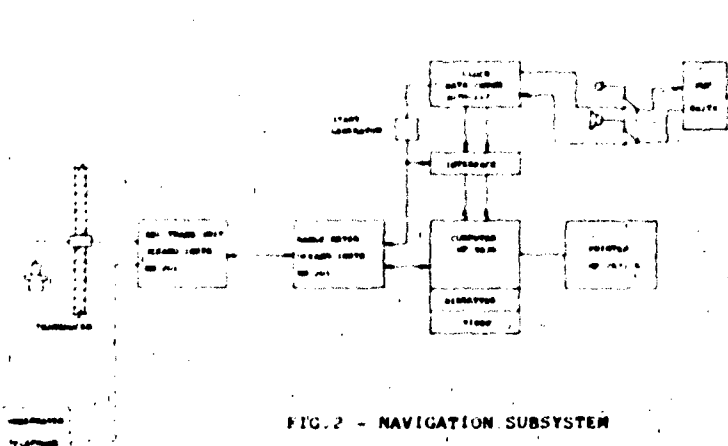


FIG. 2 - NAVIGATION SUBSYSTEM

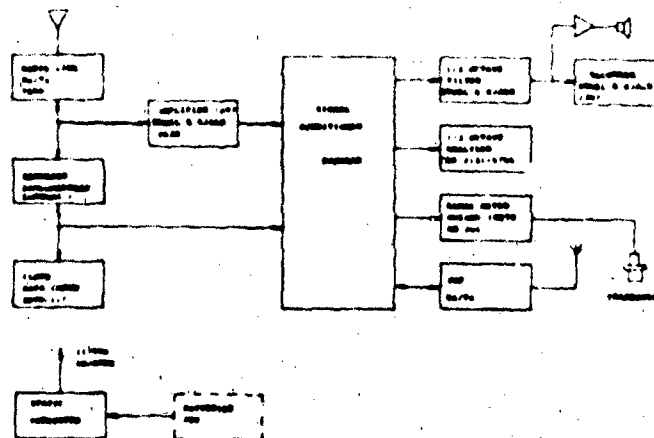


FIG. 3 - SIGNAL ACQUISITION SUBSYSTEM ABOARD ASSIST SHIP

CERNICH & VETTORI: Mobile range

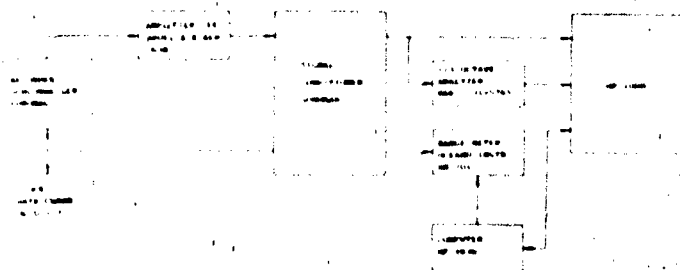


FIGURE 1 - N-LAND ANALYSIS SUBSYSTEM



FIG.5 - DEFORMATION OF THE RANGE
CURRENT | PLANE Y-Z

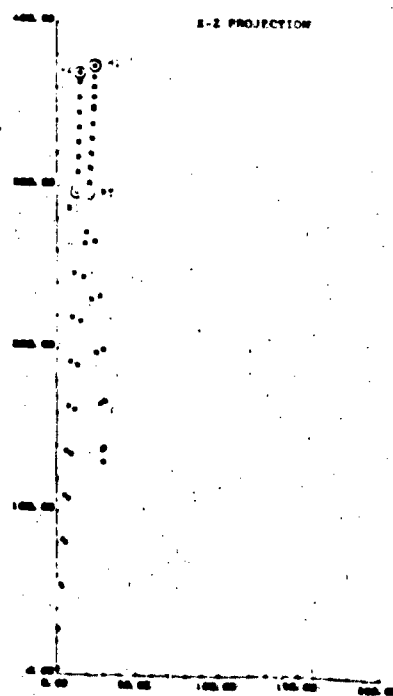


FIG.6 - DEFORMATION OF THE RANGE
CURRENT | PLANE X-Z

CERNICH & VETTORI: Mobile range

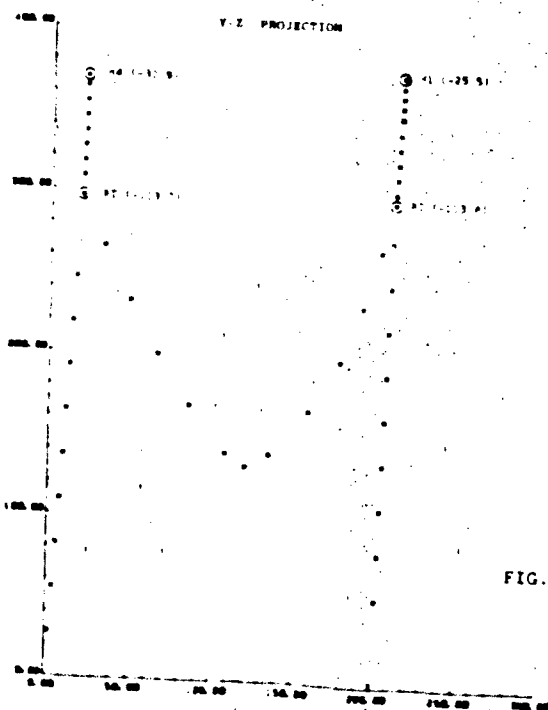


FIG.7 - DEFORMATION OF THE RANGE
CURRENT \perp PLANE Y-Z

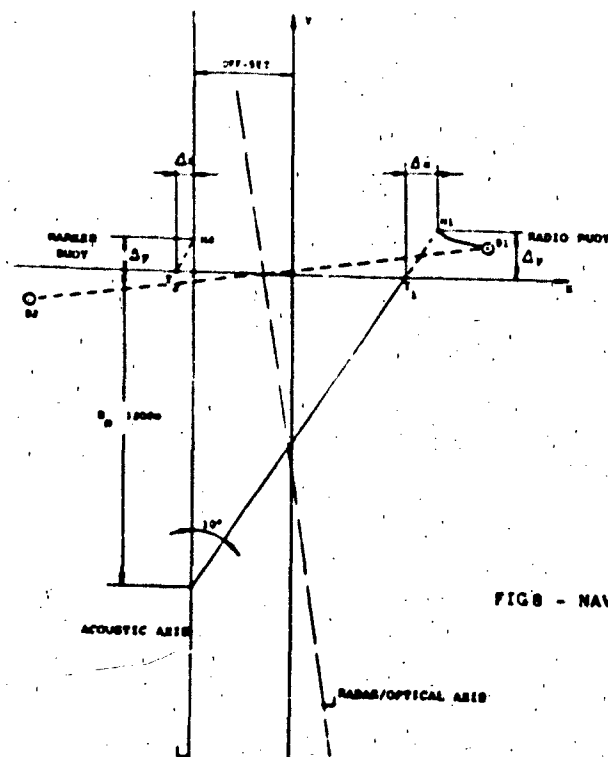


FIG 8 - NAVIGATION GEOMETRY

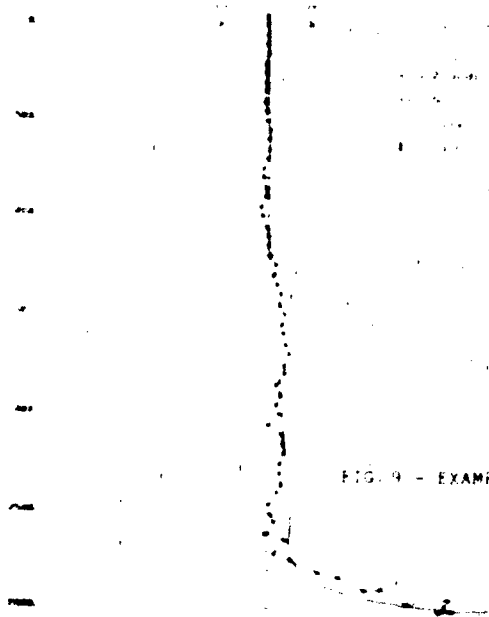


FIG. 9 - EXAMPLE OF SIMULATED NAVIGATION COURSE

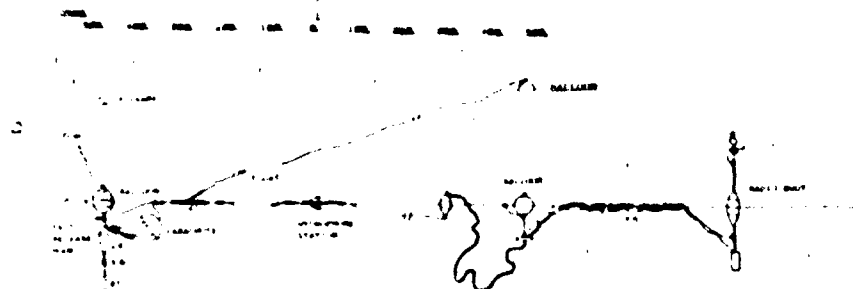


FIG. 10 - LAUNCHING OF THE TWO SECTIONS OF MOORING A

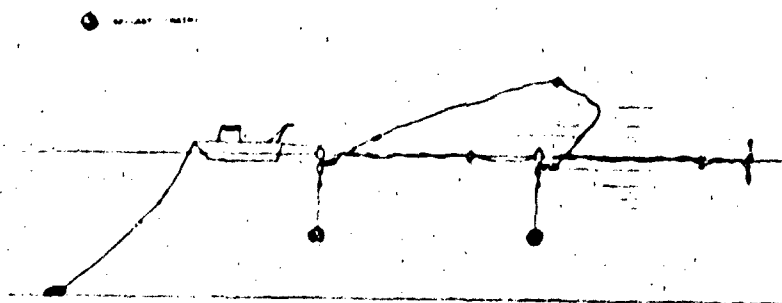


FIG. 11 - ARRANGEMENT OF MOORINGS A AND B BEFORE SINKING

DISCUSSION

A.D. Stuart (United States): Does the measurement range have the ability to monitor the aspect angle of the "target" or "test" vessel, as well as its range? If so, how is this to be done?

E. Cernich: Monitoring equipment installed on board the assist ship does not have the capability to monitor the aspect of the test vessel. However, the estimated aspect angle of the test vessel can be made available on-line onboard the test vessel by reference to the transponders' base line; ashore it can be measured by reference to the hydrophone H1-H4 baseline. Real-time ranges to hydrophones H1 and H4 are continuously displayed on board the assist ship.

A.W. George (United States): Does the on-board monitoring (quick-look) system have range correction?

E. Cernich: Ranges are measured direct to the two transponders. On board the assist ship ranges to hydrophones H1 and H4 are directly displayed, thereby providing correct ranges to the above hydrophones.

C.C. Leroy (France): Is there any security danger in transmitting the received signals by radio?

E. Cernich: The need to avoid broadcasting the data was taken into consideration. We should not forget that the transmitting and receiving antennae are operating over the sea surface. By an appropriate choice of the transmitting frequency, the vertical directivity pattern of the transmitting antennae, and the transmitter output power, the surface reflection allows the useful reception distance from the buoy to be limited to a range of about one mile centred at one mile.

SACLANTCEN CP-36

INITIAL DISTRIBUTION

| | Copies | | Copies |
|------------------------------|--------|----------------------------------|--------|
| <u>MINISTRIES OF DEFENCE</u> | | <u>SCNR FOR SACLANTCEN</u> | |
| DSHQ Belgium | 2 | SCNR Belgium | 1 |
| DND Canada | 10 | SCNR Canada | 1 |
| MOD Denmark | 8 | SCNR Denmark | 1 |
| MOD France | 8 | SCNR Germany | 1 |
| MOD Germany | 15 | SCNR Greece | 1 |
| MOD Greece | 11 | SCNR Italy | 1 |
| MOD Italy | 10 | SCNR Netherlands | 1 |
| MOD Netherlands | 12 | SCNR Norway | 1 |
| MOD Norway | 10 | SCNR Portugal | 1 |
| MOD Portugal | 2 | SCNR Turkey | 1 |
| MOD Spain | 2 | SCNR U.K. | 1 |
| MOD Turkey | 5 | SCNR U.S. | 2 |
| MOD U.K. | 20 | SEC GEN Rep. SCNR | 1 |
| SECDEF U.S. | 68 | NAMILCOM Rep. SCNR | 1 |
| <u>NATO AUTHORITIES</u> | | <u>NATIONAL LIAISON OFFICERS</u> | |
| Defence Planning Committee | 3 | NLO Canada | 1 |
| NAMILCOM | 2 | NLO Denmark | 1 |
| SACLANT | 10 | NLO Germany | 1 |
| SACLANTREPEUR | 1 | NLO Italy | 1 |
| CINVESTILANT/COMOCEANLANT | 1 | NLO U.K. | 1 |
| COMSTRIKFLANT | 1 | NLO U.S. | 1 |
| COMIBERLANT | 1 | | |
| CINCEASTLANT | 1 | <u>NLR TO SACLANT</u> | |
| COMSUBACLANT | 1 | NLR Belgium | 1 |
| COMMAIREASTLANT | 1 | NLR Canada | 1 |
| SACEUR | 2 | NLR Denmark | 1 |
| CINCNORTH | 1 | NLR Germany | 1 |
| CINCSOUTH | 1 | NLR Greece | 1 |
| COMNAVSOUTH | 1 | NLR Italy | 1 |
| COMSTRIKFORSOUTH | 1 | NLR Netherlands | 1 |
| COMEDCENT | 1 | NLR Norway | 1 |
| COMMARATIME | 1 | NLR Portugal | 1 |
| CINCHAN | 3 | NLR Turkey | 1 |
| | | NLR UK | 1 |
| | | NLR US | 1 |
| | | <u>CONFERENCE ATTENDEES</u> | 69 |
| | | Total initial distribution | 318 |
| | | SACLANTCEN Library | 10 |
| | | Stock | 22 |
| | | Total number of copies | 350 |

END